Selected Topics On Systems Far From Equilibrium

Thesis Submitted For The Degree of

Doctor Of Philosophy (Science)

of

Jadavpur University

2010

ARNAB SAHA

S. N. Bose National Centre For Basic Sciences

JD Block, Sector III

Salt Lake City

Kolkata 700098

India

Dedicated

to

my niece

Manaswita

ACKNOWLEDGEMENTS

is the love and support from my parents, my sister, my brother-in-law and most importantly my niece, that enabled me to pursue this line of study which finally culminated in this thesis.

Contents

Contents

1 Introduction and Overview

<u>Introduction:-</u> Most of the systems that we deal within physics, consist of huge number of interacting paticles ($\sim 10^{23}$). In principle, to describe such a system and its dynamical behavior, we need to know the dynamics of positions and momenta of all the particles with initial and boundary conditions. In case of quantum mechanical systems, instead of positions and momenta, we require the wave function representing the state concerned. But its equilibrium thermodynamic state is entirely specified by a few macroscopic variables like pressure, volume, temperature etc., that in turn are related through phenomenological equation of states [1, 2, 3, 4]. Question is, how all the mechanical variables and the equations of motion involving them, give rise to a complete set of a few macroscopic variables and the equations of state, which are enough to specify a thermodynamic state uniquely. Straight forward calculations from dynamical equations will not help much, because— (1) knowing all the initial momenta and coordinates exactly, is impossible and (2) available techniques to solve dynamical equations are incapable to handle such a huge number of equations ($\sim 10^{23}$), even in the simplest situation like the ideal gas.

Here is the need to develop a methodology, called statistical mechanics [5, 6, 7, 8, 9], which will prescribe a procedure to calculate macroscopic quantities from microscopic variables and related equations of motion. This development happens at two levels. In the first level we have to keep a particle-picture in our mind, i.e. our system contains N number of particles having $\{\mathbf{p_i}\}$ momenta and $\{\mathbf{x_i}\}$ coordinates ($i = 1, 2, 3, ...N$). We can also write a Hamiltonian H—a function of these microscopic variables—representing the total energy of the system. For avoiding the difficulty in counting all possible states of the isolated system because of

allowing only a narrow energy window for that, we broaden the window to access all possible energy values by assuming the system in equilibrium with a heat bath and cleverly choosing a probability distribution

$$P_{eq}(w) = \frac{e^{\frac{-H(w)}{K_B T}}}{\sum_w e^{\frac{-H(w)}{K_B T}}} \tag{1.1}$$

for a possible configuration $w(\mathbf{p_i}, \mathbf{x_i})$, making the occurrence of the system being outside the previously specified window of energy, very rare. Though we loose some information by making all possible energy states accessible to the system, it does not affect the mean values in case of large systems because the variance of any macroscopic quantity $\Delta A \sim \frac{1}{\sqrt{N}}$. The distribution in 1.1 is called Boltzmann distribution where K_B is the Boltzmann constant and T is the temperature of the heat bath. To compute a macroscopic variable A from its microscopic counterpart $A(w)$ using canonical formalism, the required prescription is

$$A = \int A(w) P_{eq}(w) dw. \tag{1.2}$$

The denominator in equation (1.1) is called partition function (Z) which directly connects with thermodynamic free energy as $F = -K_B T \ln Z$. This formalism is good enough to calculate equilibrium macroscopic properties of a system which are simple enough, like ideal gas or non-interacting Ising spin etc. But to deal with more complicated phenomena (e.g. phase transition), we need to upgrade the above formulation to the next level.

Next upgradation depends on the following observation— "*Under normal circumstances the 10^{23} or so degrees of freedom can be reduced enormously. The intensive or extensive character of observables (energy is extensive, density is intensive) allows one to reconstruct the properties of a macroscopic system given only a microscopic sample of it. Thus a liquid of only 1000 atoms, say, would probably have approximately the same energy per unit volume and density as the same liquid (at the same temperature and pressure) with 10^{23} atoms.*"—K.G.Wilson and J.Kogut[10].

But how far one can reduce the number of degrees of freedom of a system without changing its properties? This length scale of a system is called correlation length, which depends on the thermodynamic state of the system. In disordered states (e.g. gaseous state, paramagnetic

state etc.) this correlation length can be one or two atomic spacings but in special cases the correlation length is much larger than the atomic spacing, for which the critical point marking the onset of a phase transition is a prime example. Theory of critical phenomena and renormalisation group studies [11, 12, 13, 14, 15, 16, 17] in statistical mechanics suggest that the behavior of the systems having large number of degrees of freedom within their correlation length is fundamentally different from those with few degrees of freedom in the correlation length. At a first glance it is expected that the behavior of the system is governed mainly by microscopic interactions and the coupling constants of the interactions present in H. This is certainly the case when correlation length is small. But when the correlation length involves many degrees of freedom, the behavior of the system is controlled primarily by the collective behavior of those degrees of freedom. The microscopic interactions play only a secondary role and that is why universality appears. These observation implies that only the long wavelength ($\sim$ correlation length) collective excitations are important near transition.

In above situations, equation (1.1) will be too complicated starting point to arrive at some useful results and it is not at all necessary, because all the details involved in microscopic H are not important. So we change our focus from the microscopic scales to some mesoscopic scales, which are much larger from the lattice spacings but much smaller from the system size. In this length scale we define the order parameter of the concerned phase transition as a field $m(\mathbf{x})$, say. Here $L > \mathbf{x} >> a$, where a is lattice spacings or atomic/molecular length scale and L is the system size. We emphasize here that being a function of continuous variable $\mathbf{x}$, $m(\mathbf{x})$ do not exhibit any variation at distances of the order of a and so, $m(\mathbf{x})$ is called coarse-grained order parameter.

Next, ignoring unnecessary microscopic details, we will construct a mesoscopic Hamiltonian ($\mathcal{H}$) as a functional of $m(\mathbf{x})$ depending on some conditions which emerge from very generic principles. The principles and corresponding conditions are —(i) uniformity of the material over the space forbids any explicit dependence of $\mathcal{H}$ on $\mathbf{x}$ (ii) presence of short ranged non-local interactions introduces spatial derivatives of m in the expression of $\mathcal{H}$ (iii) to fulfill the demand that $\mathcal{H}$ must be an analytic function, we take it as an analytic expansion of powers of m (iv) underlying microscopic spatial symmetry should be obeyed and (v) as the probability must

not diverge at large m, the coefficient of the term containing highest even power of m in the expansion should always be positive. Guided by these conditions, one can formulate $\mathcal{H}$ with external field h as,

$$\mathcal{H} = \int d^d\mathbf{x} \left[am^2(\mathbf{x}) + bm^4(\mathbf{x}) + c(\nabla m)^2 + ... - hm) \right]. \tag{1.3}$$

It is commonly known as Landau-Ginzburg Hamiltonian. Here a, b, c... are a set of phenomenological parameters. These are unknown functions of microscopic interactions as well as the thermodynamic parameters like temperature and pressure. This is the price that we pay for avoiding the difficulty of calculations starting from (1.1). Given $\mathcal{H}$, now one can easily formulate Boltzmann weight, mesoscopic partition function ($\mathcal{Z}$) and corresponding free energy.

So, equilibrium statistical mechanics is capable enough to prescribe an elegant method of handling large number of degrees of freedom to act as a bridge between thermodynamics and laws of mechanics. Not only in equilibrium, above formulation can also be applied close to equilibrium through the linear response formalism including the fluctuation-dissipation theorem and Onsagers reciprocity relations [18, 19]. But describing systems far away from equilibrium, is beyond its scope. In fact, if one starts to study statistical dynamics which deals with the systems far from equilibrium, immediately it will appear that instead of having a unique formulation like equilibrium statistical mechanics, here we have widely different approaches to explain the dynamical properties of various systems of interest. Here we face several types of macroscopic dynamical equation. Some common examples may be — diffusion equation [20], FokkerPlanck-Kramers equation [20, 22, 18, 23, 24], Boltzmann transport equation [21, 9], Cahn-Hilliard equation [25] etc.

Though the approaches are different, it is important to note here that *all the macroscopic equations are irreversible in time, though the underlying micro-dynamics is time reversible.* It is a long standing paradoxical issue that how individual particle, obeying time reversible equations of motion, when move collectively, show time-irreversibility [21]. The fact is, irreversibility in time is a price that the system, being far from equilibrium, pays for ignoring small scale fluctuations, while going towards or away from equilibrium. Systems always ignore small scale fluctuations as long as it contains large number of degrees of freedom. That is why the canonical

formalism works so well. Another manifestation of this ignorance is calculation of critical exponents. If one computes critical exponents assuming the coarse-grained Hamiltonian $\mathcal{H}$, without going into further approximation schemes (e.g. mean field), the results are astonishingly close to the experiments. It implies that even if we calculate the exponents ignoring the microscopic fluctuations over a length scale of the order of few lattice parameters, we will be able to produce the numbers which are pretty close to the reality. But, though loosing information of microscopic fluctuations helps us to calculate macroscopic quantities in equilibrium, on the other hand it allows the number of accessible configurations to become very large. And the fact is that the systems are always prone to maximize this number, when it is relaxing towards equilibrium or driven away from it. So, at each time step the system will choose to follow only that path along which the number of allowed configurations will increase and at equilibrium it becomes the maximum. On the other hand, the time-reversed path become very rare because it reduces that number. Thus the irriversibility creeps into all natural processes, involving large number of degrees of freedom.

Derivation of Boltzmann transport equation [21, 9] is a pivotal example to understand how irreversibility in time emerges out of reversible equation of motions by introducing physically motivated assumptions. Here, without stressing on the detailed derivation, we will try to clarify the assumptions behind the derivation, which are responsible for the loss of information, resulting the time-irreversible nature of the equation.

We consider a large volume V with N molecules of dilute gas, interacting via central, pairwise, additive potential having a strong repulsive core with a finite range a. As a very large class of potentials have all these properties, the transport equation remains very general and applicable to many cases. To ensure diluteness $V/N >> a^3$ is maintained. One can define a number density of particles $f(\mathbf{r}, \mathbf{v}, t)$, so that number of the particles inside a mesoscopic volume $\delta\mathbf{r}$ $(a^3 << \delta\mathbf{r} << V)$ at time t, around the point $(\mathbf{r}, \mathbf{v})$ in phase space $\equiv f(\mathbf{r}, \mathbf{v}, t)\delta\mathbf{r}\delta\mathbf{v}$. This number can change by the following ways—(1) collision-free flow in or out of the volume $\delta\mathbf{r}$ in presence of external potential $U(r)$, (2) leaving from $\delta\mathbf{r}$ due to direct collision, (3) appearing into $\delta\mathbf{r}$ after a direct collision. To calculate the collision free contribution we consider the flow of particles into and out of a region in time δt. An expression for this flow in the x-direction

can be obtained by considering the volume $v_x \delta t \delta y \delta z$ that contain particles that move into or out of a cell with its center (x, y, z) in time δt. The flow can be expressed as the difference between the number of particles entering and leaving this small region in time δt. We consider, for example, a cubic cell and its faces perpendicular to the x-axis. The flow of the particles across the faces at $x - \frac{1}{2}\delta x$ and $x + \frac{1}{2}\delta x$ in presence of external potential U is,

$$\mathcal{N}_{free}^{x} = v_x \delta t \delta y \delta z \delta \mathbf{v} \times \left[f(x - \frac{1}{2}\delta x, y, z, v_x - \frac{1}{2}\delta v_x, v_y, v_z, t) - f(x + \frac{1}{2}\delta x, y, z, v_x + \frac{1}{2}\delta v_x, v_y, v_z, t) \right]$$

$$(1.4)$$

with similar expression for other two directions. The function f is assumed to be smooth over the mesoscopic length scale, so that it can be expanded in Taylor's series around (x, y, z). The zeroth order terms are canceled out and we neglect δ^2 and the higher order terms. Thus using $\frac{\mathbf{P}}{m} = \mathbf{v}$ we get

$$\mathcal{N}_{free} = \delta t \delta \mathbf{p} \delta \mathbf{r} \left[\nabla U . \frac{\partial}{\partial \mathbf{p}} - \frac{\mathbf{p}}{m} . \nabla \right] f \qquad (1.5)$$

If we denote the contribution from the collision by $\left[\frac{df}{dt} \right]_{coll.}$, the rate of change of $f(\mathbf{r}, \mathbf{v}, t)$ becomes,

$$\left[\frac{\partial}{\partial t} - \nabla U . \frac{\partial}{\partial \mathbf{p}} + \frac{\mathbf{p}}{m} \nabla \right] f = \left[\frac{df}{dt} \right]_{coll.} \qquad (1.6)$$

To evaluate the r.h.s we need to know the rate of change of number of particles due to collisions suffered by the particles with momentam $\mathbf{p}$ in the region $\delta \mathbf{v} \delta \mathbf{r}$ during δt assuming each such collision causes sudden change of momenta of the particle. The collisions are assumed to be *sharp* (time interval of contact is strictly zero) and binary in nature. The rate depends on the following factors.

- It depends on the probability of finding a particle of momentum $\mathbf{p}$ at $\mathbf{r}$, that suddenly alters if it undergoes a collision with another particle of momentum $\mathbf{p}'$ at $\mathbf{r}$. The probability of such a factor is proportional to the differential cross section $|\frac{d\sigma}{d\Omega}|$ of the collision, the flux of the incident particle $(\sim |\mathbf{p}' - \mathbf{p}|)$ and the joint probability of findings the two particles together— $f(\mathbf{v}', \mathbf{v}, \mathbf{r}, t)$. So the differential rate of change of the number due to this is

$$-d\mathbf{r} d\mathbf{p} d\mathbf{p}' d^2 \Omega |\frac{d\sigma}{d\Omega}||\mathbf{p}' - \mathbf{p}|f(\mathbf{v}', \mathbf{v}, \mathbf{r}, t) \qquad (1.7)$$

The negative sign signifies that this number of particles go outside the volume $\delta\mathbf{r}\delta\mathbf{v}$.

- It also depends on the probability of finding a particle of momentum $\mathbf{p}$ at $\mathbf{r}$, that suddenly appears through a collision with another two particles of momentum $\mathbf{p}''$ and $\mathbf{p}'''$ at $\mathbf{r}$. With similar reasoning one can arrive at the expression of the differential rate of change of the number as,

$$d\mathbf{r}d\mathbf{p}'''d\mathbf{p}''d^2\Omega|\frac{d\sigma}{d\Omega}||\mathbf{p}'' - \mathbf{p}'''|f(\mathbf{v}'', \mathbf{v}''', \mathbf{r}, t) \tag{1.8}$$

Here the sign is positive because it signifies that this number of particles go into the volume $\delta\mathbf{r}\delta\mathbf{v}$.

From energy and momentum conservation principles it is apparent that $|\mathbf{p}'' - \mathbf{p}'''| = |\mathbf{p}' - \mathbf{p}|$ and going into center of mass frame one can also show that $d\mathbf{p}'''d\mathbf{p}'' = d\mathbf{p}d\mathbf{p}'$. Using the above expressions for the contributions from two body collisions in equation (1.6) we get

$$\left[\frac{\partial}{\partial t} - \nabla U.\frac{\partial}{\partial \mathbf{p}} + \frac{\mathbf{p}}{m}\nabla\right]f = -\int d\mathbf{p}'d^2\Omega|\frac{d\sigma}{d\Omega}||\mathbf{p}' - \mathbf{p}|(f(\mathbf{v}', \mathbf{v}, \mathbf{r}, t) - f(\mathbf{v}'', \mathbf{v}''', \mathbf{r}, t)) \tag{1.9}$$

From above equation the existence of equilibrium state and how can it be reached—these issues are not apparent. The assumptions taken up to this point (e.g. sharp binary collisions) are not responsible for information loss—rather they are only for making the system simpler. Now we assume that the particles having momenta $\mathbf{p}$ and $\mathbf{p}'$ are *statistically independent*. This assumption is physically quite plausible because before they have arrived at the states $(\mathbf{p}, \mathbf{r})$ and $(\mathbf{p}', \mathbf{r})$, they have faced huge number of collisions with the other particles (note that the time interval δt is much more larger than the time scale coming from collision frequency), which randomise their motion and consequently they become statistically independent of each other. So we can write $f(\mathbf{v}', \mathbf{v}, \mathbf{r}, t) = f(\mathbf{v}', \mathbf{r}, t)f(\mathbf{v}, \mathbf{r}, t)$ and thus the information contained by the conditional probability $f(\mathbf{v}'|\mathbf{v}; \mathbf{r}, t)$ has disappeared. Similar thing happens when we write $f(\mathbf{v}'', \mathbf{v}''', \mathbf{r}, t) = f(\mathbf{v}'', \mathbf{r}, t)f(\mathbf{v}''', \mathbf{r}, t)$ by the same token. This assumption is called '*molecular chaos*'. The equation (1.9) now becomes

$$\left[\frac{\partial}{\partial t} - \nabla U.\frac{\partial}{\partial \mathbf{p}} + \frac{\mathbf{p}}{m}\nabla\right]f = -\int d\mathbf{p}'d^2\Omega|\frac{d\sigma}{d\Omega}||\mathbf{p}' - \mathbf{p}|(f(\mathbf{v}', \mathbf{r}, t)f(\mathbf{v}, \mathbf{r}, t) - f(\mathbf{v}'', \mathbf{r}, t)f(\mathbf{v}''', \mathbf{r}, t)$$
$$\tag{1.10}$$

The time-irreversible nature of above equation becomes transparent when Boltzmann defined the '$\mathbb{H}$'-function as

$$\mathbb{H} = \int d\mathbf{p} d\mathbf{r} f(\mathbf{v}, \mathbf{r}, t) \ln f(\mathbf{v}, \mathbf{r}, t) \tag{1.11}$$

and showed in a straight forward way from (1.10) that,

$$\frac{d\mathbb{H}}{dt} \leq 0. \tag{1.12}$$

Along the forward path value of $\mathbb{H}$ increases with time and along the time-reversed path it decreases. In equilibrium it remains constant (because, in equilibrium $\frac{d\mathbb{H}}{dt} = 0$). So, $\mathbb{H}$ function behaves as an indicator to show whether the system, following equation (1.10), is going along the forward path or along the time-reversed backward path. According to (1.12), it always decreases which clearly shows that the dynamics of the system must be irreversible in time. Not only this, it is quite straight forward to derive the equilibrium distribution (Maxwell-Boltzmann distribution) from the equilibrium condition, $\frac{d\mathbb{H}}{dt} = 0$, which is nothing but a great triumph of the theory. Later with the help of his $\mathbb{H}$-theorem, he was able to arrive at the statistical interpretation of entropy and the second law.

Thus, the resolution to the irreversibility-paradox according to Boltzmann and others, is — in all macroscopic dynamics there must exist a time-reversed backward path corresponding to each forward path, but as it is very rare, it is quite improbable to see the system actually following that path. Then, it is quite legitimate to ask the following:-

- In comparison to the paths forward in time, how rare their time-reversed paths are?

- It seems to us from above discussions that, as the degrees of freedom increase, the paths reversible in time, become more and more improbable. So, in case of small systems, can we actually see the rare trajectories?

- How does this rarity scale with system size?

- Is there any direct consequence of these rare trajectories?

It took near about a century to answer these questions after Boltzmann's work. It is only from the last decade of the last century, due to the advent of rigorous results like, fluctuation

theorems [26, 27, 28, 29, 30, 31, 32, 33, 34] and innovative techniques of single molecule experiments [35, 36] above issues are being addressed successfully. Fluctuation theorems are closely related equalities that deal with thermodynamic quantities like heat, work, entropy etc. and their probability distributions. These are valid when the systems are at equilibrium (it can reproduce equilibrium thermodynamical results with properly taken limits), close to equilibrium (it can reproduce results from linear response theory with properly taken limits) and also far away from equilibrium situations. Fluctuation theorems are the direct consequence of the rare time-reversed trajectories. So, if one wants to verify any one of the theorems, sampling rare trajectories is a must. Due to this constraint, verification or application of fluctuation theorems in case of large systems comes out to be tough computationally. Though some clever way of sampling rare events may do the job successfully. It should be mentioned here that all the thermodynamic quantities are so defined along the trajectories that, upon averaging over all possible trajectories, we get corresponding macroscopic quantities. These definitions together with the fluctuation theorems lead to a comparatively new field of research, called stochastic thermodynamics which has produced a great amount of enthusiasm in recent days. The main reason behind this enthusiasm is not only bridging the conceptual gap between reversible micro-dynamics and irreversible macro-dynamics, but also its practical implications like, extracting equilibrium results from nonequilibrium measurements [36].

Overview:- This thesis is mostly devoted to deal with some aspects of work fluctuation theorems (chapter I - chapter IV). In these works sampling rare trajectories is a must. In comparison to the large systems (i.e. systems with large number of degrees of freedom), the occurrence of rare trajectories is more frequent in small systems (i.e. system with small number of degrees of freedom), making the sampling easier. So, in these four chapters, the model systems we take, are 'small' (e.g. single oscillator in a thermal bath).

Second chapter contains a proof of work fluctuation theorems. It clearly depicts the rarity and importance of 'time-reversed' backward path. Then, in the same chapter we switch to explore generic properties of probability distribution function of thermodynamic work done on a system driven far from equilibrium. Here we show that work distribution function is in general

asymmetric.

Fluctuation theorems can extract equilibrium results from nonequilibrium measurements. **Third chapter** of this thesis contains an example where we show that work fluctuation theorem can predict zero classical diamagnetism in case of bounded, equilibrated systems. Though this is an old result (now it is in any text book of statistical mechanics in the name of Bohr-van Leeuwen theorem), work fluctuation theorems demonstrate a new way to arrive at the same result.

The importance of calculating diamagnetism in classical systems via work fluctuation theorem becomes transparent, when we apply it on a charged particle doing Brownian motion on a sphere, under the influence of z-directional magnetic field. Standard proof of Bohr-van Leeuwen theorem [37, 38, 39] tells that there will be no diamagnetism. But this proof is very subtle, because it does not care about the boundary of the system explicitly, whereas it can be shown that diamagnetic moment of bulk of any system is exactly canceled by paramagnetic moment caused by its boundary. Sphere has no such physical boundary with which the particle on it can collide and reflect back. So, the charged particle moving on a sphere may show diamagnetism. Work fluctuation theorems will allow us to explore the possibility of having diamagnetism in classical, finite but unbounded systems. Our results regarding to this problem are described in **fourth chapter** of the thesis.

In **fifth chapter**, we show how the probability distributions that include probability of occurrence of rare events, can be employed to calculate physical quantities like work distribution functions for various driven systems or multifractal exponents of a fully turbulent fluid.

Segregation or phase separation of driven colloidal mixture is a common phenomena in our daily life. For example, one can mention segregation of various particles in blood (RBC, WBC etc.) by centrifuging the sample. **Last chapter** of the thesis deals with dynamic phase separation of soft colloidal particles in a binary colloidal suspension. The phase separation occurs at nonequilibrium steady state. We study the system by *dynamical density functional theory* [40, 41] which is another example of '*time-irreversible macro-dynamics*'.

Bibliography

[1] J. C. Maxwell, Theory of Heat, Dover, (2001).

[2] E. Fermi, Thermodynamics, Dover, (1956).

[3] H.B.Callen, Thermodynamics and Introduction to Thermostatistics, Wiley, 2nd Ed., (1985).

[4] M. W. Zemansky and Richard H. Dittman, Heat and Thermodynamics, McGraw-Hill, 7th Ed., (1996).

[5] J. W. Gibbs, Elementary Principles of Statistical Mechanics, Ox Bow Press, (1981).

[6] L. D. Landau, E. M. Lifsitz, Statistical Physics, Butterworth-Heinemann, 3rd Ed., (1980).

[7] R. P. Feymann, Statistical Mechanics: A Set Of Lectures, Westview Press, 2nd Ed., (1988).

[8] R. C. Tolman, The Principles of Statistical Mechanics, Dover.

[9] M. Kardar, Statistical Physics of Particles, Cambridge University Press, 1st Ed., (2007).

[10] K. G. Wilson and J. Kogut, Physics Reports, **12**, 2, (1974), pp 75200.

[11] Leo P. Kadanoff, Statistical Physics: Statics, Dynamics and Renormalization, World Scientific, (2000).

[12] K. G. Wilson, Rev. Mod. Phys. **47**, 4 (1975).

[13] J. Cardy, Scaling and Renormalization in Statistical Physics, Cambridge University Press, (1996).

Bibliography

[14] S. K. Ma, The Modern Theory Of Critical Phenomena, Benjamin Reading, (1976).

[15] K. Kawasaki, Phase Transition and Critical Phenomena, Edited by C. Domb and M.S. Green, Academic (New York), Vol. 2, (1972).

[16] M. Kardar, Statistical Physics of Fields, Cambridge University Press, 1st Ed., (2007).

[17] N. Goldenfield, Lectures On Phase Transitions And The Renormalization Group, Westview Press, (1992).

[18] R. Zwanzig, Nonequilibrium Statistical Mechanics, Oxford University Press, USA, 1st Ed. (2001).

[19] S. R. De Groot, P. Mazur, Non-Equilibrium Thermodynamics, Dover, (1984).

[20] S. Chandrasekhar, Rev. Mod. Phys. **15**, 1 (1943).

[21] J. R. Dorfman, An Introduction to Chaos in Nonequilibrium Statistical Mechanics, Cambridge University Press, (1999).

[22] N. G. Van Kampen, Stochastic Processes in Physics and Chemistry, North Holland, 3rd Ed. (2007).

[23] H. Risken, The Fokker-Planck Equation: Methods of Solutions and Applications, Springer, 2nd Ed. (1989).

[24] C. Gardiner, Handbook of Stochastic Methods: for Physics, Chemistry and the Natural Sciences, Springer, 3rd Ed. (2004).

[25] P. C. Hohenberg, B. I. Halperin, Rev. Mod. Phys. **49**, 435 (1977).

[26] J. Kurchan, J. Stat. Mech. P07005 (2007), doi.10.1088/1742-5468/2007/07/P07005.

[27] D. J Evans and D J Searles, Phys. Rev. Lett. **96**, 120603 (2006).

[28] E. M Shevick et al, Ann. Rev. Phys. Chem. **39**, 2007.

[29] T. Bodineau and B Derrida, Phys. Rev. Lett. **92**, 180601 (2004).

[30] G. Gallavoti and E G D Cohen, Phys. Rev. Lett. **74**, 2694 (1995).

[31] D. J Evans and D J Searles, Phys. Rev. E **50**, 1645 (,) 1994.

[32] C. Jarzynski, Phys. Rev. Lett. **78**, 2690 (1997).

[33] G. E. Crooks, J. Stat. Phys. 90, 1481, 1998.

[34] U. Seifert, Phys. Rev. Lett. **95**, 040602 (2005).

[35] F. Ritort, J. Stat. Mech. Theor. Exp., P10016, (2004).

[36] J. Liphardt, S. Dumont, S. Smith, I. Tinoco, and C. Busta-mante, Science **296**, 1832 (2002).

[37] Bohr N., *Studies over Matallerners Elektrontheori*, PhD Thesis (1911).

[38] van Leeuwen J. H., J. Phys. (Paris)., **2**, 361 (1921).

[39] Vleck J. H. V., *The Theory of Electric and Magnetic Susceptibilities* (Oxford University Press, London) 1932.

[40] U. Marini Bettolo Marconi, P. Tarazona, J. Chem. Phys. **110**, 8032, 1999

[41] A. J. Archer, R. Evans, J. Chem. Phys. **121**, 4246, 2004

Bibliography

14

2 Work Fluctuation Theorems And Work Distribution Function

In this chapter we first go through the proof of Crooks' identity [1, 2] and from that we will arrive at Jarzynski equality [3, 4, 5] for systems far from equilibrium, evolving via Markov chain [6]. After that we will show that the thermodynamic work distribution is asymmetric when the system evolves via nonlinear, overdamped Langevin equation. We are interested in such dynamics because a large class of real systems, where momentum degrees of freedom dissipate very fast in presence of thermal bath, follow this dynamics.

2.1 Crooks' identity and Jarzynski equality

When a system evolves in time by discrete Markov chain:- For the proof we consider a classical system in contact with a heat bath at constant temperature T, where some degree of freedom of the system can be manipulated externally by a time dependent force, dragging the system away from equilibrium. Manipulation of this degree of freedom results in an expenditure of some amount of work and an exchange of heat with the bath, together which give rise to a net change of internal energy of the system. For example, in room-temperature water, one can take one end of a strand of RNA, attached to a small polystyrene bead and the other end to a micromechanical cantilever [7]. A laser trap is used to capture the bead. Using piezo-electric techniques to move the cantilever back and forth, the end-to-end distance of the

RNA strand can be varied. Thus the work is performed on the system (the RNA strand) and some amount of heat is delivered by the system to the bath surrounding it (the water) as this micro-manipulation to the end-to-end distance is carried out externally. Let λ_t be the current value of the controllable degree of freedom at time t, which is the end-to-end distance in our example. We consider a process where λ_t is switched between an initial and final value (λ_0 and λ_τ respectively) over some finite length of time, τ. The internal state of the system, specified by the phase space variables, at time t ($0 \leq t \leq \tau$) is labeled by i_t. The energy of the system will depend on its current state and λ_t. So, the energy at time t is denoted by $E(i_t, \lambda_t)$. We will assume discrete time and a discrete phase space. The straight forward generalisation to continuous time and phase space will be discussed later. We will consider the evolution of this system through time, as the control parameter varies through a fixed sequence as $\{\lambda_0, \lambda_1, \lambda_2...\lambda_t, \lambda_{t+1}...\lambda_\tau\}$. A particular path through phase space can be written as

$$i_0 \xrightarrow{\lambda_1} i_1 \xrightarrow{\lambda_2} .... \xrightarrow{\lambda_t} i_t \xrightarrow{\lambda_{t+1}} ..... \xrightarrow{\lambda_\tau} i_\tau. \tag{2.1}$$

Initially, (at $t = 0$) the system is in state i_0 and the control parameter is λ_0. The time evolution of the system is considered to occur stepwise i.e. discretely and one can imagine that a single step is divided into two substeps. First the control parameter is changed from λ_0 to a new value, λ_1. Thus, in this substep an amount of work, $E(i_0, \lambda_1) - E(i_0, \lambda_0)$ is performed on the system. Then the state of the system evolves from i_0, at constant λ_1, to the next state state i_1. During this evolution the system exchanges a quantity $E(i_1, \lambda_1) - E(i_0, \lambda_1)$ of heat with the reservoir. This evolution through phase space is repeated for τ time steps. We can write the total work performed on the system, W, the total heat exchanged with the reservoir, Q, and the total change in energy, ΔE, as [1, 2]

$$W = \sum_{t=0}^{\tau-1} E(i_t, \lambda_{t+1}) - E(i_t, \lambda_t) \tag{2.2}$$

$$Q = \sum_{t=1}^{\tau} E(i_t, \lambda_t) - E(i_{t-1}, \lambda_t) \tag{2.3}$$

$$\Delta E = W + Q = E(i_\tau, \lambda_\tau) - E(i_0, \lambda_0). \tag{2.4}$$

Any path through the phase space can be reversible or irreversible, depending on whether the system is in equilibrium with the bath during its evolution or not. If the path is reversible, work

done on the system $W_r = \Delta F = F(\beta, \lambda_\tau) - F(\beta, \lambda_0)$, where ΔF is the free energy difference between initial and final equilibrium ensemble and $\beta = 1/K_B T$. Therefore W_r is not a path function, rather a state function. In case of irreversible path, $W > \Delta F$ and we can define dissipative work as $W_d = W - W_r$, where both W and W_d are path functions. If an amount of work is expended in changing the free energy of the system then the change in entropy of the universe is βW_d, in units of Boltzmann's constant.

Now we need to consider the time reversed path in the phase space. Corresponding to the forward time path in equation (2.1), one can represent the time reversed path as

$$i_0 \xleftarrow{\lambda_1} i_1 \xleftarrow{\lambda_2} .... \xleftarrow{\lambda_t} i_t \xleftarrow{\lambda_{t+1}} ..... \xleftarrow{\lambda_\tau} i_\tau. \tag{2.5}$$

As the order of λ_t's is time-reversed, the sequence in which states are visited are also time-reversed. Note that the forward path begins with a change in λ, whereas the reverse path begins with a change in the internal state of the system. The definitions of work, heat and change of energy will remain unaltered. One should note here that the value of these quantities along the backward (i.e. time-reversed) path is opposite in sign to the corresponding value along the forward path.

Till now, we have not assumed any particular property, except discreteness of the path in the phase space along which the system evolves forward/backward in time. Now we are going to assume that the path is Markovian in nature, i.e. the transition probability of the system to any state i_t depends only on the previous state $i_{t\pm1}$. The '-' is for forward path and '+' is for backward path. So the system looses all the memory of states from i_0 to i_{t-2} in its forward path and from i_τ to i_{t+2} in its backward path, when it is in i_t. Employing this assumption one can write the probability of a forward and a backward path through phase space as

$$P(i_0 \xrightarrow{\lambda_1} i_1 \xrightarrow{\lambda_2} .... \xrightarrow{\lambda_t} i_t \xrightarrow{\lambda_{t+1}} ..... \xrightarrow{\lambda_\tau} i_\tau) = P(i_0 \xrightarrow{\lambda_1} i_1)P(i_1 \xrightarrow{\lambda_2} i_2)...P(i_{\tau-1} \xrightarrow{\lambda_\tau} i_\tau) \tag{2.6}$$

$$P(i_0 \xleftarrow{\lambda_1} i_1 \xleftarrow{\lambda_2} .... \xleftarrow{\lambda_t} i_t \xleftarrow{\lambda_{t+1}} ..... \xleftarrow{\lambda_\tau} i_\tau) = P(i_0 \xleftarrow{\lambda_1} i_1)P(i_1 \xleftarrow{\lambda_2} i_2)...P(i_{\tau-1} \xleftarrow{\lambda_\tau} i_\tau).$$

The trajectories through the phase space need to be 'microscopically reversible'[1, 2, 8, 9]. Before explaining microscopic reversibility, we need to explain the dynamics and its constraints. The single time step dynamics of the whole Markov chain is determined by the transition matrix

$M(t)$ whose elements are the transition probabilities,

$$M(t)_{i_{t+1},i_t} \equiv P(i_t \to i_{t+1}). \tag{2.7}$$

A transition matrix M has the properties that all elements must be non-negative and all columns sum up to one due to the normalization of probabilities. Let $\rho(t)$ be a (column) vector whose elements are the probability of being in state i at time t. Then the single time step dynamics can be written as,

$$\rho_i(t+1) = \sum_j M(t)_{ij}\rho_j(t). \tag{2.8}$$

The product of all transition matrices corresponding to every time step can describe the dynamics completely. Here the state energies $E(t)$ and the transition matrices $M(t)$ are functions of time due to the external perturbation of the system, and the resulting Markov chain is non-homogeneous in time [10]. Now we place following additional constraints to the dynamics: the state energies are always finite and the single time step transition matrices must preserve the corresponding canonical distribution. This canonical distribution is determined by the temperature of the heat bath and the state energies at that time step. So, for an arbitrary time step we can write,

$$\frac{P(i_{t-1} \xrightarrow{\lambda_t} i_t)}{P(i_{t-1} \xrightarrow{\lambda_t} i_t)} = \frac{e^{-\beta E(i_t,\lambda_t)}}{e^{-\beta E(i_{t-1},\lambda_t)}}. \tag{2.9}$$

The above constraint essentially implies that accessible state energies are always finite, and that the dynamics are Markovian, and if unperturbed preserve the equilibrium distribution. These conditions are valid independently of the strength of the external perturbation, or the distance of the ensemble from equilibrium. Now we can establish the condition for the phase space trajectories to be microscopically reversible as follows,

$$
\begin{aligned}
&\frac{P(i_0 \xrightarrow{\lambda_1} i_1 \xrightarrow{\lambda_2} .... \xrightarrow{\lambda_t} i_t \xrightarrow{\lambda_{t+1}} ..... \xrightarrow{\lambda_\tau} i_\tau)}{P(i_0 \xleftarrow{\lambda_1} i_1 \xleftarrow{\lambda_2} .... \xleftarrow{\lambda_t} i_t \xleftarrow{\lambda_{t+1}} ..... \xleftarrow{\lambda_\tau} i_\tau)} \\
&= \frac{P(i_0 \xrightarrow{\lambda_1} i_1)P(i_1 \xrightarrow{\lambda_2} i_2)...P(i_{\tau-1} \xrightarrow{\lambda_\tau} i_\tau)}{P(i_0 \xleftarrow{\lambda_1} i_1)P(i_1 \xleftarrow{\lambda_2} i_2)...P(i_{\tau-1} \xleftarrow{\lambda_\tau} i_\tau)} \\
&= \frac{e^{-\beta E(i_1,\lambda_1)}e^{-\beta E(i_2,\lambda_2)}...e^{-\beta E(i_\tau,\lambda_\tau)}}{e^{-\beta E(i_0,\lambda_1)}e^{-\beta E(i_1,\lambda_2)}...e^{-\beta E(i_{\tau-1},\lambda_\tau)}} \\
&= e^{-\beta Q},
\end{aligned} \tag{2.10}
$$

where Q is the heat exchanged with the reservoir as the system goes along the forward path and $-\beta Q$ is the corresponding change in entropy (in units of Boltzmann's constant) of the bath. A system with this property will be described as microscopically reversible. So, microscopic reversibility is a relation between probability ratios of forward and corresponding backward trajectories and the heat. Now, if we specify the initial states of the forward as well as the backward path are in equilibrium with the reservoir, then employing the following property of any equilibrium ensemble A where λ_t is fixed at λ,

$$P(A|\lambda) = \frac{e^{-\beta E(A,\lambda)}}{\sum_i e^{-\beta E(i,\lambda)}} = \exp[\beta(F(\beta,\lambda) - E(\beta,\lambda))] \tag{2.11}$$

and from the microscopic reversibility condition one can write,

$$\begin{aligned}
&\frac{P(i_0|\lambda_0)P(i_0 \overset{\lambda_1}{\rightarrow} i_1 \overset{\lambda_2}{\rightarrow} \dots \overset{\lambda_t}{\rightarrow} i_t \overset{\lambda_{t+1}}{\rightarrow} \dots \overset{\lambda_\tau}{\rightarrow} i_\tau)}{P(i_\tau|\lambda_\tau)P(i_0 \overset{\lambda_1}{\leftarrow} i_1 \overset{\lambda_2}{\leftarrow} \dots \overset{\lambda_t}{\leftarrow} i_t \overset{\lambda_{t+1}}{\leftarrow} \dots \overset{\lambda_\tau}{\leftarrow} i_\tau)} \\
&= \exp[\beta(\Delta F(\beta,\lambda) - \Delta E(\beta,\lambda) - Q)] \\
&= e^{\beta W_d}.
\end{aligned} \tag{2.12}$$

If we represent any path in the phase space along which the system evolves as $\mathbf{x}$ and its time reversed counterpart by $\tilde{\mathbf{x}}$, then from the above analysis it is clear that the average of any path function $\mathcal{O}$ over all possible forward trajectories (denoted by 'F') can be written in terms of averaging over time reversed trajectories (denoted by 'R') as,

$$\langle \mathcal{O}(\mathbf{x}) \rangle_F = \langle \tilde{\mathcal{O}}(\tilde{\mathbf{x}}) e^{-\beta W_d(\tilde{\mathbf{x}})} \rangle_R \tag{2.13}$$

where the angular brackets are representing the averaging over initial equilibrium ensemble and also over all possible paths.

From the above analysis a detailed fluctuation theorem (Crooks' identity) and an integrated fluctuation theorem (Jarzynski identity) for work can come out easily. To arrive on Crooks' identity we consider $\mathcal{O} = \delta(\beta(W_d - W_d[\mathbf{x}]))$ and its time reversed counterpart as $\tilde{\mathcal{O}} = \delta(\beta(W_d + W_d[\tilde{\mathbf{x}}]))$. Using these into equation (2.13) and noting that ΔF, being a macroscopic state function, is not a random variable, we get

$$\frac{P_F(W_F)}{P_R(W_R)} = e^{\beta W_d}. \tag{2.14}$$

To get Jarzynski equality from above, first we note that $W_d = W_F - \Delta F$. Then from the normalisability condition of the probability distributions, after integrating both side of the above identity we get

$$\langle e^{-\beta W} \rangle = e^{-\beta \Delta F}, \tag{2.15}$$

omitting the notation 'F' for convenience. From here on we will suppress the subscript 'F' in case of all the quantities measured in the forward direction for notational convenience, except where mentioning both the directions (forward as well as reverse) are necessary. We stress that the above identities are valid far from equilibrium situations and independent of the strength of external perturbation because they are more-or-less direct implication of the microscopic reversibility condition, which was derived in a similar way. The only point of difference is when the microscopic reversibility condition is valid for any initial state (equilibrium or nonequilibrium), to use these two identities one must start from an equilibrium ensemble. One should note that standard equilibrium results can be derived from the above identities as special cases. Another important point should be mentioned here that though in principle microscopic reversibility and the identities discussed here are applicable to any system but those systems where fluctuations are comparable with $K_B T$, are preferred. Otherwise the convergence of the above identities will require large number of realisations which are practically impossible to take. Thus, the relevance of Crooks' identity or Jarzynski equality as a tool for measuring free energy differences is usually restricted to small systems[11].

When a system evolves in time by continuous Markov chain:- Now we will quickly go through the microscopic reversibility condition in case of continuous Markov processes. Though there are many advantages in working with a finite, discrete state space, most physical systems studied in statistical mechanics have a continuous phase space. So it is worthwhile to look into that.

Let $x(t)$ be the state of the system at time t. The phase space probability density is $\rho(x,t)$. The time evolution of the probability density can be described by an operator U, i.e. $\rho(x, t_2) =$

$U(t_1, t_2)\rho(x, t_1)$. U has the following properties

$$\lim_{t_2 \to t_1} U(t_1, t_2) = \mathbf{I} \qquad t_2 \geq t_1 \tag{2.16}$$

$$U(t_3, t_1) = U(t_3, t_2)U(t_2, t_1) \qquad t_3 \geq t_2 \geq t_1$$

where $\mathbf{I}$ is identity operator. The operators U can also be written as integral operators of the form,

$$\rho(x, t_2) = U(t_2, t_1)\rho(x, t_1) \tag{2.17}$$

$$= \int P(x, t_2 | x', t_1)\rho(x', t_1)dx' \qquad t_2 \geq t_1$$

For Markovian processes the propagators are transition probability densities and they have the following properties

$$\lim_{t_2 \to t_1} P(x, t_2 | x', t_1) = \delta(x - x') \tag{2.18}$$

$$P(x, t_3 | x'', t_1) = \int P(x, t_3 | x', t_2)P(x', t_2 | x'', t_1)dx'$$

Now we assume that the energy of the system always remain finite though due to the external perturbation at discrete set of times, it has discrete jumps in its profile and the propagator always returns the same equilibrium state on which it was applied if the system is unperturbed. These are constraints to the dynamics analogous to those we had in case of discrete Markov process described in previous section. We can also define time reversal of the trajectories in the phase space as it was described before and again assume that the canonical ensemble remains unaffected by the time reversal. Thus we can write analogous to equation (2.9), as

$$\rho(x, t | \beta, E)P(x, t | x, t') = \rho(\tilde{x}, \tau - t | \beta, E)P(\tilde{x}, \tau - t' | \tilde{x}, \tau - t) \tag{2.19}$$

where ρ depicts canonical distribution determined by the bath temperature and energy at the corresponding time. Here $\tilde{x}$ denotes the time reversed state of x. Using the above relation we can arrive at microscopic reversibility condition for the present scenario for given set of U as,

$$P(x(t) | x(0), U) = \prod_{j=0}^{J-1} P(x, t_{j+1} | x, t_j) \tag{2.20}$$

$$
\begin{aligned}
&= \prod_{j=0}^{J-1} P(\tilde{x}, t_{j+1}|\tilde{x}, t_j) \frac{\rho(x(t_j)|\beta, E(t_j))}{\rho(x(t_{j+1})|\beta, E(t_j))} \\
&= \tilde{P}(\tilde{x}(t)|\tilde{x}(0), \tilde{U}) \exp(-\beta Q(x))
\end{aligned}
$$

From here, Crooks' identity and Jarzynski equality follow in straight forward fashion. Therefore we can conclude that even if the system traverses along continuous Markov chain in the phase space being far from equilibrium, we can estimate the change of free energy between the initial and final equilibrium state by using Jarzynski or Crooks' identity.

2.2 Asymmetry In Work Probability Distribution

From the statement of the work fluctuation theorems, it should be clear enough that free energy difference is We take a nonlinear system that follows overdamped Langevin dynamics, being in contact with a heat bath at constant temperature. The thermal noise coming from the bath variables is Gaussian and delta correlated. We consider this particular system because the dynamics is a nice example of continuous Markov process discussed earlier and more importantly, it can explain the physical properties and dynamics of a large class of real systems, for example soft materials including polymers, colloids etc. Huge amount of literature exists in this field. Some typical examples may be [12, 13]. One can also take the experiment of pulling RNA polymers, mentioned at the beginning of this chapter. According to the discussions in the previous sections, microscopic reversibility, Jarzynski equality and Crooks' identity all are valid (provided we set the initial conditions properly for the last two) for the system under consideration. What we ask here is about the generic properties of the work distribution which takes an important role to extract information about free energy landscape from nonequilibrium measurements. We will show that if the system is arbitrarily dragged from one equilibrium state to another by an external time dependent force via arbitrarily irreversible paths, the thermodynamic work probability distribution is in general asymmetric, even if the evolution dynamics has a symmetry.

A couple of years ago a simple but effective experiment on a mechanical oscillator was done by Douarche, Ciliberto, Patrosyan and Rabbiosi (DCPR)[14, 15] who showed that for a linear oscillator in the overdamped limit,

$$\Delta F = \langle W \rangle - \frac{\langle (W - \langle W \rangle)^2 \rangle}{2KT} \tag{2.21}$$

This is consistent with equation (2.15) if the distribution of W is Gaussian and has been studied by various authors [16, 17, 18, 19]. This relation which is similar to a relation found by Landau and Lifshitz [20] in the context of thermodynamic perturbation theory, was demonstrated experimentally and also analytically for a particular kind of forcing by DCPR for linear oscillators.

The particularly convenient form of equation (2.21) made us investigate whether it holds for nonlinear systems. In what follows, we have looked first at the linear system with an arbitrary forcing in the highly viscous limit. The Green function technique used for that proof is then extended to treat the nonlinear system in a perturbative manner. The general dynamics is for the system is,

$$m\ddot{x} + k\dot{x} = -\frac{\partial V}{\partial x} + M(t) + f(t) \tag{2.22}$$

where $M(t)$ is an externally applied time dependent force and $f(t)$ is a random force that allows the system to be in equilibrium in absence of $M(t)$. The viscous limit corresponds to dropping the inertial term $m\ddot{x}$. The system is supposed to be in equilibrium (state A) at $t = 0$ and then we switch on $M(t)$ for a time τ, after which $M(t)$ takes a constant value $M(\tau)$. The system reaches the state B. In going from state A to state B, the thermodynamic work done on the system is

$$W = -\int_0^\tau \dot{M}(t)x(t)dt \tag{2.23}$$

Above is nothing but the continuum version of the definition given in equation (2.2). We are interested in the moments of W. We will work in the highly damped limit where the inertial term in equation (2.22) can be dropped. For a quadratic $V(x)$ (linear system), we will prove equation (2.21) for an arbitrary $M(t)$ and then go on to show that equation (2.21) needs to be modified for arbitrary $V(x)$. The most significant finding is that, even for a symmetric $V(x)$,

the odd moments of $\Delta W = W - \langle W \rangle$ are non-vanishing and hence the distribution of ΔW is asymmetric for all non-quadratic $V(x)$. We will show this analytically, using perturbation theory; suggest a generalization of equation (2.21) and numerically establish that the probability distribution $P(\Delta W)$ is indeed asymmetric in general. It should be noted that an asymmetric work probability distribution has been obtained by various authors such as, Bena et.al [21], Cleuren et.al[22], Blickle et.al[23],Lua-Grosberg [11] etc. In all these cases the potential has been asymmetric. We will specializing the work with a symmetric potential (i.e. $V(x) = V(-x)$) and show that $P(W)$ is still asymmetric.

We begin with the linear harmonic oscillator under the action of a deterministic force $M(t)$ and random force $f(t)$. In the highly viscous limit with unit friction coefficient k, the system evolves according to

$$\dot{x} + \Gamma x = M(t) + f(t) \tag{2.24}$$

where the random force $f(t)$ has the correlation function

$$\langle f(t)f(t') \rangle = 2KT\delta(t - t') \tag{2.25}$$

We calculate the moments of the work done, from the above dynamics. The solution for $x(t)$ can be written down as

$$x(t) = \int G(t - t')[M(t') + f(t')]dt' \tag{2.26}$$

where $G(t - t')$ is the causal Green function,

$$G(t - t') = \Theta(t - t')e^{-\Gamma(t-t')} \tag{2.27}$$

Clearly, the average of the work is

$$\langle W \rangle = -\int^\tau dt_1 \dot{M}(t_1) \int^{t_1} G(t_1 - t_2)M(t_2)dt_2 \tag{2.28}$$

while, the deviation from the average is

$$\Delta W = W - \langle W \rangle = -\int^\tau dt_1 \dot{M}(t_1) \int^{t_1} G(t_1 - t_2)f(t_2)dt_2 \tag{2.29}$$

which has the mean square value of

$$\langle (\Delta W)^2 \rangle = 2KT \int^\tau dt_1 \dot{M}(t_1) \int^\tau dt_2 \dot{M}(t_2) \tag{2.30}$$

$$\int^{t_2} dt'' \int^{t_1} dt' G(t_1 - t')G(t_2 - t'')\delta(t' - t'')$$

where equation (2.25) has been used. Noting the identity, derived from the time translational invariance

$$\int_0^{t_2} G(t_2 - t'')G(t_1 - t'')dt'' = G(t_1 - t_2)/2\Gamma \tag{2.31}$$

we arrive at

$$\frac{\langle(\Delta W)^2\rangle}{2KT} = \frac{1}{\Gamma} \int^\tau dt_1 \dot{M}(t_1) \int_1^t dt_2 \dot{M}(t_2)G(t_1 - t_2) \tag{2.32}$$

Using the above and equation (2.28)

$$\langle W\rangle - \frac{\langle(\Delta W)^2\rangle}{2KT} = -\int^\tau dt_1 \dot{M}(t_1) \int_1^t dt_2 G(t_1 - t_2)[M(t_2) + \frac{\dot{M}(t_2)}{\Gamma}] \tag{2.33}$$

Integrating by parts the first term in the integral above and using $G(0) = 0$ due to causality, we find

$$\langle W\rangle - \frac{\langle(\Delta W)^2\rangle}{2KT} = -\frac{M^2}{2\Gamma} \tag{2.34}$$

The free energy change is precisely this amount, and that establishes equation (2.21) for an arbitrary forcing M(t).
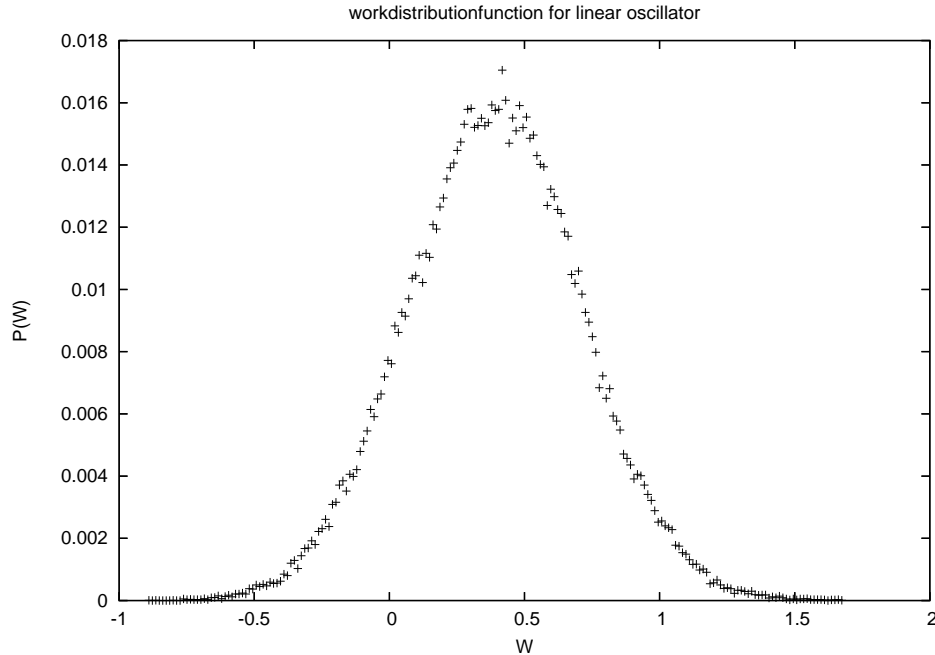
Figure 2.1: Work probability distribution for $\lambda = 0$. Note the symmetry of the distribution.
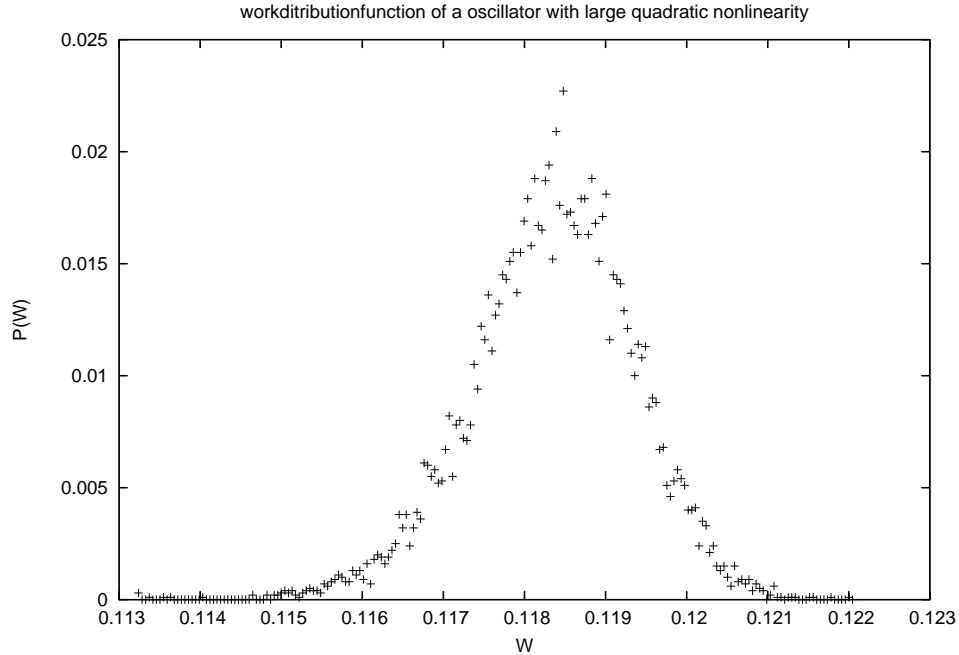
Figure 2.2: Work probability distribution for $\lambda = 20$. The tail in left side signifies the asymmetrical nature of the distribution here. Here $V(x) = (1/2)x^2 + (20/3)x^3$.

We now consider the inclusion of a non linear term in the motion, which becomes

$$\dot{x} + \Gamma x + \lambda x^3 = M(t) + f(t) \tag{2.35}$$

preserving the $x \rightarrow -x$ symmetry of $V(x)$ in equation (2.22). The question to ask is whether the equality in equation 2.21 still holds? To investigate this, we specialize to the case of $M(t) = M_0 t$ as studied by DCPR and carry out a perturbative calculation to $O(\lambda)$.

We write

$$x = x_0 + \lambda x_1 + \lambda^2 x_2 + ... \tag{2.36}$$

and substituting in equation (2.35) and equating the coefficients of equal powers of λ on either side we get

$$\dot{x}_0 + \Gamma x_0 \; = \; M(t) + f(t) \tag{2.37}$$
$$\dot{x}_1 + \Gamma x_1 \; = \; -x_0^3$$

workdistributionfunction of nonlinear oscillator with small cubic nonlinearity in restoring force
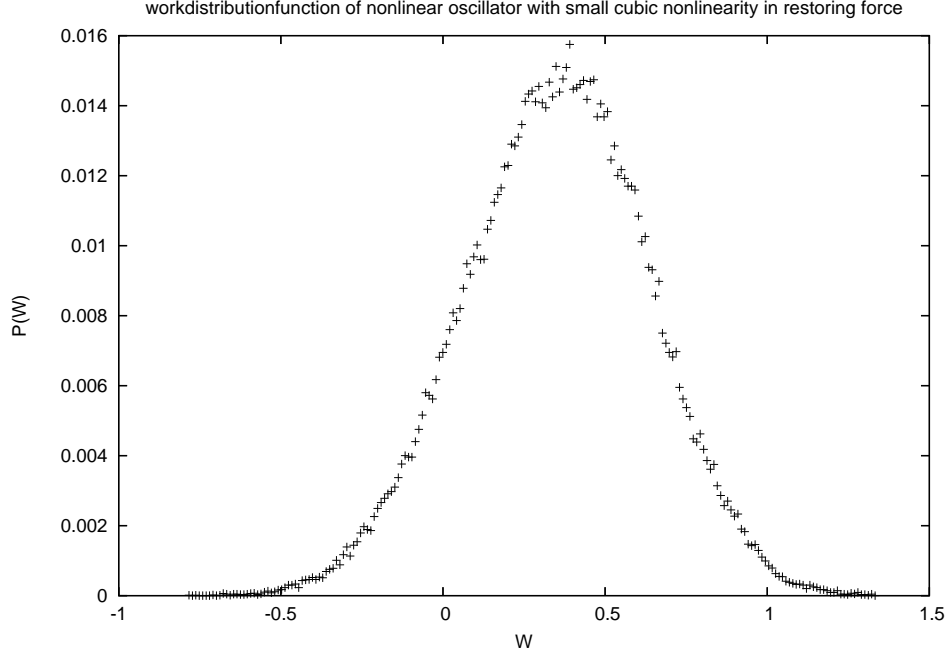
Figure 2.3: Work probability distribution for $\lambda = 0.1$. The tail in left side signifies the asymmetrical nature of the distribution here. Here $V(x) = (1/2)x^2 + (0.1/4)x^4$.

and so on. We can now expand $W(\tau)$ according to the equation (2.36),

$$W = W_0 + \lambda W_1 + ... \tag{2.38}$$

where

$$W_0 = -\int^\tau \dot{M}(t)x_0(t)dt \tag{2.39}$$

$$W_1 = -\int^\tau \dot{M}(t)x_1(t)dt$$

From equation (2.37) we get

$$x_0 = \int_0^t G(t-t')[M(t') + f(t')]dt' \tag{2.40}$$

$$x_1 = -\int_0^t G(t-t')x_0^3 dt'$$

We note that in the way we have set it up, $G(t_1 - t_2)$ is exactly the same G that we had for the linear problem. We have already calculated $\langle W_0 \rangle$ and now we concentrate on $\langle W_1 \rangle$. We write

$$\langle W_1 \rangle = \int^\tau \dot{M} dt \int^t dt' G(t-t') \left[\int^{t'} dt_1 G(t'-t_1)M(t_1)\right]^3$$

27
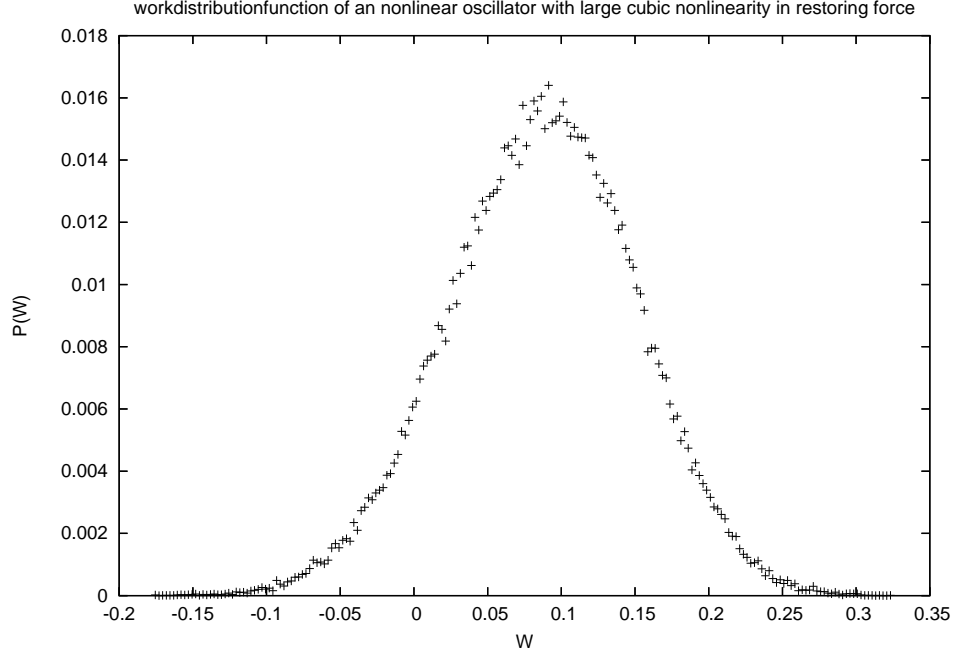
Figure 2.4: Work probability distribution for $\lambda = 20$. The symmetrical nature is due to dominance of $\langle (W - \langle W \rangle)^4 \rangle$ of the distribution here. Here $V(x) = (1/2)x^2 + (20/4)x^4$.

$$+ \quad 3 \int^{\tau} \dot{M} dt \int^{t} dt' G(t - t') \int^{t'} dt_1 dt_2 dt_3 \tag{2.41}$$
$$M(t_1) \quad G(t' - t_1) G(t' - t_2) G(t' - t_3) \langle f(t_2) f(t_3) \rangle$$

The second term in the r.h.s vanishes once we use equation (2.31) and causality. We are left with

$$\langle W_1 \rangle = \int^{\tau} \dot{M} dt \int^{t} dt' G(t - t') \left[\int^{t'} dt_1 G(t' - t_1) M(t_1) \right]^3 \tag{2.42}$$

We now use $M(t) = M_0 t$ and carry out the the integration to arrive at

$$\langle W_1 \rangle = \frac{M_0^4}{\Gamma^3} \left[\frac{\tau^4}{4\Gamma} - \frac{2\tau^3}{\Gamma^2} + \frac{15\tau^2}{2\Gamma^3} - \frac{16\tau}{\Gamma^4} \right], \tag{2.43}$$

keeping the leading order terms, i.e. terms which increase with τ.

Let us now turn to the calculation of the variance $\langle (W - \langle W \rangle)^2 \rangle$. The perturbative calculation generates the following upto $0(\lambda)$

$$\langle (\Delta W)^2 \rangle = \langle (\Delta W_0)^2 \rangle + 2\lambda \langle \Delta W_0 \Delta W_1 \rangle \tag{2.44}$$

Workdistributionfunction for linear (liny plot) and nonliear (with small cubic nonlinearity) oscillator (dotted plot)
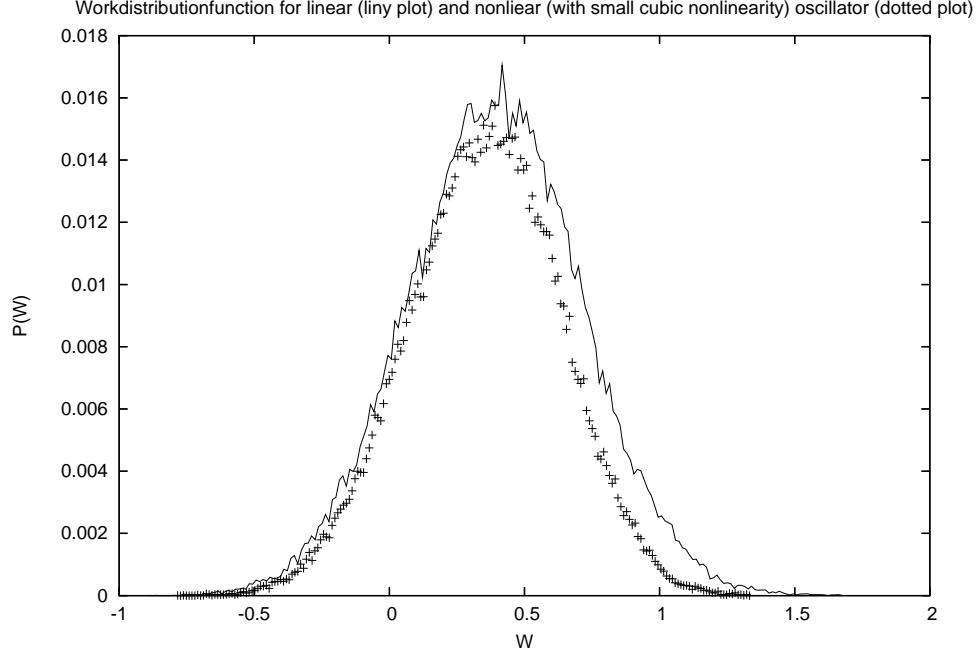
Figure 2.5: Work probability distributions for $V(x) = (1/2)x^2$ and $V(x) = (1/2)x^2 + (0.1/4)x^4$ are plotted above by line and dots respectively. The striking asymmetry in nonlinear case is clear here.

where $\Delta W_0 = W_0 - \langle W_0 \rangle$ and $\Delta W_1 = W_1 - \langle W_1 \rangle$. We have already calculated the first term in the r.h.s. Now we will concentrate on the second term. In the $O(\lambda)$ correction in the variance, we have found that the disconnected parts (i.e. where the averaging is over ΔW and ΔW_1 separately.) do not contribute. Specializing to the case $M(t) = M_0 t$, calculation leads to the $O(\lambda)$ term of the variance as,

$$0(\lambda) \ \ part \ \ of \frac{\langle (\Delta W)^2 \rangle}{2KT} = -\frac{M_0^4}{\Gamma^3} \left[\frac{2\tau^3}{\Gamma^2} - \frac{27\tau^2}{2\Gamma^3} + \frac{16\tau}{\Gamma^4} \right], \qquad (2.45)$$

keeping the leading order terms. Thus,

$$\langle W \rangle - \frac{\langle (\Delta W)^2 \rangle}{2KT} = \langle W_0 \rangle - \frac{\langle (\Delta W_0)^2 \rangle}{2KT} + \frac{\lambda M_0^4 \tau^4}{4\Gamma^4} - \frac{6\lambda M_0^4 \tau^2}{\Gamma^6} + O(\tau) \qquad (2.46)$$

Now, ΔF upto $O(\lambda)$ is $\Delta F_0 + \lambda \frac{M_0^4 \tau^4}{4\Gamma^4}$ and hence according to equation (2.46) the difference $\Delta F - \langle W \rangle + \frac{\langle (\Delta W)^2 \rangle}{2KT}$ shows up at $O(\tau^2)$. That $\Delta F \neq \langle W \rangle - \frac{\langle (\Delta W)^2 \rangle}{2KT}$ in this case is not surprising since the general result is given by equation (2.15). What is noteworthy is that in

29
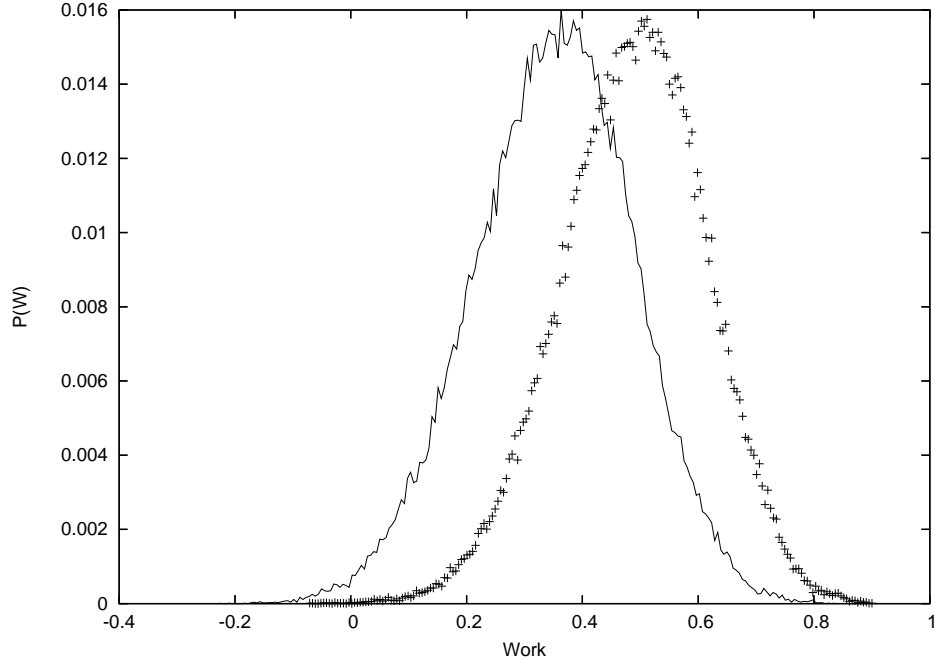
Figure 2.6: For $\lambda = 0.5$, the line-plot of the work distribution function is for forward process and other one (dotted plot)is for backward process. Work corresponding to their crossing point gives the free energy difference precisely.

the dynamics with $V(x) = V(-x)$, the work distribution is not symmetric about $\langle W \rangle$. To find a convenient modification of equation (2.21), we return to equation (2.15) starting with a work probability distribution $P(W)$ of the form,

$$P(W) \propto e^{[-\frac{(W-W_0)^2}{2\sigma^2} - \frac{\mu_1(W-W_0)^3}{\sigma^3} - \frac{\mu_2(W-W_0)^4}{\sigma^4}]} \tag{2.47}$$

where μ_1, μ_2 and σ are parameters, arrive at the cumulant expansion

$$\Delta F = \langle W \rangle - \frac{\langle (W - \langle W \rangle)^2 \rangle}{2KT} + \frac{\langle (W - \langle W \rangle)^3 \rangle}{6(KT)^2} \tag{2.48}$$
$$+ \frac{1}{24} \left[\frac{3 \langle (W - \langle W \rangle)^2 \rangle^2 - \langle (W - \langle W \rangle)^4 \rangle}{(KT)^3} \right]$$

assuming small departure from Guassian behaviour. The immediate question is whether the dynamics generates $\langle (\Delta W)^3 \rangle$. We note that if it does not, then the symmetric correction to

the Guassian distribution- the flatness factor, proportional to $\Xi = -[\langle (\Delta W)^4 \rangle - 3 \langle (\Delta W)^2 \rangle^2]$ would not be able to satisfy the Jarzynski Equality since the dynamics yields for this term a leading behaviour proportional to τ, while the leading discrepancy is at $O(\tau^2)$. This correction can only come from $\langle (\Delta W)^3 \rangle$. Within perturbation theory, we note that to the leading order,

$$\langle (\Delta W)^3 \rangle = 3\lambda \langle (\Delta W_0)^2 (\Delta W_1) \rangle \tag{2.49}$$

and a cursory inspection of the solution of the equation of motion shows that $\langle (\Delta W)^3 \rangle$ is nonzero and the leading order term is indeed $O(\tau^2)$.

To test equation (2.48) numerically, we decided to work first with the quadratic nonlinearity in equation of motion,

$$\dot{x} + \Gamma x + \lambda x^2 = M(t) + f(t) \tag{2.50}$$

We will restrict ourselves to those values of λ (with $\Gamma = 1$), that the trajectory does not run away. In this case, it is the cubic deviation which is the most significant and that would imply an asymmetric probability distribution for the work W. This is not unexpected since the potential for equation (2.50) is cubic and hence asymmetric. We have taken,

$$
\begin{aligned}
M(t) &= 0 & t = 0 \\
&= M_0 t & 0 < t < \tau \\
&= M_0 \tau & t \geq \tau
\end{aligned}
\tag{2.51}
$$

In between the interval τ we generate the values of x at different points by the following,

$$x(t + \Delta t) = x(t) - (x(t) + \lambda x^2(t))\Delta t + M(t)\Delta t + \sqrt{2KT\Delta t}\eta(t) \tag{2.52}$$

where $\eta(t)$ is a random number between 0 and 1. We calculate all the quantities in the unit of $2KT$. We calculate a trajectory $[x(t)]_\tau$ starting from an initial value and evaluate the work according to equation (2.23). The ensemble is one of initial conditions $x(0)$ and we calculate $\langle W \rangle$, $\langle (\Delta W)^2 \rangle$, $\langle (\Delta W)^3 \rangle$.

λ	$-\langle W \rangle$	$\dfrac{\langle (\Delta W)^2 \rangle}{2K_B T}$	$\dfrac{\langle (\Delta W)^3 \rangle}{6(K_B T)^2}$
0.3	0.357	0.078	-0.003
1.0	0.304	0.052	-0.005

2 Work Fluctuation Theorems And Work Distribution Function

We have also found the work distribution function $P(W)$. For $\lambda = 0$ (i.e. the system with quadratic potential) and for $\lambda = 20$ the distributions are shown in figures (2.1) and (2.2) respectively. For nonzero λ the distribution is asymmetric, which is expected for an asymmetric potential.

We repeated the numerics with quartic oscillator (i.e. $V(x) = \frac{1}{2}x^2 + \frac{\lambda}{4}x^4$) and found that $\langle(\Delta W)^3\rangle$ is certainly nonzero, indicating an asymmetric distribution. For small values of λ, the asymmetry is striking. For large values of λ due to dominating $\langle(\Delta W)^4\rangle$ the distribution becomes sharply peaked, and the asymmetry is difficult to make out, although its existence is guaranteed by the nonzero value of $\langle(\Delta W)^3\rangle$. The distribution for $\lambda = 0.1$ and $\lambda = 20$ is shown in figure (2.3) and (2.4) respectively. In figure(2.5) comparison between the work distribution functions for the cases when $\lambda = 0.1$ and $\lambda = 0$ are shown by plotting together. The asymmetry is clear from it. Recently Mai and Dhar [24]have found an asymmetric distribution for $V(x) = ax^2 + bx^3 + cx^4$. Our contention is that the asymmetry exists even if $b = 0$. First, we have to calculate F by the following

$$F = -KT \left[\ln \int \exp[-\beta(\frac{1}{2}x^2 + \frac{\lambda}{4}x^4 - Mx)]dx\right] \tag{2.53}$$

We have calculated ΔF using equation (2.53) at $t = 0$ and $t = \tau$, exactly. Then after calculating required moments from the work probability distribution obtained, and using equation (2.48), we have calculated ΔF again, which matches well with the previous one. Here we tabulate the numerical results in units of KT for $\lambda = 0.3$, $\lambda = 0.5$, $\lambda = 1$ to show how equation (2.48) works.

λ	ΔF(from equation (2.53))	$-\langle W\rangle$	$\frac{\langle(\Delta W)^2\rangle}{2K_BT}$	$\frac{\langle(\Delta W)^3\rangle}{6(K_BT)^2}$	$\frac{1}{24}\left[\frac{\Xi}{(KT)^3}\right]$	ΔF(from equation (2.48))
0.5	0.4301	0.361	0.077	-0.006	-0.002	0.430
0.3	0.4499	0.373	0.085	-0.007	-0.001	0.450
1.0	0.4010	0.339	0.065	-0.004	-0.006	0.394

Now we will verify Crooks' identity given in equation(2.14). A very important check on the accuracy of our numerical work can be obtained if we try to verify Crooks theorem for our data. Here we will verify this at $\lambda = 0.5$. To verify the theorem we will use the fact that, at the

crossing point of the two probability distributions, that is the point where $P_F(W_F) = P_R(W_R)$, W_F is precisely ΔF. From figure (2.6) it is clear that, work at the crossing point, matches well with the corresponding free energy difference from the table.

We can also point out a possible application. We consider a ferromagnet or an Ising magnet near but above its critical point T_c. We can imagine being close to T_c, but sufficiently far away so that the mean field Landau model is valid. If we now switch on an time dependent magnetic field, then the dynamics of the mean magnetisation will be given by an equation of the form shown by equation (2.35). If we are in the region $T < T_c$, then the dynamics will be governed by equation (2.35) with an added quadratic nonlinearity. It will be interesting to check the veracity of equation (2.48) in this case.

2.3 Summary

In this chapter we have proved work fluctuation theorems for the systems evolving via Markov chains and we show, both analytically and numerically, that for a nonlinear system making a transition from one equilibrium state to another under the action of an external time dependent force, the work probability distribution is in general asymmetric, even if the evolution dynamics has a symmetry.

Bibliography

[1] G.E.Crooks Phys. Rev. E **60**, 2721 (1999)

[2] G.E.Crooks Phys. Rev. E **61**, 2361 (2000)

[3] C.Jarzynski Phys. Rev. Lett. **78**, 2690 (1997)

[4] C.Jarzynski Phys. Rev. E **56**, 5018 (1997)

[5] C.Jarzynski J. Stat. Phys. **98**, 77 (2000)

[6] J. R. Norris, Markov Chains. Cambridge University Press, 1997.

[7] J. Liphardt, S. Dumont, S. Smith, I. Tinoco, and C. Busta-mante, Science **296**, 1832 (2002).

[8] S. R. de Groot and P. Mazur, Nonequilibrium Thermodynamics (North-Holland, Amsterdam, 1962).

[9] D. Chandler, Introduction to Modern Statistical Mechanics (Oxford University Press, New York, 1987), pp. 165.

[10] P. C. G. Vassiliou, The evolution of the theory of non-homogeneous Markov systems Appl. Stoch. Model. D. A. 13, 59176 (1997).

[11] R. C. Lua and A. Y. Grosberg, J. Phys. Chem. B **109**, 6805, 2005

[12] Shi-Qing Wang, Phys. Rev. A 40 2137 1989

Bibliography

[13] T. G. Mason1,2 and D. A. Weitz1 Phys. Rev. Lett. **74**, , (1250) 1995

[14] F.Douarche, S.Ciliberto, A.Patrosyan I.Rabbiosi Europhys. Lett. **70**, 593 (2005)

[15] F.Douarche, S.Ciliberto, A.Petrosyan J. Stat. Mech. **P09011** 28 2005

[16] Hermans J. Chem. Phys. **95** 1991 9029

[17] Ritort Poincare Seminar **2** 2003 195

[18] Gore et al. PNAS **100** 2003 12564

[19] Park-Schulten J. Chem. Phys. **120** 2004 5946

[20] Statistical Physics by L. D. Landau and E. M. Lifshitz Pergamon Press 1959

[21] Bena et.al EuroPhys. Lett. **71** 2005 879

[22] Cleuren et.al Phys. Rev. Lett. **96**, 2006 (050601)

[23] Blickle et.al Phys. Rev. Lett. **96**, 2006 (070603)

[24] Mai T and Dhar A Phys. Rev. E **75**, 061101 (2007)

3 Work Fluctuation Theorems Vs. Bohr-van Leeuwen Theorem: Part(I)

In this chapter we will study the dynamics of a trapped, charged Brownian particle in the presence of a time-dependent magnetic field. We will calculate work distributions for different time-dependent protocols numerically. In our problem, thermodynamic work is related to variation of the vector potential with time as opposed to the case in previous chapter where the work is related to time variation of the scaler potential, a quantity that depends only on the coordinates of the particle. Using the Jarzynski and the Crooks equalities, we will show that the free energy of the particle is independent of the magnetic field, thus complementing the Bohr-van Leeuwen theorem. We also show that our system exhibits a parametric resonance in a certain parameter space.

3.1 Work fluctuation theorems and Bohr-van Leeuwen theorem

Equilibrium statistical mechanics provides us an elegant framework to explain properties of a broad variety of systems in equilibrium. Close to equilibrium the linear response formalism is very successful in the form of fluctuation-dissipation theorem and Onsager's reciprocity relations. But no such universal framework exists to study systems driven far away from equilibrium. Needless to say that the most processes that occur in nature are far from equilibrium.

3 Work Fluctuation Theorems Vs. Bohr-van Leeuwen Theorem: Part(I)

In recent years there has been considerable interest in the nonequilibrium statistical mechanics of small systems. This has led to discovery of several rigorous theorems, called fluctuation theorems (FT) and related equalities [1, 2, 3, 4, 5, 6, 7, 8, 9, 10, 11] for systems far away from equilibrium. Some of these theorems have been verified experimentally [12, 13, 14, 15, 16] on single nanosystems in physical environment where fluctuations play a dominant role. We will focus on the Jarzynski identity [4] and Crooks' equality [5] which deal with systems which are initially in thermal equilibrium and are driven far away from equilibrium irreversibly. Jarzynski identity relates the free energy change(ΔF) of the system when it is driven out of equilibrium by perturbing its Hamiltonian (H_λ) by an externally controlled time dependent protocol $\lambda(t)$, to the thermodynamic work (W) done on the system, given by

$$W = \int_0^\tau \dot{\lambda} \frac{\partial H_\lambda}{\partial \lambda} dt, \tag{3.1}$$

over a phase space trajectory. Here τ is the time through which the system is driven. Jarzynski identity is,

$$\left\langle e^{-\beta W} \right\rangle = e^{-\beta \Delta F}. \tag{3.2}$$

Crooks' equality relates the ratio of the work distributions in forward and backward (time reversed) paths through which the system evolves. This relation is given by,

$$\frac{P_f(W)}{P_b(-W)} = e^{\beta W_d}, \tag{3.3}$$

where, P_f and P_b are the distributions of work along forward and backward paths respectively. Here, the dissipative work $W_d = W - W_r$ and W_r is the reversible work which is same as the free energy difference (ΔF) between the initial and the final states of the system when driven through a reversible, isothermal path. If the system is driven reversibly all along the path, the work distribution will be $\delta(W - \Delta F)$, $W_d = 0$ and $P_f = P_b$. Thus, the above identities are trivially true for reversibly driven system. Jarzynski identity follows from equation (3.3). Crooks relation follows from a more general Crooks identity which relates ratio of work probabilities of forward path and that of the reverse path to the dissipative work expended along the forward trajectory. Both of the above relations are proved in the previous chapter.

In this chapter we will study the applicability of Jarzynski identity and Crooks equality in case of velocity dependent as well as time dependent Lorentz force which is derivable from a generalised potential, $U = q(\phi - \mathbf{A}(t).\mathbf{v})$. Here, $\mathbf{A}$ is time dependent vector potential, ϕ is scalar potential, q is the charge of a particle and $\mathbf{v}$ is its velocity. Different time dependent protocols for magnetic fields are considered. Consequently, we find that, the free energy difference obtained using Jarzynski and Crooks equality complements Bohr-van Leeuwen theorem [17, 18, 19]. This theorem states that in case of classical systems the free energy is independent of magnetic field and hence the theorem concludes absence of diamagnetism in classical thermodynamical equilibrium systems. For completeness a proof of Bohr-van Leeuwen theorem is given in appendix A. We finally show that our system, in presence of ac magnetic field exhibits parametric resonance in certain parameter regime. In presence of dynamical instabilities the nature of the distributions of various path dependent thermodynamic functions like work, heat etc are interesting issues which we will not discuss in this thesis.

In an earlier related work [19, 20] a charged particle dynamics in overdamped limit is studied in the presence of harmonic trap and static magnetic field. The work distribution have been obtained analytically for different protocols. It is shown that work distribution depends explicitly on the magnetic field but not the free energy difference (ΔF).

3.2 Model

The model Hamiltonian for our isolated system is,

$$H = \frac{1}{2m}\left[\left(p_x + \frac{qB(t)y}{2}\right)^2 + \left(p_y - \frac{qB(t)x}{2}\right)^2\right] + \frac{1}{2}k(x^2 + y^2), \qquad (3.4)$$

where k is the stiffness constant of harmonic confinement. The magnetic field $B(t)$ is applied in the z direction. The x and y components of the vector potential, A_x A_y are given by $-\frac{qB(t)y}{2}$ and $\frac{qB(t)x}{2}$ respectively. We have chosen symmetric guage here. The particle-environment interaction is modeled via Langevin equation including inertia [21], namely,

$$m\ddot{x} = \frac{q}{2}\left[y\dot{B}(t) + 2\dot{y}B(t)\right] - kx - \Gamma\dot{x} + \eta_x(t), \tag{3.5}$$

$$m\ddot{y} = -\frac{q}{2}\left[x\dot{B}(t) + 2\dot{x}B(t)\right] - ky - \Gamma\dot{y} + \eta_y(t), \tag{3.6}$$

where Γ is the friction coefficient and η_x and η_y are the Gaussian white noise along x and y direction respectively. This thermal noise has the following properties,

$$< \eta_i >= 0; < \eta_i(t)\eta_j(t') >= \delta_{ij}2\Gamma k_B T\delta(t - t'). \tag{3.7}$$

With the above prescription for the thermal noise, the system approaches a unique equilibrium state in the absence of time dependent potentials. Denoting the protocol $\lambda(t) = \frac{q}{2}B(t)$ the thermodynamic work done by external magnetic field on the system upto time τ is,

$$W = -\frac{q}{2}\int_0^\tau (x\dot{y} - y\dot{x})\dot{B}(t)dt. \tag{3.8}$$

We will like to emphasize that this thermodynamic work is related to the time variation of the vector potential and can be identified as time variation of magnetic potential $-\mu.\mathbf{B}$, $W = -\int_0^\tau \mu.\frac{d\mathbf{B}}{dt}dt$, where induced magnetic moment is $\frac{q}{2}(x\dot{y}-y\dot{x}) = \frac{q}{2}(\mathbf{r}\times\mathbf{v})$. To obtain value of work and its distribution, we have solved equation (3.5) and (3.6) numerically using verlet algorithm [22]. We first evolve the system upto a large time greater than the typical relaxation time so that the system is in equilibrium and then apply a time dependent protocol for the magnetic field. We have calculated values of the work for 10^5 different realisations to get better statistics. The values of work obtained for different realisations can be viewed as random samples from the probability distributions $P(W)$. We have fixed friction coefficient, mass, charge and $k_B T$ to be unity. All the physical parameters are taken in dimensionless units.

3.3 Results and discussions

First we have taken magnetic field to vary linearly in time, i.e., $\mathbf{B} = \mathbf{B_0}\frac{t}{\tau}\hat{\mathbf{z}}$. Work distributions for both forward and backward protocols are obtained. In figure (3.1) we have plotted the distributions $P_f(W)$ and $P_b(-W)$, for forward and backward protocol respectively, which are

depicted in the insets of figure (3.1). Using Jarzynski identity (equation (3.2)) we have computed
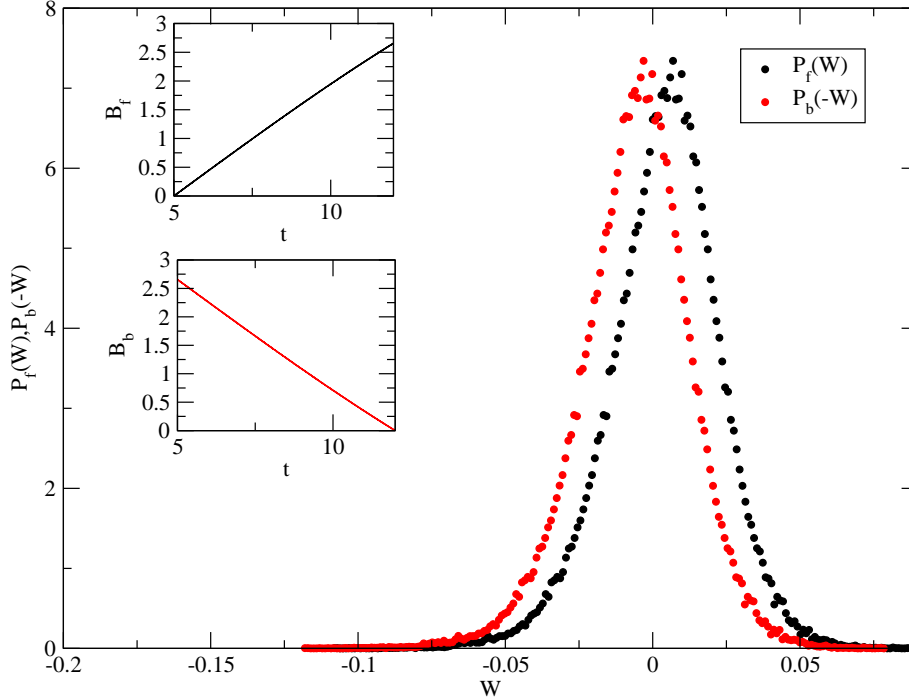
Figure 3.1: Forward $P_f(W)$ and backward work probability distribution $P_b(-W)$ for a ramp magnetic field.

free energy difference ΔF. We have obtained $\left\langle e^{-\beta W} \right\rangle$ to be unity (1.0 ± 0.04) implying $\Delta F = 0$. It may be noted that $\Delta F = F(B) - F(0)$, where B is the value of the field at the end of the protocol. In the beginning of the protocol, the value of B is zero. For different values of final magnetic field we have obtained $\Delta F = 0$ within our numerical accuracy. This implies that free energy itself (and not the free energy difference) is independent of the magnetic field, thereby satisfying the Bohr-van Leeuwen theorem as stated earlier. We can also employ Crooks' equality (equation (3.3) to determine the free energy difference. It follows from Crooks' equality that P_f and P_b distributions cross at value $W = \Delta F$. This value, where the two distributions cross each other (that is, $W = 0$), can be readily inferred from figure (3.1). This again suggests that, $\Delta F = 0$ which is consistent with the result obtained using Jarzynski identity.

To strengthen our assertion (that is, the free energy being independent of magnetic field) further in figure (3.2) and (3.3) we have plotted $P_f(W)$ and $P_b(-W)$ for two other different protocols as shown in insets of corresponding figures. For figure (3.3) we have considered sinusoidally varying magnetic field $B = B_1 \sin \omega t$ in z direction. From the crossing point of P_f and P_b we observe that $\Delta F = 0$, consistent with earlier result.

In figure (3.4) we have plotted $P_f(W)$ and $P_b(-W)e^{\beta W_d}$, corresponding to the protocol
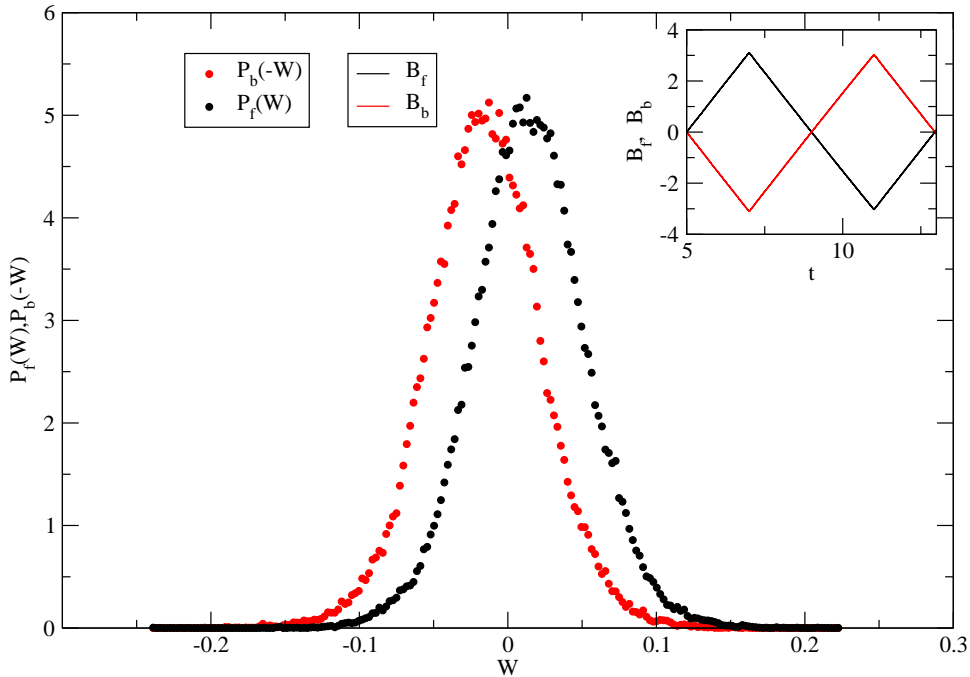
Figure 3.2: $P_f(W)$ and $P_b(-W)$ for symmetric ramp for B(t).

shown in figure (3.3). Both the graphs fall on each other (within numerical error), thus verifying Crooks' equality. It may be noted that reverse protocol also implies reversing the magnetic field [23]. In all our figures the distribution of work is asymmetric and depends on the magnetic field protocol explicitly as opposed to ΔF. Moreover, all the distributions show significant tail in the negative work region. This is necessary so as to satisfy Jarzynski identity.

We now discuss briefly the occurrence of parametric resonance [24] in our system in presence of sinusoidally oscillating magnetic field $B(t) = B_1 \sin \omega t$. In the parameter range $\frac{q_1 B_1}{4\sqrt{2L_1}} - \Gamma_1 > 0$
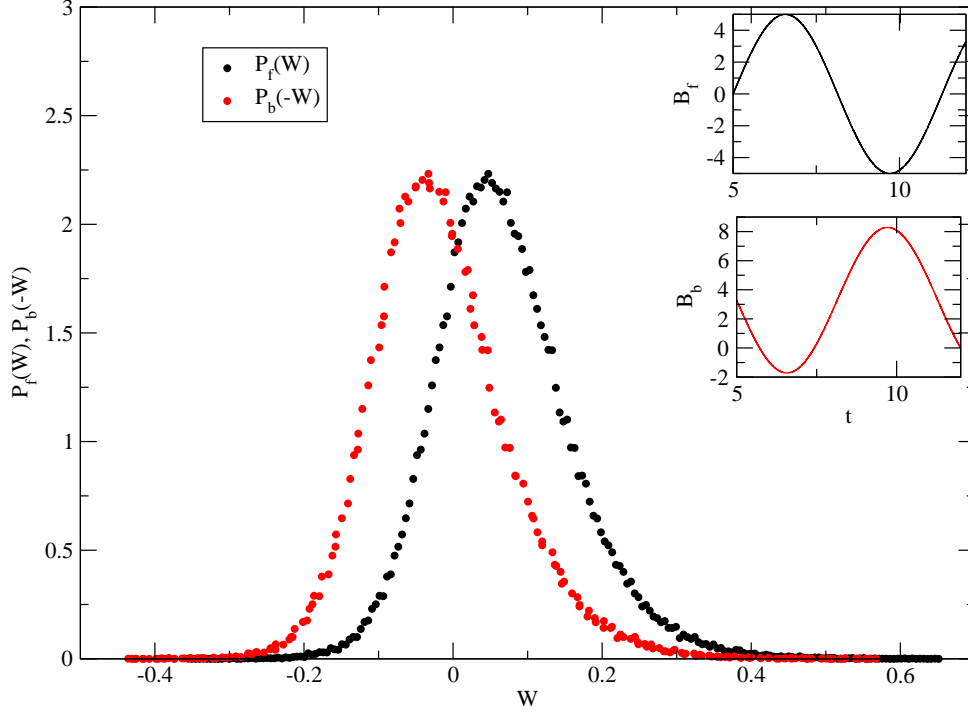
Figure 3.3: $P_f(W)$ and $P_b(-W)$ for oscillatory magnetic field

where $L_1 = 1 + \frac{2(k_1 - \Gamma_1^2)}{q_1^2 B_1^2}$ (see Appendix B), our system exhibits instability. Here $k_1 = \frac{k}{m}$, $\Gamma_1 = \frac{\Gamma}{2m}$ and $q_1 = \frac{q}{2m}$. The external parametric magnetic field injects energy into the system and this pumping is expected to be strongest near twice the systems frequency ($\sqrt{L_1}$). The trajectory of the Brownian particle grows exponentially in time also exhibiting oscillatory motion at twice the frequency of external magnetic field. This is shown in figure (3.5), where the coordinates of the particle and the protocol are plotted as a function of time. The parameters are $B_1 = 60$ and $\omega = 1$. For these graphs noise strength $k_B T$ is taken as one. In presence of this instability (large variation in coordinate values) it becomes difficult to calculate work distributions as it requires large number of realisations and better accuracy. One should also take care about the energy of the system so that it remains finite while computing the work along the path when the system is instable. Because if the energy becomes very large the microscopic reversibility condition will be under threat. Further work in analysing the nature of the parametric resonance and other instabilities in context to the work distributions is in progress.
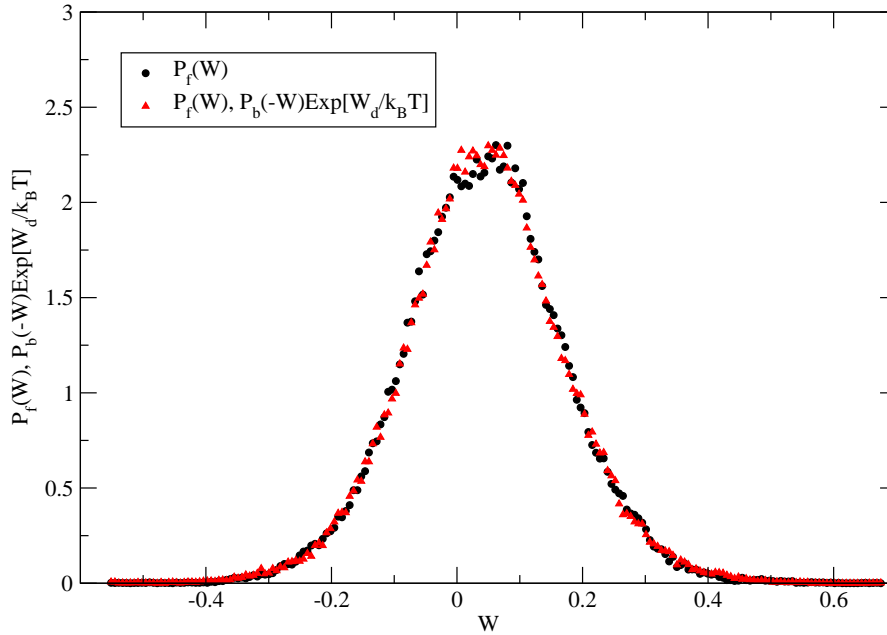
Figure 3.4: $P_f(W)$ and $P_b(-W)e^{\beta W_d}$ are plotted together.

3.4 Summary

In conclusion, by considering the dynamics of a trapped charged Brownian particle in a time dependent magnetic field we have verified Jarzynski identity and Crooks' equality. As a by product our result complements Bohr-van Leeuwen theorem. Work done on the system by external field arises due to the time variation of vector potential. This is in contrast to earlier studied models where the input energy to the system comes from time variation of the coordinate dependent potentials. Finally, we have discussed very briefly the occurrence of parametric resonance in our system. Our results are amenable to experimental verification.
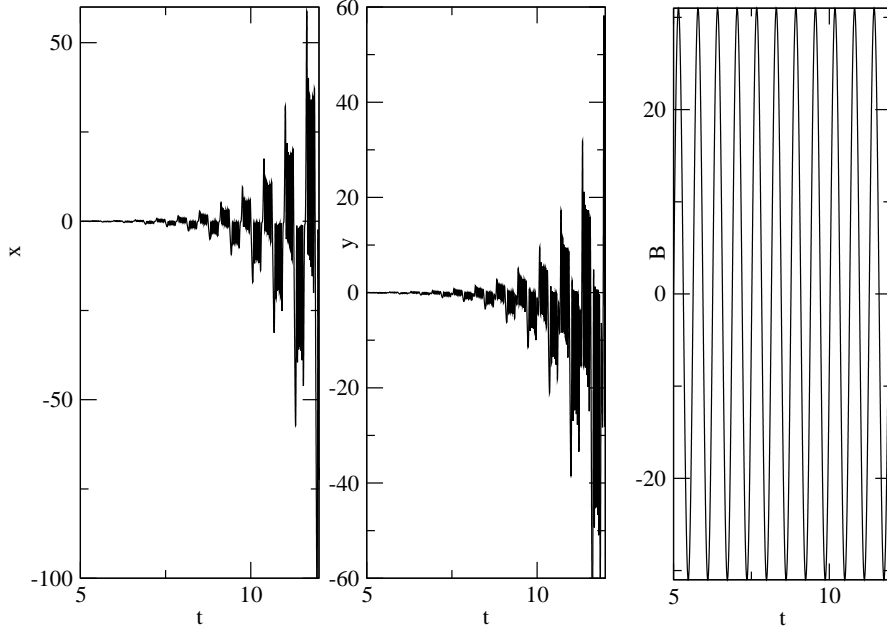
Figure 3.5: x and y Coordinates of the particle and the $B(t)$ are plotted as a function of time.

3.5 Appendix A

Proof Of Bohr-van Leeuwen Theorem:- N number of charged particles at temperature T interacting through a potential V is considered, so that, we can write a Hamiltonian of the system as,

$$H(\mathbf{P_i}, \mathbf{r_i}) = \sum_i \frac{\mathbf{P_i^2}}{2m_i} + V(\{\mathbf{r_i}\}) \qquad (\mathbf{A1})$$

where i is the particle index and $\mathbf{P_i}$ and $\mathbf{r_i}$ are the canonically conjugate momenta and coordinates of the particles. The corresponding partition function is (with usual notation)

$$Z = \sum_{allstates} e^{-\beta H(\mathbf{P_i}, \mathbf{r_i})} = \int_{all P_i, r_i} e^{-\beta H(\mathbf{P_i}, \mathbf{r_i})} \prod_i d\mathbf{P_i} d\mathbf{r_i}. \qquad (A2)$$

The free energy is

$$F = -K_B T \ln Z \qquad (A3)$$

Now a static magnetic field $\mathbf{B}(\mathbf{r_i})$, is applied to the system. So, the new Hamiltonian becomes

$$H_1(\mathbf{P_i}, \mathbf{r_i}) = \sum_i \frac{1}{2m_i}(\mathbf{P_i} - \mathbf{q_i}\mathbf{A}(\{\mathbf{r_i}\}))^2 + \mathbf{V}(\{\mathbf{r_i}\}) \qquad (\mathbf{A4})$$

where, $\mathbf{A}$ is the corresponding vector potential. Here, the new partition function is

$$Z_1 = \int_{allP_i, r_i} e^{-\beta H_1(\mathbf{P_i}, \mathbf{r_i})} \prod_i d\mathbf{P_i}d\mathbf{r_i} \qquad (A5)$$

Now, we transform the variables as

$$\mathbf{P_i} \to \mathbf{P'_i} = \mathbf{P_i} - \mathbf{q_i}\mathbf{A}(\{\mathbf{r_i}\}) \qquad (\mathbf{A6})$$

and

$$\mathbf{r_i} \to \mathbf{r'_i} = \mathbf{r_i} \qquad (A7)$$

Clearly, the Jacobian of the transformation is unity. Hence,

$$\prod_i d\mathbf{P'_i}d\mathbf{r'_i} = \prod_i d\mathbf{P_i}d\mathbf{r_i} \qquad (A8)$$

Thus, the new partition function with static magnetic field (Z_1) is same as the older one without magnetic field (Z), and hence,

$$F_{without\mathbf{B}} = -K_BT\ln Z = -K_BT\ln Z_1 = F_{with\mathbf{B}} \qquad (A9)$$

where, F is the free energy of the system and K_B is the Boltzmann constant. So, the difference between the free energies with and without magnetic field is given by

$$\Delta F = 0 \qquad (A10)$$

The obvious consequence of the above analysis is Bohr-van Leeuwen theorem, according to which, within the domain of classical statistical mechanics the magnetic susceptibility is zero.

3.6 Appendix B

Occurrence of parametric resonance in our system:- In presence of oscillatory magnetic field $B(t) = B_1 \sin \omega t$, the mean values of coordinates $< x >$, $< y >$ of the particle (averaged over thermal noise) obey the following equation for $z = < x > + i < y >$

$$m\ddot{z} + (\Gamma + iqB_1 \sin \omega t)\dot{z} + (k + i\frac{qB_1\omega}{2}\cos \omega t)z = 0 \quad (B1),$$

With $k = mk_1$, $\Gamma = m\Gamma'$, $q = mq'$ the above equation becomes

$$\ddot{z} + (\Gamma' + iq'B_1 \sin \omega t)\dot{z} + (k_1 + i\frac{q'B_1\omega}{2}\cos \omega t)z = 0 \quad (B2).$$

Now, using the following transformation,

$$z(t) = \xi(t)\exp[-\frac{1}{2}\int^t (\Gamma' + iq'B_1 \sin \omega t)dt], \qquad (B3)$$

equation (A2) becomes

$$\ddot{\xi} + [k_1 - \frac{1}{4}(\Gamma' + iq'B_1 \sin \omega t)^2]\xi = 0. \qquad (B4)$$

Redefining Γ' and q' as $\Gamma_1 = \Gamma'/2$ and $q_1 = q'/2$ we get,

$$\ddot{\xi} + [k_1 - (\Gamma_1 + iq_1B_1 \sin \omega t)^2]\xi = 0. \qquad (B5)$$

Again after transforming t as $t = \frac{\sqrt{2}t_1}{q_1B_1} - \frac{\pi}{2\omega}$ and ω as $\omega = \frac{\omega_1 q_1 B_1}{\sqrt{2}}$ we get,

$$\frac{d^2\xi}{dt_1^2} + [L_1 + \cos 2\omega_1 t_1 + i\epsilon \cos \omega_1 t_1]\xi = 0, \qquad (B6)$$

where, $L_1 = 1 + \frac{2(k_1 - \Gamma_1^2)}{q_1^2 B_1^2}$ and $\epsilon = \frac{4\Gamma_1}{q_1 B_1}$. For large B_1, ϵ is a small parameter and hence $i\epsilon \cos \omega_1 t_1$ can be treated as perturbative term as long as ω_1 is far from $2\sqrt{L_1}$. The condition $L_1 > 1$ should be maintained. Thus ξ can be expanded as $\xi = \xi_0 + \epsilon\xi_1 + ...$ Using this in equation(A6), we get (keeping only ϵ^0 order term),

$$\frac{d^2\xi_0}{dt_1^2} + [L_1 + \cos 2\omega_1 t_1]\xi_0 = 0. \qquad (B7)$$

The above equation exhibits parametric resonance [24]when $\omega_1 \approx \sqrt{L_1}$. Near resonating frequency, ξ_0 goes as $\xi_0 \sim e^{st_1}$, where $s \approx \frac{1}{4\sqrt{L_1}}$. Hence, z will grow exponentially, if $st_1 - \Gamma_1 t > 0$, i.e., $\frac{q_1 B_1}{4\sqrt{2L_1}}(t + \frac{\pi}{2\omega}) - \Gamma_1 t > 0$.The condition given above can be maintained if $\frac{q_1 B_1}{4\sqrt{2L_1}} - \Gamma_1 \geq 0$. For small amplitude of magnetic field, the trajectories of the particles is stable.

Bibliography

[1] C. Bustamante, J.Liphardt and F. Ritort Physics Today 58 45 2005

[2] R. J. Harris and G. M. Scuetz, cond-mat/0702553

[3] D. J. Evans and D. J. Searles Adv.Phys. 51 1529 2002

[4] C. Jarzynski Phys. Rev. Lett. **78**, 2690 (1997);C. Jarzynski Phys. Rev. E **56**, 5018 (1997)

[5] G.E.Crooks Phys. Rev. E **60**, 2721 (1999); G.E.Crooks Phys. Rev. E **61**, 2361 (2000)

[6] F. Hatano and S. Sasa, Phys. Rev. Lett. **86**, 3463 (2000)

[7] W. Letchner et.al, J. Chem. Phys. 124, 044113 (2006); G Hummer and A. Szabo, Proc. Natl.Acad. Sci. 98 3658 2001

[8] R. van Zon and E. G. D. Cohen, Phys. Rev. E **67**, 046102 (2002); Phys. Rev. E **69**, 056121 (2004)

[9] U. Seifert. Phys. Rev. Lett. **95**, 040602 (2005)

[10] J. J. Kurchan Phys.A 31 3719 1998

[11] O. Narayan and A. Dhar J. Phys. A 37 63 2004

[12] J. Liphardt et.al., Sciences 296,1832 (2002)

[13] F.Douarche, S.Ciliberto, A. Patrosyan I. Rabbiosi Europhys. Lett. **70**, 593 (2005)

[14] D. Collin et.al., Nature 437, 231 (2005)

Bibliography

[15] V. Bickle et.al. Phys. Rev. Lett. **96**, 07063 (2006)

[16] C. Tietz, et.al. Phys. Rev. Lett. **97**, 050602 (2006)

[17] N. Bohr, Dissertation, Copenhegen (1911); J. H. van Leewen, J. Phys. 2 3619 1921; R. E. Peierls, Surprises in theoretical Physics (Princeton University Press, Princeton,1979)

[18] A. M. Jayannavar and N. Kumar, J. Phys. A 14 1399 1981

[19] A.M.Jayannavar and Mamata. Sahoo Phys. Rev. E **75**, 032102 (2007)

[20] A.M.Jayannavar and Mamata. Sahoo, Cond-mat 0704.2992

[21] H. Risken, The Fokker Planck Equation, Springer Verlag, Berlin,1984.

[22] Understanding Molecular Simulation D.Frankel, B.Smit Academic Press (1996)

[23] V. Y. Chernyak, M. Chertkov and C. Jarzynski J. Stat. Mech Theory and Experiment P08001 (2006)

[24] L.D.Landau and E.M.Lifshitz, in Mechanics, Course of Theoretical Physics Vol. 1 (Pergamon, Oxford, England, 1976)

4 Work Fluctuation Theorems Vs. Bohr-van Leeuwen Theorem: Part(II)

4.1 Classical diamagnetism: Two dimensional infinite plane

The Gibbsian approach to equilibrium statistical mechanics forbids the presence of a finite magnetic moment (M_{eq}) in a classical system at canonical equilibrium. This result was proved by Bohr in his PhD thesis [1] and also by van Leeuwen in a now classic paper [2]. The obvious consequence of this well known result, now called Bohr-van Leeuwen (BvL) theorem [3, 4, 5, 6, 7, 8], is the nonexistence of orbital diamagnetism in such a system in general. The essential point of the proof of the theorem (given also in the previous chapter) is that the partition function becomes independent of the magnetic field implying vanishing susceptibility, and hence the absence of the diamagnetism. This can readily be seen by recalling that the magnetic field $\mathbf{B}$, or equivalently the vector potential $\mathbf{A}$, can be incorporated in the Hamiltonian by the canonical replacement $\mathbf{p} \to (\mathbf{p} + \frac{q\mathbf{A}}{c})$, where q is the charge of the particle. Since, the partition function involves integration of the momenta over the entire momentum space, the origin of p can be trivially shifted by $\frac{q\mathbf{A}}{c}$ and as a result, the vector potential disappears when the momenta are integrated over during the evaluation of the partition function. The demonstrated absence of classical diamagnetism is, however, somewhat paradoxical inasmuch as each particle must trace a cyclotron orbit and therefore contribute a diamagnetic moment given by $\frac{q}{2c}(\mathbf{r} \times \mathbf{v})$, where $\mathbf{r}$ is its position and $\mathbf{v} = \dot{\mathbf{r}}$. This was resolved by noting that the cuspidal orbits of the electron skipping the boundary generate a paramagnetic moment equal and opposite to the

(a)   (b)
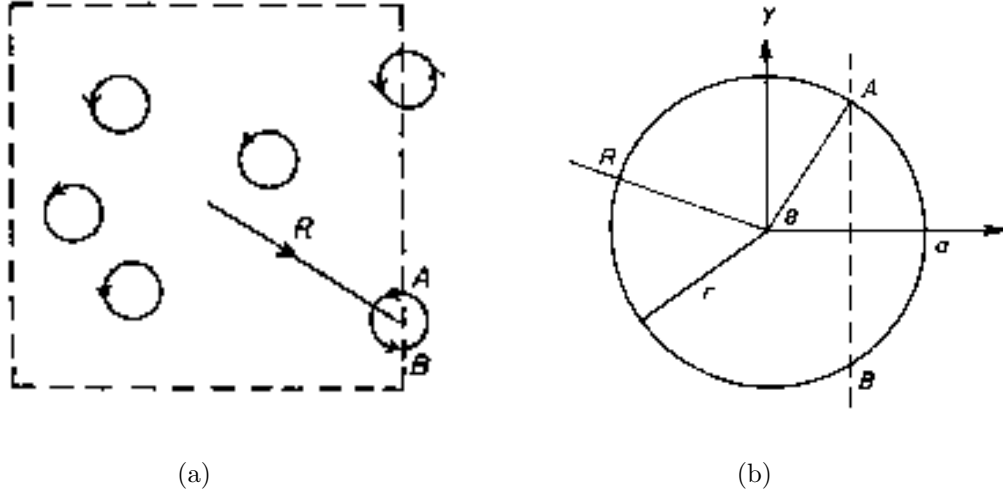
Figure 4.1: (a) Above is a schematic diagram for the circular orbits of the positively charged particles on **x-y** plane in a bounded area, under the influence of constant magnetic field going into the paper perpendicularly. (b) Above is a schematic diagram of an incomplete orbit at the boundary.

the diamagnetic moment due to the charges in the bulk [1, 3, 4, 5] and thus they cancel each other's contribution exactly. This cancellation can easily be demonstrated if we consider some cyclotron orbits for positive charges on a two dimensional plane ($\mathbf{x} - \mathbf{y}$ plane, say) in a bounded area, moving in a magnetic field pointing into the the plane (see figure (4.1a))[9]. The magnetic moments of the circular orbits are pointing upward. Orbits totally within the region contribute an upward magnetic moment, proportional to $\pi a^2 n \mathbf{A}$, where a is radius of an orbit, n is the density of the orbits and $\mathbf{A}$ is the area vector. As the charges cannot go outside the bounded area, they reflect back from the boundary and thus the orbits at the boundary are cuspidal. If $\mathbf{R}$ is the position vector of the center of an orbit at the boundary and $\mathbf{r}$ is the position vector of the charge moving along the orbit from its center, then the magnetic moment due the charge is proportional to

$$\sigma = \frac{1}{2}\mathbf{R} \times \int d\mathbf{r} + \frac{1}{2}\int \mathbf{r} \times d\mathbf{r} \tag{4.1}$$

We will neglect the second term of the above in large area limit because its contribution to the magnetic moment will be proportional to the perimeter of the concerned area while the contribution of the first term will be proportional to the area itself. For a single orbit at the boundary (see figure (4.1b)) $\int d\mathbf{r} = -2a\sin\theta\hat{y}$ where $\hat{y}$ is the unit vector along $\mathbf{y}$. All orbits within $\pm a$ of the boundary lie partially within the region. There are $2nadR$ such orbits along a segment dR of the boundary. Therefore, the total magnetic moment of those orbits along the boundary is proportional to

$$\Sigma = \int 2na\sigma dR = 2na \int \frac{dR}{2}\mathbf{R} \times (-2a\langle\sin\theta\rangle)\hat{y} \tag{4.2}$$

where $\langle . \rangle$ represents integration over all possible θ and so $\langle\sin\theta\rangle = \frac{1}{2}\int_0^\pi \sin\theta d(\cos\theta) = \frac{\pi}{4}$. Now Σ can be written as,

$$\Sigma = -\frac{\pi a^2 n}{2} \oint \mathbf{R} \times d\mathbf{R} = -\pi a^2 n\mathbf{A}, \tag{4.3}$$

Thus, the magnetic moment due to orbits along the boundary is same in magnitude but opposite in direction to that of due to the orbits wholly within the region and consequently they cancel each other.

The Gibbsian treatment of van Leeuwen, however, makes no appeal to such a boundary effect. This may at once be taken as the strength and the weakness of the equilibrium statistical mechanical approach. The purpose of this chapter is thus to make explicit the subtle role of boundary via a real space-time (Einsteinian) approach.

In a previous paper by Kumar and Jayannavar[5], it was shown by space-time approach that if a charged particle moving on two dimensional infinite plane, is subjected to a perpendicular constant magnetic field, then a non-zero diamagnetic moment is exhibited. On the other hand, if the particle is confined within a harmonic well, then this diamagnetic contribution is exactly canceled by the paramagnetic contribution coming from the boundary skipping orbits. The motion of the charge particle, in presence of the confinement, is described by the following equation of motion:

$$m\ddot{\mathbf{r}} = -k\mathbf{r} - \Gamma\dot{\mathbf{r}} + \frac{q}{c}(\dot{\mathbf{r}} \times \mathbf{B}) + \xi(t), \tag{4.4}$$

where $\xi(t)$ is the Gaussian white noise: $\langle\xi_i(t)\xi_j(t')\rangle = 2T\Gamma\delta_{ij}\delta(t - t')$ for $k_B = 1$. Here the particle-environment interaction is modeled via a Langevin equation including inertia. Defining

a variable $z \equiv x + iy$, the equation of motion reduces to

$$\ddot{z} = -kz - (\omega_r + i\omega_c)\dot{z} + F(t),$$

with $\omega_r = \Gamma/m$ and $\omega_c = qB/mc$, while $F(t) = \xi_x(t) + i\xi_y(t)$, with the property $\langle F(t)F^*(t') \rangle = 4k_BT\delta(t - t')$. Solving the above equation for z and noting that $M_{eq} = \frac{q}{2c}(\mathbf{r} \times \mathbf{v}) = \frac{q}{2c}\text{Im}\langle z^*\dot{z} \rangle$, they finally obtained

$$\lim_{t \to \infty} \lim_{k \to 0} M_{eq} = \frac{q}{mc} \frac{k_BT\omega_c}{\omega_r^2 + \omega_c^2} \neq 0. \tag{4.5}$$

However, if we do not take the $k \to 0$ limit, the M_{eq} vanishes as $t \to \infty$, hence upholding the subtle role of the boundary. Above result can also be derived in real space-time approach [10, 11, 12].

We have numerically verified the above results and have found them to be in excellent agreement with the analytical ones. This should certify the accuracy of the numerical results. These results and numerics will serve as the bench mark of our calculations further in this chapter. First we have solved the equation of motion numerically using the Heun's method (Runge-Kutta 2) [13] for $k = 0$ and for different constant magnetic fields, keeping temperature and friction coefficient constant to evaluate ensemble averaged as well as time averaged M_{eq} at long time limit. This is shown in figure (4.2a), where the numerical data (solid circles) has been compared with the exact analytical result (solid line) given by equation (4.5), thereby supporting the role of absence of cuspidal orbits in unbounded systems. Next, in figure (4.2b), we have plotted $M_{eq}(\tau)$ as a function of the observation time τ, for three different cases: (i) when the particle is freely moving on an infinite two dimensional plane; (ii) particle is trapped in a two dimensional harmonic potential; and (iii)particle is trapped in a quartic potential. We observe that in the unbounded case (case (i)), M_{eq} saturates to a non-zero value which is the same as computed from the analytical result (4.5), while in either of the later two cases (with confining potentials) M_{eq} saturates to zero, as expected.

However one should note here that, above discussion is for the manifestation of the role played by the boundary to cancel the diamegnetic moment in bulk exactly. In absence of boundary the cancellation will not happen and we get nonzero magnetic moment on two dimensional
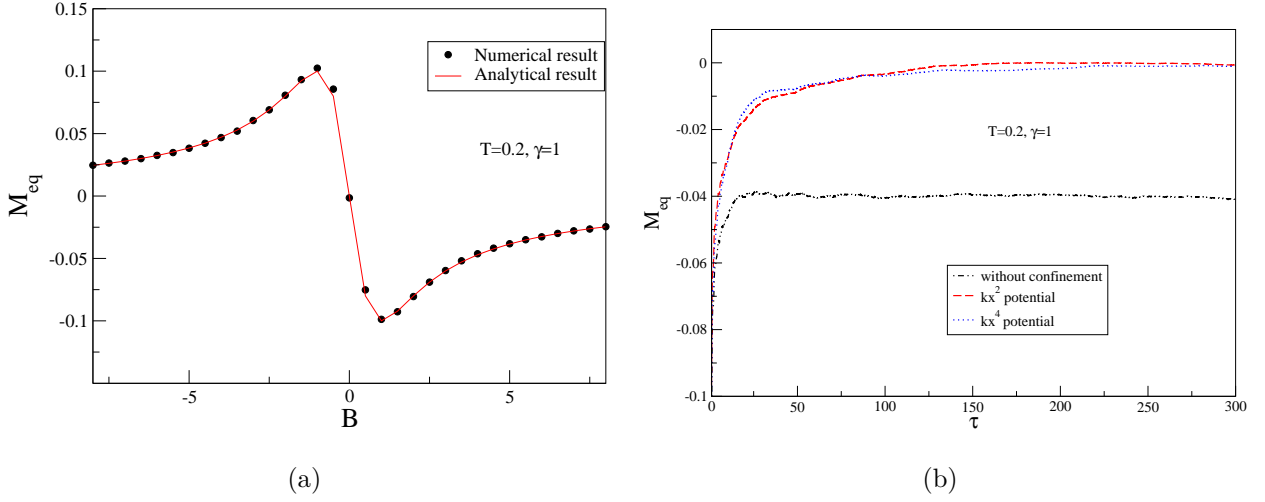
Figure 4.2: In figure (a) diamagnetic moment is plotted against various magnetic field and in figure (b) the same is plotted against time for confined and unconfined cases, magnetic field is kept fixed.

infinite plane. But this nonzero magentic moment should not launch a contradiction to BvL simply because the particle cannot equilibrate on an infinite plane without boundary and consequently it is not an equilibrium result whereas BvL deals with only those systems which are in equilibrium. We will discuss this point a bit more in the next section.

4.2 Classical diamagnetism: Finite unbounded space

In case of a particle following equation (4.4) on two dimensional infinite plane $(\mathbf{x} - \mathbf{y})$, the fluctuations along $\mathbf{x}$ and $\mathbf{y}$ at long time limit, are given by

$$\langle x^2 \rangle - \langle x \rangle^2 = \langle y^2 \rangle - \langle y \rangle^2 = \frac{k_B T / \Gamma}{1 + \frac{q^2 B^2}{c^2 \Gamma^2}} t. \tag{4.6}$$

The long time fluctuations along v_x and v_y are given by

$$\langle v_x^2 \rangle - \langle v_x \rangle^2 = \langle v_y^2 \rangle - \langle v_y \rangle^2 = \frac{k_B T}{2} \tag{4.7}$$

which indicates that the particle relaxes to equilibrium in velocity space after a long time but in position space it cannot equilibrate. So, the joint probability distribution of position and velocity of the particle at time t, namely $P(\mathbf{x}, \mathbf{v}; t)$, is explicitly time dependent and consequently $\frac{\partial P}{\partial t} \neq 0$. Therefore the particle is not in equilibrium. But BvL is an equilibrium result. So, one may argue that the result in the previous section should not be compared with BvL.

This motivate us to take the particle following the same dynamics given in equation (4.4) but on a *finite and unbounded* space like sphere. The magnetic field is taken along z direction as before. Due to finiteness of the space, after a long time each and every point on the sphere will expected to be equally probable position for the particle. So, along with the velocity space, in position space also the particle can be equilibrated with the thermal bath surrounding it. This equilibration is achieved and verified by simulating the dynamics on the sphere.

4.3 Classical diamagnetism: On sphere

Let us consider a finite classical system where the particle does not hit a geometrical boundary all along its motion. In such a situation, classical diamagnetism is expected as the skipping trajectories carrying paramagnetic current along the boundary are absent [5]. This subtle role of the boundary has been revisited by Kumar and Kumar [14] by considering the motion of a charged particle which is constrained to move on the surface of a sphere, i.e., on a finite but unbounded system. The surface of a sphere has no boundary, and to the pleasant surprise of the authors, they did find non-zero classical orbital diamagnetic moment by following the space-time approach. This effect has been attributed to the dynamical correlation induced by Lorentz force between velocity and transverse acceleration when the problem is treated as per the Einsteinian approach, i.e., in this case, via the Langevin dynamics [15, 16]. Such subtle dynamical correlations are presumably not captured by the classical Gibbsian statistical

mechanics based on equilibrium partition function.

In our present work, we explore this system further using the recently discovered fluctuation Theorems (FTs), namely, the Jarzynski Equality (JE) and the Crooks' Fluctuation Theorem (CFT) [17, 18]. These FTs address the calculation of equilibrium free energy difference ΔF between two thermodynamic states derivable from irreversible (nonequilibrium) trajectories. We come across other intriguing consequences. If the system is driven out of equilibrium by perturbing its Hamiltonian (H_λ) by an externally controlled time-dependent protocol $\lambda(t)$, the thermodynamic work done on the system is given by [17]

$$W = \int_0^\tau \dot{\lambda} \frac{\partial H}{\partial \lambda} \, dt \tag{4.8}$$

over a phase space trajectory, where τ is the time through which the system is driven. $\lambda(0) = A$ and $\lambda(\tau) = B$ are the thermodynamic parameters of the system. The JE states

$$\langle e^{-\beta W} \rangle = e^{-\beta \Delta F}, \tag{4.9}$$

where $\Delta F = F_B - F_A$ is the free energy difference between the equilibrium states corresponding to the thermodynamic parameters B and A, and the angular brackets denote average taken over different realizations for fixed protocol $\lambda(t)$. In equation(4.9), $\beta = 1/k_B T$, T being the temperature of the medium and k_B is the Boltzmann constant. Initially the system is in equilibrium state determined by the parameter $\lambda(0) = A$. The work done W during each repetition of the protocol is a random variable which depends on the initial microstate and on the microscopic trajectory followed by the system. The JE acts as a bridge between the statistical mechanics of equilibrium and nonequilibrium systems and has been used experimentally [19] to calculate free energy differences between thermodynamic states. The CFT predicts a symmetry relation between work fluctuations associated with the forward and the reverse processes undergone by the system. This theorem asserts that

$$\frac{P_f(W)}{P_r(-W)} = e^{\beta(W - \Delta F)}, \tag{4.10}$$

where $P_f(W)$ and $P_r(W)$ denote distributions of work values for the forward and its time-reversed process. During the forward process, initially the system is in equilibrium with parameter A. During the reverse process, the system is initially in equilibrium with parameter B and the protocol is changed from λ_B to λ_A over a time τ in a time reversed manner $(\lambda(\tilde{t}) = \lambda(\tau - t))$ and in our present problem, magnetic field also has to be reversed in sign [6]. From equation (4.10), it is clear that the two distributions cross at $W = \Delta F$, thus giving a prescription to calculate ΔF.

In the present work, we show that the case of a charged particle moving on a sphere leads to free energy of the system which depends on the magnetic field and on the dissipative coefficient, which is inconsistent with the prediction of canonical equilibrium statistical mechanics. The same system gives orbital diamagnetism when calculated via the space-time approach, again in contradiction with the equilibrium statistical mechanics [14]. For the recently studied case of a particle moving on a ring [20], the Langevin approach predicts zero orbital magnetism, just as in the present treatment. Thus, in this case, the free energy obtained by using FTs is consistent with the canonical equilibrium statistical mechanics.

We take up the model proposed in [14], which consists of a Brownian particle of charge $-e$ constrained to move on the surface of a sphere of radius a, but now with a time-dependent magnetic field $\mathbf{B}(t)$ in the $\hat{\mathbf{z}}$ direction. The Hamiltonian of the system in the absence of heat bath is given by:

$$H = \frac{1}{2m}\left(\mathbf{p} + \frac{e\mathbf{A}(\mathbf{r},t)}{c}\right)^2,$$ (4.11)

which in polar coordinates reduces to

$$H = \frac{1}{2m}\left[\left(\frac{p_\theta}{a} + \frac{eA_\theta(t)}{c}\right)^2 + \left(\frac{p_\phi}{a\sin\theta} + \frac{eA_\phi(t)}{c}\right)^2\right].$$ (4.12)

In a symmetric gauge, $A_\theta = 0$ and $A_\phi = (1/2)aB(t)\sin\theta$. In presence of the heat bath, the dynamics of the particle is described by the Langevin equation [6]:

$$m\frac{d\mathbf{v}}{dt} = -\frac{e}{c}(\mathbf{v}\times\mathbf{B}(t)) - \Gamma\mathbf{v} - \frac{e}{2c}\left(\mathbf{r}\times\frac{d\mathbf{B}(t)}{dt}\right) + \sqrt{2T\Gamma}\,\xi(t),$$ (4.13)

where m is the particle mass and Γ is the friction coefficient. $\xi(t)$ is a Gaussian white noise with the properties $\langle\xi(t)\rangle = 0$ and $\langle\xi_k(t)\xi_l(t')\rangle = \delta_{kl}\delta(t - t')$. The first term on the right hand side

is the Lorentz force. If the magnetic field varies with time, it also produces an electric field $\mathbf{E}$, hence the presence of the force term $-e\mathbf{E} = -(e/2c)(\mathbf{r} \times \frac{d\mathbf{B}}{dt}(t))$ in equation (4.13). This is an additional element of physics not present in reference [14]. Switching over to the spherical polar coordinates, equation (4.13) assumes the following form in terms of dimensionless variables:

$$\ddot{\theta} - \dot{\phi}^2 \sin\theta\cos\theta = -\frac{a\omega_c(B(t))}{c}\dot{\phi}\sin\theta\cos\theta - \frac{a\gamma}{c}\dot{\theta} + \sqrt{\eta}\,\xi_\theta; \tag{4.14}$$

$$\begin{aligned}
\ddot{\phi}\sin\theta + 2\dot{\theta}\dot{\phi}\cos\theta &= \frac{a\omega_c(B(t))}{c}\dot{\theta}\cos\theta + \frac{ab}{c}\dot{B}(t)\sin\theta \\
&\quad - \frac{a\gamma}{c}\dot{\phi}\sin\theta + \sqrt{\eta}\,\xi_\phi.
\end{aligned} \tag{4.15}$$

In the above equations, the dots represent differentiation with respect to the dimensionless time $\tau = (c/a)t$. Here $\gamma = \Gamma/m$, $\omega_c(B(t)) = eB(t)/mc$, $b = e/(2mc)$ and $\eta = 2Ta\gamma/mc^3$.

First we consider the case of static magnetic field $\mathbf{B}$ of magnitude B in the $\hat{\mathbf{z}}$ direction. The ensemble averaged orbital magnetic moment which by symmetry is also in the $\hat{\mathbf{z}}$ direction is given by

$$\langle M(t) \rangle = -\frac{ea}{2}\langle \dot{\phi}\sin^2\theta \rangle \tag{4.16}$$

where $\langle \cdots \rangle$ denote ensemble average over different realizations of the stochastic process. We have calculated the equilibrium magnetic moment by double averaging first over a large observation time and then over the ensemble:

$$M_{eq} = \langle\langle M(t) \rangle\rangle = \frac{1}{\tau}\int_0^\tau dt\,\langle M(t) \rangle \tag{4.17}$$

as $\tau \to \infty$. For a numerical check, we have obtained the same results as figures 2 and 3 of [14]. Throughout our analysis, we have used dimensionless variables. e, c, m and a are all taken to be unity.

The thermodynamic work done by the external time-dependent magnetic field on the system up to time t is given by

$$W(t) = \int_0^t \frac{\partial H}{\partial t'}dt' = \frac{ea}{2}\int_0^t dt'\,\dot{\phi}(t')\sin^2\theta(t')\dot{B}(t'). \tag{4.18}$$

In our case, $B(t)$ acts as the external protocol $\lambda(t)$. The Langevin equations are solved numerically by using the Euler method of integration with time step $\Delta t = 0.01$. While simulating the
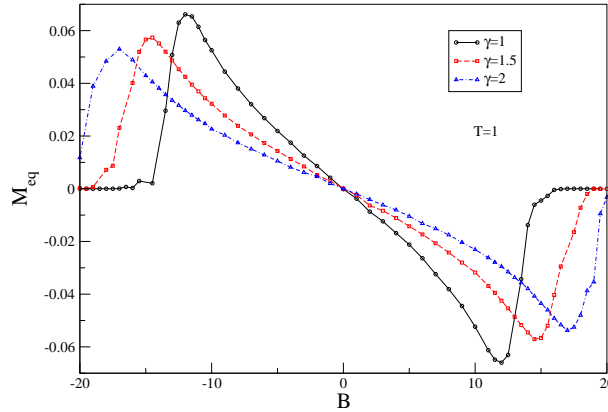
Figure 4.3: Plots of magnetic moment M_{eq} versus magnetic field B for different γ and for a given temperature $T = 1$. The different plots are for γ=1, 1.5 and 2, as mentioned in the figure.

dynamics, we have to be careful near the poles where $1/\sin\theta$ diverges. This is regularised by replacing $1/\sin\theta$ with $1/\sqrt{\sin^2\theta + \epsilon}$ where ϵ is the small positive number of the order of Δt. The periodic boundary conditions for θ and ϕ co-ordinate are fixed carefully.

In figure (4.3), we have plotted the dimensionless magnetic moment $M_{eq}(\equiv \frac{M_{eq}}{ea})$ versus the magnetic field in dimensionless units $B(\equiv \frac{eBa}{mc^2})$ for different values of the friction coefficient $\gamma(\equiv \frac{\Gamma a}{mc})$, as mentioned in the figure. At each point, the signature of M_{eq} is opposite to that of B, providing clear evidence of diamagnetism. Initially, M_{eq} increases with B (linear response) and after showing a peak at high fields, it approaches zero. At high fields, it is expected that the radius of the cyclotron orbits will tend towards zero, and hence naturally the magnetic moment also vanishes. With increase in the friction coefficient γ, the peak shifts towards higher magnitudes of magnetic field. We noted that this behaviour is qualitatively consistent with the exact result obtained for the orbital magnetic moment M_{2d} for a charged particle in a two-dimensional plane in the absence of a boundary, following the real space-time approach. Compared to the analysis in [14], we have gone beyond the linear response regime.

In figure (4.4) we have plotted the magnitude of M_{eq} as a function of B for different values of temperature T. From figures (4.3) and (4.4), it can be inferred that the magnetic moment can be monotonic or non-monotonic in T and γ, depending on the whether the values of B
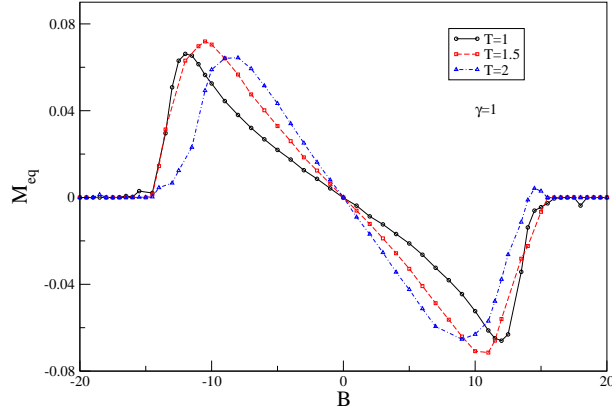
Figure 4.4: Plots of M_{eq} versus B for different T and for a given friction coefficient $\gamma = 1$. We have taken different plots for T=1, 1.5 and 2.

lie within the linear response regime or beyond. To this end, in figures (4.5) and (4.6), we have plotted the equilibrium magnetic moment as a function of temperature T and friction coefficient γ respectively, for various values of B. The magnetic moment is zero at $T = 0$ as well as at $T = \infty$. It exhibits a minimum in the intermediate range of temperature. This minimum shifts towards lower temperature with the increase in B. It should be noted that for larger temperatures, a higher number of realizations are required to generate more accurate data points.

In figure (4.6), we notice that in the parameter range that we have considered, the equilibrium magnetic moment decreases monotonically with friction coefficient. For large γ, the particle motion gets impeded by the medium and as expected, $M_{eq} \to 0$ as $\gamma \to \infty$. As $\gamma \to 0$, there is a saturation in the value of magnetic moment, which depends on the value of the parameters B and T. This we have not shown in the figure. It is evident from figure (4.3) that for large values of B ($B > 10$), dependence of M_{eq} on γ is non-monotonic. This is shown in the inset where M_{eq} is plotted as a function of γ for $B = 12$ and for $B = 15$. It is observed that the dip in M_{eq} shifts towards higher γ for higher value of B. For small friction coefficients, the saturation value is very small (for large B) and it requires a much larger number of realizations to achieve reliable results. Our results clearly indicate that the temperature and the friction dependence of
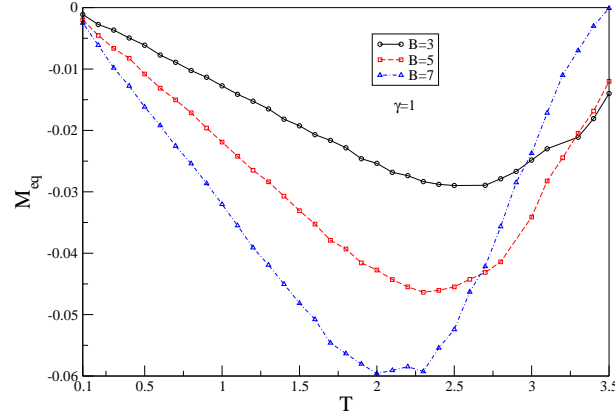
Figure 4.5: Plots of M_{eq} as a function of T for $\gamma = 1$ and for three different values of the external magnetic field: B=3, 5 and 7.

the classical magnetic moment obtained via real space-time approach are qualitatively different for an infinite unbounded system (equation (4.5)) from that for a finite unbounded system considered here. From equation (4.5) we can readily infer that the dependence of M_{2d} on temperature T and on friction coefficient γ is monotonic.

Having shown that the space-time approach leads to a finite diamagnetic moment in contrast to its absence in canonical equilibrium, we can now turn to the calculation of free energy differences for the same problem using the FTs. We subject the system to the time-dependent magnetic field (protocol) in the form of a ramp, $B(t) = B_0 t/\tau$, where τ denotes the total time of observation. We use the ramp with an observation time $\tau = 2000$. The final value of magnetic field is $B(\tau) = B_0$. To calculate the free energy difference, $\Delta F = F(B_0) - F(0)$, we have used the JE (equation (4.9)). To calculate ΔF numerically, we have generated 10^4 realizations of the process, making sure that the system is initially in canonical equilibrium in the absence of magnetic field ($B(0) = 0$). The results for ΔF are plotted as a function of $B(\tau)$ in figure (4.7) for two values of γ. All physical parameters are in dimensionless units and are as mentioned in the figure. Surprisingly, we notice that ΔF depends on the magnetic field $B(\tau)$. This is in sharp contrast to the equilibrium result, namely, ΔF should be identically zero. To our knowledge, this is the *first* example wherein the Fluctuation Theorem fails to reproduce the result obtained from equilibrium statistical mechanics. This is yet another surprise in the field
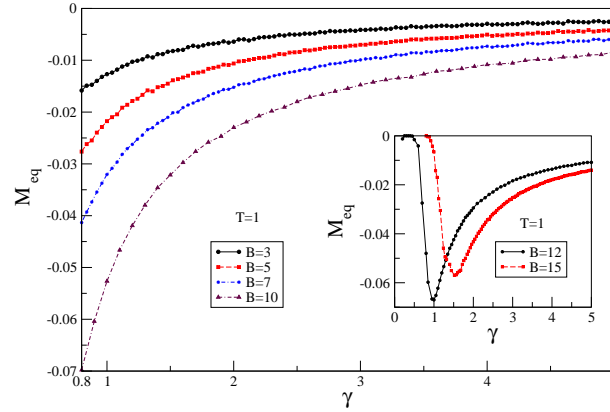
Figure 4.6: Plots of M_{eq} as a function of the friction coefficient γ, for 4 different values of B: B=3, 5, 7 and 10, with T=1. Note that the axis for γ starts from 0.8. In the inset we have plotted the curves M_{eq} versus γ for B=12 and 15.
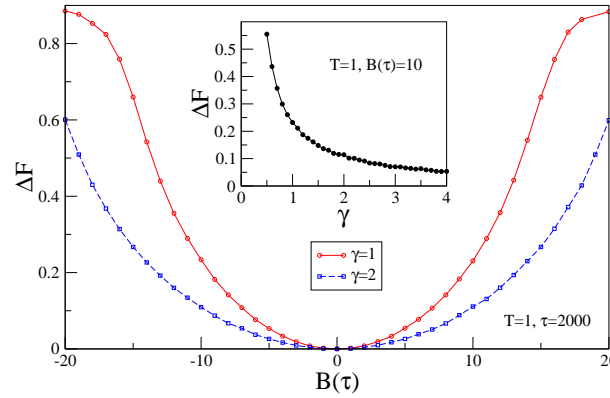
Figure 4.7: Plots of ΔF versus the final value of the magnetic field $B(\tau)$ for $\gamma = 1$ and $\gamma = 2$. The protocol used is a ramp, $B = B_0 t / \tau$, for a time of observation $\tau = 2000$, with the temperature fixed at T=1. The inset shows the variation of ΔF as a function of the friction coefficient γ, with the parameters T=1, $B(\tau) = B_0$=10.
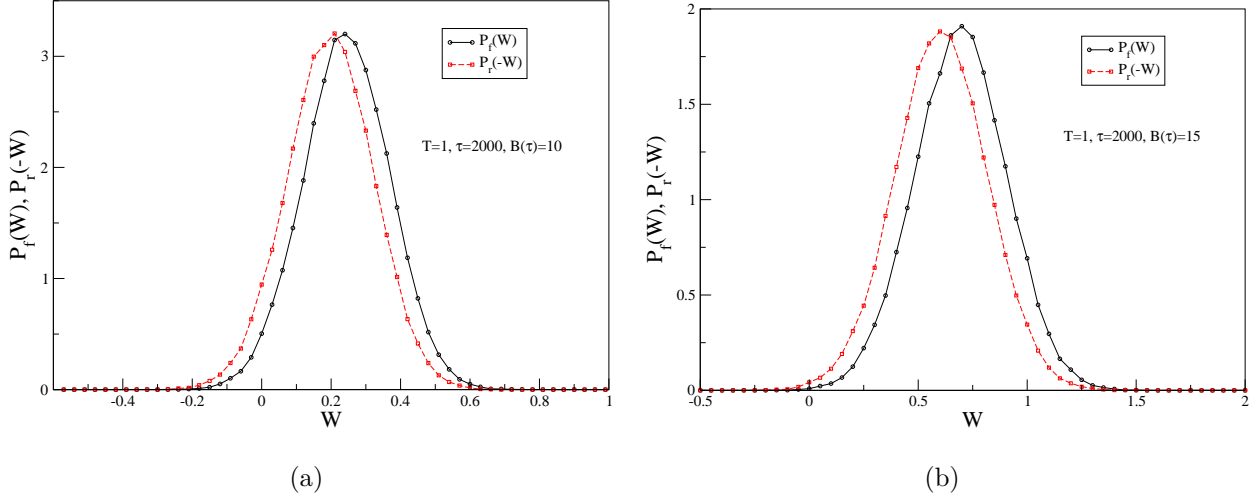
Figure 4.8: Determination of ΔF using the CFT. (a) Plots of $P_f(W)$ and $P_r(-W)$ at $B(\tau) = B_0 = 10$, which cross at $W(=\Delta F) = 0.22$. (b) Plots of $P_f(W)$ and $P_r(-W)$ at $B(\tau) = B_0 = 15$, which cross at $W(=\Delta F) = 0.65$.

of classical diamagnetism. Moreover, ΔF depends on the type of protocol. The dependence of ΔF on the friction coefficient is shown in the inset of figure (4.7). In classical equilibrium, it should be noted that the free energy does not depend on friction coefficient. From this free energy, one can get moment by calculating the derivative of the obtained free energy with respect to B. However, the magnetic moment thus obtained does not agree with that obtained through the simulation of the Langevin equations.

In figure (4.8) (a) and (b), we have plotted $P_f(W)$ and $P_r(-W)$ as a function of W for the same protocol ending with two different values of the magnetic field ($B(\tau) = 10$ and 15). The crossing point of $P_f(W)$ and $P_r(-W)$, according to the CFT, gives the value of ΔF, which we have found to be equal to 0.22 for $B_0 = 10$ and 0.65 for $B_0 = 15$, which are in turn equal to the obtained values using the JE, namely, 0.22 and 0.65 respectively, within our numerical accuracy. Thus we have shown that a charged particle on a sphere exhibits finite diamagnetic moment and magnetic field dependent free energy calculated via real space-time approach and the Fluctuation Theorems respectively. As mentioned earlier, these results contradict equilib-

rium statistical mechanics.

4.4 Classical diamagnetism: On ring

Now we turn to a simpler problem of a charged particle moving on a ring in a magnetic field perpendicular to the plane of the ring, i.e., in the $\hat{\mathbf{z}}$ direction. This problem has been studied recently [20] in connection with the BvL for a particle motion in a finite but unbounded space, where it was shown that this system analised via the Langevin dynamics does not exhibit orbital diamagnetism, consistent with equilibrium statistical mechanics. It is not surprising as the equation of motion for the relevant dynamical variable, namely the azimuthal angle ϕ, does not depend on the strength of the static magnetic field. Hence, the magnetic field has no effect on the motion of a particle constrained to move in a circle of fixed radius a. We analyze the same problem, however in the presence of time-dependent magnetic field (protocol), within the framework of Jarzynski equality to obtain the free energy dependence on magnetic field in this case. To this end, the Hamiltonian of the system is given by

$$H = \frac{1}{2m}\left(\frac{p_\phi}{a} + \frac{eA_\phi(t)}{c}\right)^2, \tag{4.19}$$

where, for a magnetic field in the $\hat{\mathbf{z}}$ direction, $A_\phi(t) = (a/2)B(t)$. The corresponding Langevin equation for the relevant variable ϕ is given by

$$ma\ddot{\phi} = -\Gamma a\dot{\phi} + \frac{ea}{2c}\dot{B}(t) + \sqrt{2T\Gamma}\,\xi_\phi. \tag{4.20}$$

The above equation can be written in a compact form

$$\ddot{\phi} = -\gamma\dot{\phi} + \lambda_1\dot{B}(t) + \sqrt{\eta}\,\xi_\phi, \tag{4.21}$$

with $\gamma = \frac{\Gamma}{m}$, $\lambda_1 = \frac{e}{2mc}$ and $\eta = \frac{2\gamma T}{ma^2}$. In this section, the dots represent differentiation with

respect to real time t. It may be noted that if the magnetic field is independent of time, i.e., $\dot{\mathbf{B}} = 0$, then the field has no effect on the ϕ variable, as can be seen from equation (4.21). The thermodynamic work W, using equation (4.8) and (4.19), is given by

$$W(t) = \int_0^t \frac{\partial H}{\partial t'} \, dt' = \frac{ea^2}{2c} \int_0^t \dot{\phi}(t') \dot{B}(t') \, dt'. \tag{4.22}$$

The formal solution for $\dot{\phi}$ is given by

$$\dot{\phi}(t) = \dot{\phi}(0)e^{-\gamma t} + e^{-\gamma t} \int_0^t dt' \, e^{\gamma t'} [\lambda_1 \dot{B}(t') + \sqrt{\eta} \, \xi_\phi(t')]. \tag{4.23}$$

Substituting this solution in equation (4.22) for W, we get

$$
\begin{aligned}
W(t) &= g \int_0^t dt' \dot{B}(t') [\dot{\phi}(0)e^{-\gamma t'} + e^{-\gamma t'} \int_0^{t'} \{\lambda_1 \dot{B}(t'') \\
&\quad + \sqrt{\eta} \, \xi_\phi(t'')\} e^{\gamma t''} \, dt''],
\end{aligned}
\tag{4.24}
$$

where $g = ea^2/2c$. Since the expression for W in the above equation is linear in the Gaussian stochastic variable $\xi_\phi(t)$, W itself follows a Gaussian distribution. To obtain $P(W)$, we simply need to evaluate the average work $\langle W \rangle$ and the variance $\sigma_W^2 = \langle W^2 \rangle - \langle W \rangle^2$. the full probability distribution $P(W)$ is given by

$$P(W) = \frac{1}{\sqrt{2\pi\sigma_W^2}} \exp\left[-\frac{(W - \langle W \rangle)^2}{2\sigma_W^2} \right]. \tag{4.25}$$

Averaging equation (4.24) over random realizations of $\xi_\phi(t)$, and noting that $\langle \xi_\phi(t) \rangle = 0$, we get for average work done till time τ:

$$\langle W \rangle = g\lambda_1 \int_0^\tau dt' \dot{B}(t')e^{-\gamma t'} \int_0^{t'} dt'' \, \dot{B}(t'')e^{\gamma t''}. \tag{4.26}$$

Again using equation (4.24) and (4.26), after tedious but straightforward algebra, the variance σ_W^2 can be readily obtained and is given by

$$\sigma_W^2 = \frac{g^2}{2\gamma}\eta \int_0^\tau dt' \, \dot{B}(t') \int_0^\tau dt_1 \dot{B}(t_1)e^{-\gamma|t'-t_1|}. \tag{4.27}$$

In arriving at the above expression, we have used the fact that the variance of the initial equilibrium distribution of angular velocity $\dot{\phi}(0)$ is given by $\langle \dot{\phi}^2(0) \rangle = \frac{T}{ma^2} = \frac{1}{2}\eta$ (because

$P(v_\phi) = \sqrt{\frac{m}{2\pi T}} \exp(-mv_\phi^2/2T) \Rightarrow P(\dot\phi) = \sqrt{\frac{ma^2}{2\pi T}} \exp(-m\dot\phi^2 a^2/2T))$. Comparison between (4.26) and (4.27) gives the result

$$\sigma_W^2 = 2T\langle W\rangle, \tag{4.28}$$

a fluctuation-dissipation relation. Using equation (4.25) and (4.28), we get

$$\langle e^{-\beta W}\rangle = 1, \tag{4.29}$$

which, according to the JE, implies $\Delta F = F(B(\tau)) - F(B(0)) = 0$, where $B(0)$ and $B(\tau)$ are the values of the magnetic field at the initial and final times of the protocol respectively. The magnitudes of $B(0)$ and $B(\tau) = B$ can take any value. Thus, $\Delta F = 0$ implies that the free energy is independent of the magnetic field, the result being consistent with equilibrium statistical mechanics. It is interesting to note that the averaged work $\langle W\rangle$ (equation (4.26)) and its variance σ_W^2 (equation (4.27)) depend on the functional form of $B(t)$ and on the magnetic fields at the end points of the observation time and yet $\langle \exp(-\beta W)\rangle$ is independent of magnetic field. We have obtained this exact result which is independent of the functional form the protocol $B(t)$.

4.5 Summary

In conclusion, whenever the real space-time approach for a charged particle in the presence of a magnetic field predicts a finite diamagnetic moment, the Fluctuation Theorems too fail to reproduce results consistent with equilibrium statistical mechanics. These conclusions have also been supported by the results for the motion of a charged particle in a two-dimensional plane in the absence of boundary [5, 21]. In cases where real space-time approach to diamagnetism is not in conflict with the equilibrium statistical mechanics, an example being a charged particle on a ring or in the presence of a confining boundary [6], the Fluctuation Theorems lead to results consistent with equilibrium statistical mechanics. Only experiments can resolve whether really orbital diamagnetism exists in classical equilibrium systems (like charged particle on the surface of a sphere).

Bibliography

[1] Bohr N., *Studies over Matallerners Elektrontheori*, PhD Thesis (1911).

[2] van Leeuwen J. H., J. Phys. (Paris)., **2**, 361 (1921).

[3] Vleck J. H. V., *The Theory of Electric and Magnetic Susceptibilities* (Oxford University Press, London) 1932.

[4] Peierls R. E., *Surprises in Theoretical Physics* (Princeton University Press, Princeton) 1979.

[5] Jayannavar A. M. and Kumar N., J. Phys. A **14**, 1399 (1981).

[6] Saha A. and Jayannavar A. M., Phys. Rev. E **77**, 022105 (2008).

[7] Jayannavar A. M. and Sahoo M., Phys. Rev. E **75**, 032102 (2007).

[8] Jayannavar A. M. and Sahoo M., Pram. J. Phys. **70**, 201 (2008).

[9] Ma Shang-Keng, Statistical Mechanics, World Scientific, Philadelphia, 1985.

[10] Furuse H., J. Of The Phys. Soc. Of Jap **28** 3 (1970)

[11] Lemons S. Don, Kaufman L. David, IEEE Transaction On Plasma Science **27** 5 (1999)

[12] Hou L. J. *et. al.* Phys. Of Plasma, **16** 053705 (2009)

[13] R. Mannela Stochastic Process in Physics, Chemistry and Biology, Lecture Notes in Physics, Vol. 557, Springer-Verlag, Berlin (2000).

Bibliography

[14] Kumar N. and Kumar K. V., Europhys. Lett. **86**, 17001 (2009).

[15] H. Risken, *The Fokker-Planck Equation* (Springer-Verlag) 1984.

[16] Coffey W. T., Kalmykov Y. P. and Waldron J. T., *The Langevin equation* (World Scientific, Singapore) 1996; Li X. L., Ford G. W. and O' Connell R. F., Phys. Rev. A **41**, 5287 (1990).

[17] Jarzynski C., Phys. Rev. Lett. **78**, 2690 (1997); Phys. Rev. E **56**, 5018 (1997).

[18] Crooks G. E., Phys. Rev. E **60**, 2721 (1999); 6123612000.

[19] Ritort F., J. Phys. Condens. Matter **18**, R531 (2006).

[20] Kaplan T. A. and Mahanti S. D., Europhys. Lett. **87**, 17002 (2009).

[21] Saha A. and Jayannavar A. M., manuscript under preparation.

5 Rare Events And Systems Far from Equilibrium

Rare events in the context of physics can have various connotations. An obvious one is the phenomenon where a barrier exists and one has to hop across the barrier to activate the event. Decay of metastable states and the occurrences of certain chemical reactions are examples of such processes. It is the thermal noise that activates these hopping processes and the rareness of the events is characterized by the large time-scale involved. The relevant time-scales are of the order $\exp(\Delta V / K_B T)$, where V is the height of the barrier to be overcome, T is the temperature and K_B is the Boltzmanns constant. Here, however, our focus will be on rare events which happen with a probability that lies at the tail of the probability distribution in the case of certain problems in statistical physics.

The role of large deviations in physics as a uniform theme of problems in statistical physics was employed by Oono [1] two decades ago. It is in the last decade that the view has become more widespread and study of such systems becomes plentiful [2, 3, 4, 5]. One such area is the fluctuation theorems [3, 4, 6, 7, 8, 9, 10] which relate to nonequilibrium systems, characterized by irreversible heat losses between the system and its environment; typically a thermal bath. For systems in equilibrium with time reversal symmetry, the probability of absorbing a given amount of heat is equal to the probability of releasing the same amount. This ratio of heat absorbed to heat released is not unity in nonequilibrium situations.

The steady-state nonequilibrium systems are more likely to deliver heat to the surroundings than absorb heat from it. If the system is macroscopic in size, then the probability of heat ab-

sorption is insignificant. For small systems (e.g. molecular motors) the probability of absorbing heat can be significant. On an average, heat would be produced but there would be processes that imply occasional absorption of heat. This actually goes back to Loschmidts objection to Boltzmanns derivation of the second law of thermodynamics from Newtons laws of motion. Since the microscopic laws of motion are invariant under time reversal, Loschmidt argued that there must also be entropy decreasing evolutions which violate the second law of thermodynamics. The fluctuation theorems delineate the occurrence of macroscopic irreversibility from the time reversal invariant microscopic equations of motions. Time reversed trajectories do occur but they become rarer and rarer with increasing size of the system. These are the rare events and their occurrence is a signature of large deviations. A particular form of the fluctuation theorem will be discussed in the next section, where we will show how it relates to the general theory of large deviations.

Probably the earliest that large deviations entered the domain of physics was the 1960s when Kolmogorov and Obukhov reconsidered Kolmogorovs theory of homogeneous isotropic turbulence of 1941 in the light of Landaus objection. In a nonequilibrium steady-state situation for the turbulent velocity eld, Kolmogorov had assumed that the energy supplied per unit time at large scales was exactly equal to the energy dissipated at the smallest (molecular) scales. It was assumed that the energy dissipation rate was a constant at all scales and that was contradicted by Landau. Phenomenologically, Kolmogorov and Obukhov [11] introduced fluctuations in the dissipation rate in 1962. Careful experiment revealed the existence of these fluctuations. The fluctuations occurred rarely these were the rare events of turbulence [12, 13, 14, 15, 16, 17, 18, 19]. These rare events constitute one of the most difficult issues to understand in the theory of turbulence. In this chapter we will see how the theory of large deviation, applied in a purely intuitive manner can immediately show a connection between this longstanding problem and the rare events in simple coin toss experiment.

While our focus here will be on the fluctuation theorem and turbulence, it should be mentioned that yet another set of problems where the tail of the probability distribution is the key to the problem of persistence [20, 21, 22, 23, 24]. In its simplest incarnation, this is the issue of a one-dimensional random walker starting out from the origin at $t = 0$. As it takes random

steps to the right and left, there is always the possibility of its crossing the origin in the course of its meandering. We ask what is the probability that after a time t has elapsed, the walker has not returned to the origin even once. This constitutes the rare event. The probability for not returning has to go to zero as $t \to \infty$ and the long time behaviour is characterized by $P(t) \sim 1/t^\theta$, where is the persistence exponent. Over the last decade, a wide variety of physical systems (e.g. the simple diffusion process, Ising model, Ginzberg-Landau model, model of growth etc.) have been found to exhibit this slow decay in the probability distribution.

5.1 Work probability distribution and tossing a biased coin

Now we show that the rare events present in dissipated work that enters Jarzynski equality[8], when mapped appropriately to the phenomenon of large deviations found in a biased coin toss, are enough to yield a quantitative work probability distribution for Jarzynski equality. This allows us to propose a recipe for constructing work probability distribution independent of the details of any relevant system. Our contention is: in the large deviation theory [25, 26, 27, 28], the central role is played by the distribution associated with tossing of a coin and the simple coin toss is the "Gaussian model" of problems where rare events play significant role. Here we illustrate our contention by applying it to the study of some aspects of Jarzynski equality. The equality says if W is the work done during a period of duration τ, during which an external force acts on the system and does work, then Jarzynski established that in units of $K_B T$

$$\langle e^{-W} \rangle = e^{-\Delta F} \tag{5.1}$$

where angular brackets denote ensemble average and ΔF is the free energy difference for the equilibrium free energies corresponding to the initial and final states. Here K_B is Boltzmann constant and T is the temperature of the concerned system in the initial equilibrium state or, equivalently, the temperature of the heat reservoir with which the system was thermalized before the process took place. It is important to note that here W is a path (trajectory followed by the system during τ) dependent variable. So, if we consider the ensemble of all possible paths (each

path originating from one of the several microstates corresponding to the initial equilibrium macrostate), different values of W along different path can be identified with a set of random variable. Now, if we define another random variable — dissipative work along a path — as

$$W_D \equiv W - \Delta F \tag{5.2}$$

Jarzynski equality (5.1) shows that

$$\langle e^{-W_D} \rangle = 1 \tag{5.3}$$

Clearly, to satisfy above equality, W_D should take both positive and negative values. Again, we know that since $\langle W \rangle$ is the thermodynamic work done in going from initial state to the final state, the second law of thermodynamics would assert that $\langle W \rangle \geq \Delta F$ (i.e., $\langle W_D \rangle \geq 0$), with the equality holding for the reversible process where the system remains always in the equilibrium with its surrounding. So, negative values of W_D are relatively rare events, yet important enough to make the equality of equation(5.3) to hold.

The strategy for demonstrating the validity of our approach will be as follows. As the paradigm for the distribution of rare events we will take, as mentioned earlier, the distribution associated with tossing a coin. The random variable associated with a coin toss can range between two finite numbers which we will take to be 0 and 1. The mean value p, of the variable for an unbiased coin is 1/2 and for a biased coin it lies between 0 and 1 but $p \neq 1/2$. Dissipative work along a path W_D ranges from $-\infty$ to $+\infty$ and we will first carry out a transformation that maps it onto the range 0 to 1. Further, according to the second law of thermodynamics, the events corresponding to $W > \Delta F$ (or, $W_D > 0$) are more likely than the ones corresponding to $W < \Delta F$ (or, $W_D < 0$) and hence there will be an asymmetry or *bias* about the events corresponding to $W = \Delta F$ (or, $W_D = 0$). The amount of bias in the statistics of W due to irreversibility is clearly: $\langle W \rangle - \Delta F$. The corresponding coin has to be biased as well and hence we shall take the asymmetric situation of $p \neq 1/2$. Needless to say that for reversible process, since $\langle W \rangle = \Delta F$, this bias is zero.

Having defined the mapping — which, of course, is not unique — the first check would be to verify if Jarzynski equality in the form of (5.3) is satisfied. This can be tested since we have an explicit distribution — namely, the one associated with the biased coin toss. Such a

check is depicted in figure (5.1), details regarding which follows later in this section. From the distribution for W_D one can also have the distribution for W. The distributions of work and dissipative work have drawn a lot of attraction. For various systems these distributions are now known from experiments as well as numerical studies (*e.g.* [29, 30, 31, 32, 33, 34, 35, 36]). Here we obtain these distributions from very general requirements, which are independent of the dynamics (that usually varies from system to system) followed by the systems. Hence it is important to ask whether the experiments on the systems obeying widely different dynamics really exhibit similar distributions. We find the answer here by comparing our results with actual experimental results and numerical simulations. The probability distribution for W_D, $P(W_D)$, was obtained experimentally by Liphardt *et al.* [33]; and, $P(W)$ has been obtained by Blickle *et al.* [34] for a different system. We have also used an anharmonic oscillator driven by a linear time dependent force to simulate the dynamics and numerically construct $P(W)$ [35]. A similar system has also been studied in [36].

In this work, we calculate $P(W)$ from the biased coin toss distribution which we have taken as a starting ansatz based on the principle of large deviations. The only connection between the experiments and the method we use, is the fact that, the experiment is carried out far from equilibrium and hence must feature negative values of W_D (large deviations) and we have started with a distribution which has large deviations built in it. As will turn out, our method will have two parameters which we fix by comparing with the distribution obtained from the experiment. The appropriateness of $P(W)$, we calculate employing the theory of large deviations, is borne out by comparison as well be demonstrated below. The point we want to stress here is that the present theory, which explicitly takes care of large deviations, does not require explicit knowledge of dynamics. Consequently, it has wide range of applicability. The parameters of the distribution need to be fixed in each case from the scales of measured distribution — *e.g.*, peak position and peak magnitude.

5.1.1 Coin toss

We begin by recalling the situation of coin tossing experiment. If we assign a value 1 to the outcome 'heads' and 0 to the outcome 'tails', then the mean after N trials is

$$M_N = \frac{1}{N} \sum_i^N X_i \tag{5.4}$$

This is an experimental mean which belongs to a set of independent and identically distributed $(i.i.d)$ random numbers lying between 0 and 1 since each individual X_i is either 0 or 1. For an unbiased coin where "heads" and "tails" are equally probable, this mean goes towards $1/2$ as $N \to \infty$. However, for a biased coin where the probability of obtaining "heads" is $p(\neq 1/2)$, the mean will converge towards p as $N \to \infty$. If in N trials 'heads' appear X times, then the probability of finding a mean $M_N = X/N$ is

$$P\left(\frac{X}{N}\right) = {}^NC_X p^X (1-p)^{(N-X)} \tag{5.5}$$

This is the binomial distribution, which is the most commonly used example of a theory exhibiting large deviations $i.e.$ even when $N \gg 1$, we find a P which falls off slower than Gaussian. $P\left(X/N\right) \sim \exp[-N\left(X/N - p\right)^2/\sigma^2]$. Taking log of both side of equation (5.5), we arrive at:

$$\ln P\left(\frac{X}{N}\right) = X \ln p + (N - X) \ln(1 - p) +$$
$$\ln N! - \ln X! - \ln(N - X)!. \tag{5.6}$$

We know from Stirling's formula that for large N, $N! \simeq N^N e^{-N} \sqrt{2\pi N}$. Applying Stirling's approximation for large N, X, $(N - X)$, the above relation becomes

$$\ln P(x) = -N J(x), \tag{5.7}$$

where,

$$J(x) \equiv x \ln \frac{x}{p} + (1 - x) \ln \left(\frac{1 - x}{1 - p}\right) +$$
$$\frac{1}{2N} \ln x(1 - x) + \frac{1}{2N} \ln N \tag{5.8}$$

and $x \equiv X/N$. This leads to

$$P(x) \quad \sim \quad \frac{1}{\sqrt{Nx(1-x)}} \exp(-NI(x)) \tag{5.9}$$

where,

$$I(x) \equiv x \ln \frac{x}{p} + (1-x) \ln \frac{1-x}{1-p} \tag{5.10}$$

For large enough N the pre-factor changes slowly compared to the exponential term and we get Chernoff's formula where $I(x)$ is the rate function.

5.1.2 The mapping

In order to appreciate the analogy between the large deviation theory and the Jarzynski equality, we need to consider evolution of a relevant system to have a stochastic component, *i.e.* there is a regular time dependent force acting on the system from $t = 0$ to $t = \tau$ as it proceeds from an initial equilibrium state to a final state and in addition there is a random component. Langevin dynamics of a particle of mass m can be considered as a simple example of such a stochastic dynamics:

$$m\ddot{x} = -\frac{\partial V}{\partial x} - \lambda \dot{x} + f(t) + \eta(t) \tag{5.11}$$

where V is a potential function, $f(t)$ is a regular time dependent force, λ is damping coefficient and $\eta(t)$ is random noise. Here dots represent time derivative. Fluctuation theorems are proved for such a system by Kurchan [37] and subsequently by several authors [38, 39, 40, 41]. The time dependent force is switched on at $t = 0$ and switched off at $t = \tau$. At $t = 0$ the system resides in a macroscopic equilibrium state, corresponding to which there exist a large number of microstates. Since we are considering stochastic evolution, we can start from the *same microstate* and do the experiment N times, each time getting different value of the dissipative work. If w_D^i is the dissipative work for i^{th} realisation then we can define W_D [the analogue of M_N is equation (5.4)] as

$$W_D = \frac{1}{N} \sum_{i=1}^{N} w_D^i. \tag{5.12}$$

The distribution of W_D is sought from the large deviation principle.

We now note that $\langle W \rangle \geq \Delta F$ (or, $\langle W_D \rangle \geq 0$) according to the second law of thermodynamics — the equality holds for reversible processes. To implement our scheme, we need to define a transformation which maps W_D to another variable Z such that, $0 \leq Z \leq 1$, in accordance with the experimental mean in coin toss scenario, given in equation (5.4). We consider the variable $W_D + c$, where 'c' is a quantity that we shall fix later. The class of transformation we consider here is

$$Z(W_D) = \frac{1}{2}[1 - \tanh\alpha(W_D + c)], \tag{5.13}$$

where 'α' is a parameter which eventually will have to be fixed using experimental results. Actually, only the positive constant 'α' defines this class of transformations because a constraining relation for c will be established. Our ansatz is that, Z, like W_D, satisfies large deviation principle and the rate function for the coin toss problem is the rate function for Z. So, the rate function for Z is

$$I(Z) = Z \ln\frac{Z}{p} + (1 - Z)\ln\frac{1 - Z}{1 - p}. \tag{5.14}$$

The probability distribution for Z is simply

$$P(Z) \sim \frac{1}{\sqrt{NZ(1 - Z)}} e^{-NI(Z)} \tag{5.15}$$

where N is the number of trajectories used in constructing the experimental mean of the *i.i.d* variables. In our case, X_i in coin tossing experiment and dissipative work w_D^i in equation (5.12) are *i.i.d* variables. We note that $I(Z = 1) = \ln(1/p)$, while $I(Z = 0) = \ln[1/(1 - p)]$. For $p < 1/2$, $I(Z = 0) < I(Z = 1)$. The function $I(Z)$ has a minimum at $Z = p$. Thus the probability $P(Z)$ has a peak at $Z = p$ and is exponentially small at $Z = 0$ and $Z = 1$, but with $P(Z = 0) > P(Z = 1)$, because of the inequality in $I(Z)$. From second law of thermodynamics, we need $\langle W_D \rangle > 0$ for irreversible process, *i.e.* realizations with the outcome $W_D > 0$ is more probable than that of $W_D < 0$. All the above constraints are met since $Z \to 0$ as $W_D \to \infty$ and $Z \to 1$ as $W_D \to -\infty$. We now return to equation (5.13); noting that $e^{-W_D} = e^c[Z/(1 - Z)]^{1/2\alpha}$, we have

$$\langle e^{-W_D} \rangle = \frac{e^c \int_0^1 \left(\frac{Z}{1-Z}\right)^{\frac{1}{2\alpha}} P(Z)dZ}{\int_0^1 P(Z)dZ} \tag{5.16}$$
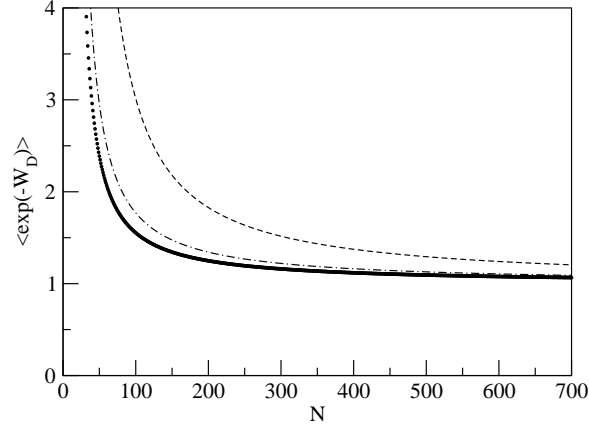
Figure 5.1: In this figure we show the convergence of $\langle \exp(-W_D) \rangle$ with respect to N for different values of α. The thick-dotted, dot-dashed, and dashed lines are respectively for $\alpha = 0.17, 0.57, 0.96$. The curves in the figure are obtained by numerically integrating equation (5.16) by employing Simpson's one-third rule.

The right hand side of equation (5.16) is plotted as a function of N in figure (5.1) for different values of α. As $N \to \infty$, we find $\langle e^{-W_D} \rangle$ converges to unity for all α, as it should according to Jarzynski equality. From figure (5.1) one can see that as α decreases, lesser number of trajectories (or, realizations) are required for the convergence. The convergence is verified for various values of p. The result shown in figure (5.1) is for $p = 0.25$.

5.1.3 Comparison with experiments

We will now obtain $P(W)$ from $P(W_D)$ following the theoretical technique discussed above and compare with the work distribution function obtained experimentally and numerically. From equation (5.13) we write

$$W = \Delta F - c + \frac{1}{2\alpha} \ln \frac{1-Z}{Z} \tag{5.17}$$

We fix $c = \Delta F$ to get the following simple form

$$W = \frac{1}{2\alpha} \ln \frac{1-Z}{Z} \tag{5.18}$$

79

We can now find $P(W)$ by noting the normalisation condition:

$$\int_0^1 P(Z)dZ = \int_{-\infty}^{\infty} P(Z = f(W)) \left| \frac{dZ}{dW} \right| dW = 1 \qquad (5.19)$$

where, $P(Z)$ is given in equation (5.15). The work distribution is then found as

$$P(W) = P(Z = f(W)) \left| \frac{dZ}{dW} \right| \qquad (5.20)$$

with $f(W) = (1 - \tanh \alpha W)/2$ and $P(Z)$ as given by equation (5.15). The parameter N in equation (5.15) can be linked to the width σ of the distribution by appealing to the Gaussian limit which shows that $\sigma^2 = 2p(1-p)/N$. In principle we need to fix three unknown parameters in equation (5.20), *viz.*, σ, α and p. To reduce the task of parameter-adjustments, we pre-assign a value of p. As a result, only α and σ will be used as fitting parameters.

We now show the comparison between our assertion of the form of $P(W_D)$ [and hence $P(W)$] and different experimental and numerical results.

Experiment by Liphardt *et al.*: This experiment tests Jarzynski equality by stretching a single RNA molecule between two conformations — both reversibly and irreversibly. The experiment has been done for three different molecular end-to-end extensions and for each extension, three different stretching rates are considered. For all combinations of extensions and pulling rates, the experiment provides $P(W_D)$. For the present purpose, we consider three distributions corresponding to 15 nm extension, which are shown in the inset of the figure (5.2). Other distributions can also be taken care of similarly. In this work, $P(W_D)$ we compute, depends on two parameters *viz.*, α and σ. We determine these two parameters by comparing with $P(0)$ and $P_{max}(W_D)$ [maximum value of $P(W_D)$] of the corresponding distribution given by Liphardt *et al.*. After fixing these two parameters as $(\alpha, \sigma) \simeq (0.12, 0.07), (0.12, 0.13), (0.14, 0.20)$ for three different pulling rates, we arrive at the full distributions for every pulling rate. This is shown in figure (5.2). We fix $p = 0.48$ here.

Experiment by Blickle *et al.*: This experiment deals with the thermodynamics of an over-damped colloidal particle in a time dependent nonharmonic potential. Blickle *et al.* have not only measured $P(W)$, they have also computed $P(W)$ from the relevant Fokker-Planck dynamics. Our explanation of their $P(W)$ is dependent on the choice of the two parameters α
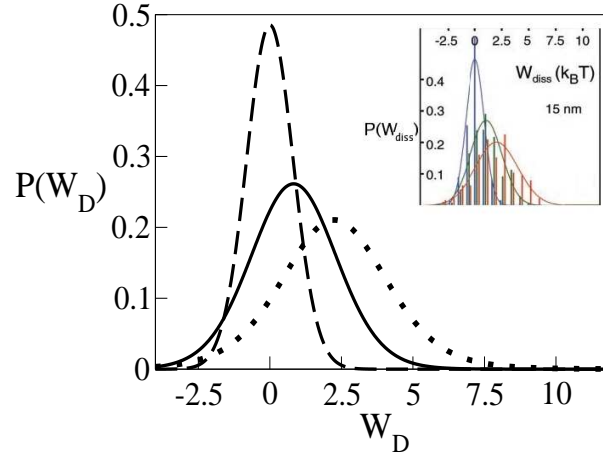
Figure 5.2: The figure of the inset is taken from [33] where dissipated work probability distributions are experimentally obtained for a particular end-to-end extension ($= 15nm$) of P5abc RNA molecule but for three different pulling rates indicated by three different curves — dashed, solid and dotted. In main figure we obtain $P(W_D)$ by fixing α and σ, as required by the theory presented here.

and σ. We determine these parameters by comparing $P(0)$ and $P_{max}(W)$. This fixes $\alpha \simeq 0.1$ and $\sigma \simeq 0.2$. This comparison is shown in figure (5.3). We fix $p = 0.24$ here. The moments found by Blickle *et al.* and us compare as follows (Table I)

Moments	Values from experiment by Blickle *et al.*	Values from the theory presented here
$\langle W \rangle$	2.4	2.40
$\langle W^2 \rangle$	11.6	11.74
$\langle W^3 \rangle$	63.7	64.11

Since we use only two parameters (α and σ) to get the distribution, it implies that only $\langle W \rangle$ and $\langle W^2 \rangle$ have been used. This leaves the $\langle W^3 \rangle$ as a prediction which can be compared with the experimental data. A more sensitive quantity to measure asymmetry of a distribution is $\langle \Delta W^3 \rangle$, where $\Delta W = W - \langle W \rangle$. Our distribution shows that this moment is nonzero. If $p \neq 1/2$, then $|\langle \Delta W^3 \rangle|/(\sigma|1 - 2p|\langle \Delta W^2 \rangle^{3/2})$ is a constant, the value of which in our case is
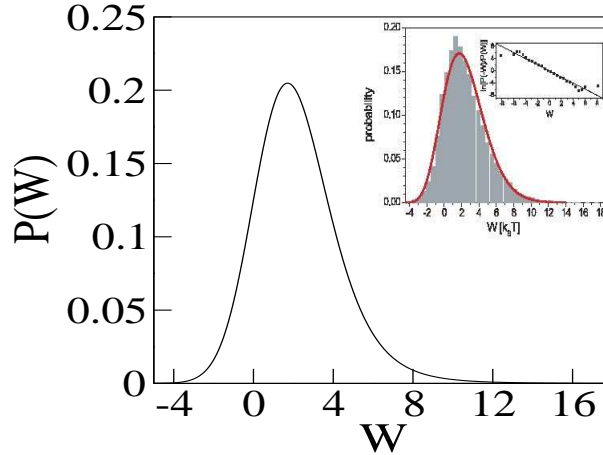
Figure 5.3: The figure of the inset is taken from [34], which shows experimentally as well as numerically obtained work probability distribution function for an overdamped colloidal particle in a time-dependent nonharmonic potential. In the main figure we obtain $P(W)$ from the theory presented here.

$\sim$10. Nonzero $\langle \Delta W^3 \rangle$ corresponds to asymmetry of $P(W)$ that has been observed whenever the dynamics has been nonlinear[35, 36]. In those cases the cause of the asymmetry is the strength of the nonlinear term. Here the role is played by $(1 - 2p)$ (though, no particular dynamics is explicitly involved here) and it can be considered as a measure of asymmetry.

Driven anharmonic oscillator: We consider here a Brownian particle, trapped by the potential $V(x) = kx^2 + \gamma x^4$ (where k and γ are constants) and driven by a linearly time-dependent force $f(t)$. The evolution is taken to be governed by following overdamped Langevin dynamics,

$$\lambda \dot{x} + \frac{\partial V}{\partial x} = f(t) + \eta(t). \tag{5.21}$$

Here $\eta(t)$ is the random noise coming from heat bath. We assume $\langle \eta(t) \rangle = 0$ and $\langle \eta(t)\eta(t') \rangle = 2T\lambda\delta(t - t')$, where T is temperature of the bath. The force $f(t)$ acts from $t = 0$ to $t = \tau$ and $P(W)$ (where $W = -\int_0^\tau \dot{f}(t)x(t)dt$) is numerically obtained. The comparison between numerically obtained $P(W)$ and that obtained from equation (5.20) with $\alpha \simeq 0.15$ and $\sigma \simeq 0.062$ is shown in figure (5.4). We fix $p = 0.28$ here. Thus, one should note here that the strength of the discussed framework is due to its simplicity because we require only few parameters
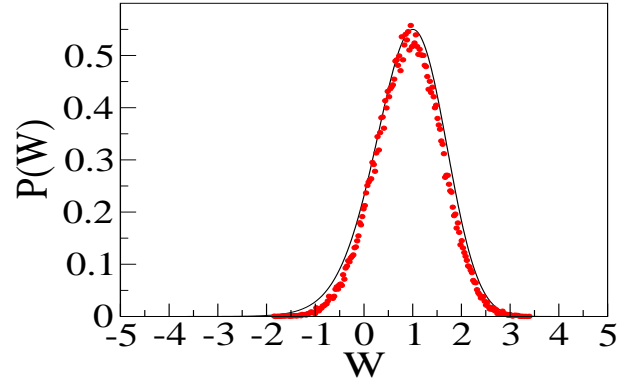
Figure 5.4: In this figure we show how $P(W)$, calculated by simulating the dynamics of a driven Brownian particle obeying equation (5.21) (shown in dots) collapses to the $P(W)$ calculated from the distribution for tossing a biased coin (shown in black solid line), as it is prescribed here. For simulating the dynamics we take $k = 1, T = 1, \lambda = 1$ and $\gamma = 0.1$.

from experiments and elementary results from large deviation theory to construct a full work probability distribution and its applicability to various systems which may differ widely by the dynamical rules they follow. We believe that it is possible to make better contact with experiments by constructing more appropriate form for the function Z. Readers would also appreciate that we could derive results concerning Jarzynski equality merely by focusing on the rare events — rare negative dissipation — that enter into Jarzynski equality and mapping them onto the biased coin-toss-experiments. Here we have discussed situations where the evolution had a stochastic component in addition to the regular time dependent force. We hope to extend it to the deterministic situations. In the deterministic case, we envisage the following picture. The evolution of a nonlinear system under time dependent drive is intrinsically chaotic and we can exploit that to define an "experimental mean" for w_D^i. In this case, we need to consider the different initial conditions around an ϵ-neighbourhood ($\epsilon \to 0$) of a given microstate and since the evolution of each initial microstate (from same initial macrostate) will be different from each other due to the chaotic flow, we can define W_D as in equation (5.12). Therefore, in accordance with our contention, above is an example where the simple coin toss is the 'Gaussian

model' for the problems where rare events play significant role. In the next section we will show that another natural phenomena—turbulence—where fluid in vigorous motion is certainly far away from equilibrium, can be viewed with the rare outcomes of a coin tossing experiment.

5.2 Turbulence and rare events in tossing a coin

Fully developed turbulence in fluid [11, 42, 43, 14, 15, 16, 17, 18, 19, 44, 13] is basically multifractal — a term coined for the very first time in a paper by Benzi et. al.[45]. The multifractal formulation has been documented in great details by Parisi *et. al.*[46] (also see [47]). Among the precursors to the multifractal formulation are the works by Kolmogorov[11], Obukov[42] and Mandelbort[48]. It is widely accepted that the concept of multifractality, technically speaking, stands on the shoulders of the large deviation theory[25, 26, 27, 28]. However, one should be careful enough while using large deviation theory in turbulence for deriving exponents of the velocity structure functions because Frisch *et. al.*[49] have shown that one must make use of 'refined' large deviation theorem[50] as had already been anticipated by experimentalists[51] on the basis of a normalization requirement.

The scaling exponents of the structure functions of the velocity field difference between two points in a turbulent fluid are known to be related nonlinearly on the orders of the structure functions. In the model of Kolmogorov and Obukhov, the nonlinearity was for the first time, attributed to large fluctuations in the velocity difference which in turn was supposed to be triggered by large fluctuations in the dissipation rate coarse grained at the same scale. Since then a number of models have been proposed to understand the essential features of this 'intermittent' behavior. Among these there is the multifractal model referred to above which interprets the experimental results by assuming multifractal nature for the probability distribution function of the energy dissipation rate. This model does not make predictions, rather interprets the exponents of the scaling laws for the coarse grained dissipation field in terms of a singularity spectrum, defined as the Legendre transform of the exponents.

Within the paradigm of multifractal model of turbulence, where one assumes that the velocity has a local scale invariance, it is not quite hard to find phenomenological models that can

faithfully enough reproduce anomalous scaling exponents. However, what we have focused on in this paper is quite different than what the usual research on multifractality is all about. We emphasize that the rare events present in the distribution of energy dissipation in real space, when 'mapped' appropriately on the phenomenon of large deviations found in simple coin toss, are enough to yield anomalous exponents. Quite interestingly, here one does not has to fall back on any explicit model of energy cascade e.g. random multiplicative model[49] etc.

In what follows in this section shortly, we propose an approach that allows us to construct a simple (tunable) parameter dependent model that has the amazing potential of yielding quantitative results. While constructing such a model, we mainly rely on the observation that the concerned physical process (here, turbulence) has certain relevant rare events present in it. In the case of turbulence, our model's success can be interpreted as the re-confirmation that the phenomenon of multifractality owes itself to the rare events present in the distribution of energy dissipation. To be precise, to construct our model for turbulence, we have assumed that square of one-dimensional velocity gradient (scaled appropriately as shown later in equations (5.24) to (5.26)) minus the expected mean of the energy dissipation rate is a bounded, independent and identically distributed random variable. On the face of the fact that velocity field is random in a turbulent flow, this assumption is not very artificial. We want to stress here that our model does not stand against the multifractal model of turbulence. Rather, our model suppliments the multifractal model and also, uses its results for benchmarking. Our framework, on the top of it, has the advantage of being applicable to any other physical phenomenon where there is no known multifractal (or any other) explanation of the results due to the presence of rare events therein. Our methodology may look like a 'black-box' but the point is that it is capable of delivering genuine results that can be experimentally verified.The central result from the coin tossing experiment we will use, is given in (5.9) and (5.10).

Turning to turbulence, in 1941 Kolmogorov[52] invoked the concept of Richardson's cascade[53] of eddies to propose a phenomenological model (K41) for three dimensional incompressible turbulence at high Reynolds number. Even today this is the cornerstone of our understanding of turbulence. Understanding turbulence is understanding the small scale behaviour of the velocity structure function $S_q(l)$, where $S_q(l) \equiv \langle |\Delta \vec{v}.(\vec{l}/|l|)|^q \rangle$, with $\Delta \vec{v} \equiv \vec{v}(\vec{r} + \vec{l}) - \vec{v}(\vec{r})$ and

'*l*' is a distance which is short compared to macroscopic length scales like the system size but is large compared to molecular scale where viscous dissipation takes place. The angular bracket denotes ensemble average (i.e. average over different values of '$\vec{r}$'). The observation is that $S_q(l)$ has a scaling behaviour l^{ζ_q} where l is in the range indicated (so called inertial range). Finding ζ_q can be described as the holy grail of turbulence. K41 gives $\zeta_q = q/3$ — a result which is exact for $q = 3$ and very close to experimental findings for low value of q. There is systematic departure from $q/3$ at relatively higher values of q. This is the phenomenon of intermittency. Of particular interest is the case $q = 6$. Since $|\Delta v|^3/l$ is a measure of the local energy transfer rate (same as energy input and energy dissipation rate in K41 and thus a constant), we expect $\zeta_6 = 2$. The deviation $2 - \zeta_6$ is thus a very sensitive quantity and is often singled out for special treatment. The exponent $\mu = 2 - \zeta_6$ is formally called the intermittency exponent and the experimental measurements agree on a value 0.2 for μ. It can be viewed as the co-dimension of dissipative structures.

The model of intermittency are usually constructed on a phenomenological basis by thinking of various ways of modifying the Richardson's cascade picture. The β-model, the bifractal model and the multifractal model all belong to this class. The crucial hypothesis is that the daughter eddies produced from the mother eddies are not space filling and the active part of space is in general a multifractal. The velocity field has different scaling exponents on different fractal sets that form the multifractal structure. These scaling exponents can, in principle, yield ζ_q. This multifractality can also be defined and measured in terms of the fluctuations of the local dissipation rate rather than in terms of the fluctuations of the velocity increments Δv. The key element, that is needed to define multifractality in terms of dissipation is the local space average of energy dissipation over a ball of radius l centered around a point at $\vec{r}$: $\varepsilon_l(\vec{r}) \equiv \frac{3\nu}{8\pi l^3} \int_{|\vec{r'} - \vec{r}| < l} d^3\vec{r'} \sum_{i,j} [\partial_j v_i(\vec{r'}) + \partial_i v_j(\vec{r'})]^2$. If the dissipation is multifractal, moments of ε_l follow a power law behaviour at small l, i.e. $\langle \varepsilon_l^q \rangle \sim l^{\tau_q}$. Kolmogorov's refined similarity hypothesis relates the statistical properties of fluctuation of velocity increment to those of the space averaged dissipation and yields: $\zeta_q = \frac{q}{3} + \tau_{q/3}$. We now carry out the usual speculation that since the higher order velocity structure factors differ most strongly from K41, then the probability distribution for the velocity increments must differ most strongly from that appro-

priate to K41 in the tail of the distribution. The tail of a distribution involves rare events and this is how the theory of large deviations enters the picture. Following Landau's observation on K41[11], Kolmogorov[11] and Obukhov[42] introduced fluctuations in the dissipation rate. Careful experiments revealed the existence of these fluctuations. The fluctuations, however, occur rarely and these are the rare events of turbulence. This allows us to establish a quantitative bridge between turbulence and theory of large deviations. The above discussion parallels what can be found in [19] (in particular Sec. 8.6.4). The quantitative development in [49] thereafter focuses on a particular model which has been taken to be a random cascade model. What is clearly shown over there is the fact that the general random cascade model which exhibit multifractal behavior is related to the large deviation theory in which the rate function $I(x)$ in equation(5.10) is just the $f(\alpha)$ function of a multifractal distribution. What we will do in the following will be to exploit the above discussion by a) treating the dissipation at different points inside a coarse graining volume as independent random variables and b) using a suitable mapping which makes the result from Cramers' theorem for the coin toss, relevant.

More than a decade ago, Stolovitzky and Sreenivasan[44], in a somewhat different approach tried to validate refined similarity hypothesis by viewing turbulence as a general stochastic process (fractional Brownian motion to be precise). While this was a very significant achievement, there was a shortcoming in that the theory ruled out the existence of correlation functions like S_3. It indeed is surprising since the readers may know that the only exact non-trivial result existing in the theory of turbulence is Kolmogorov law: $S_3(l) = -\frac{4}{5}\varepsilon l$. However as we shall note, their approach allows us to make direct contact with the terms of large deviation that signify the occurrence of rare events. It can be observed that deviation of ε_l from the expected mean ε plays the role of M_N of equation (5.4) and it is what we are interested in. As $l \to \infty$, this deviation variable has a distribution according to the role of equation (5.9). We hope a simplification: The $\varepsilon_l - \varepsilon$ can range from large negative to large positive values. We bring the range between 0 to 1 by defining a variable as:

$$Z_T(\varepsilon_l) \equiv \frac{1}{2}\left[1 + \tanh\left(\frac{\varepsilon_l - \varepsilon}{\Xi}\right)\right] \tag{5.22}$$

where Ξ is a constant with dimension of ε. We now make the drastic assumption that since $\varepsilon_l - \varepsilon$ is a rare event, the distribution of Z_T can be considered similar to that for the coin-toss with a biased coin and accordingly, we can hypothesize that

$$P(Z_T) \propto e^{-NI(Z_T)} \tag{5.23}$$

Here, N is number of random variables. This simple model yields value of $\mu \approx 0.16$ which is quite close to the presently accepted value. It can be taken as an *a posteriori* justification for our seemingly bold above-proposed postulate regarding the distribution of $Z_T(\varepsilon_l)$. Also, a ζ_q vs q plot has been obtained that is not only convex but also follows She-Leveque scaling[13] faithfully enough for a model as simple as this (figure 5.5).

In what follows we describe how these results are arrived at. The one dimensional velocity derivative can be use to express the global average of the full energy dissipation if local isotropy exists[54, 55]. The velocity increment is given by

$$\Delta v(l) = \int_r^{r+l} \frac{dv}{dr} dr \tag{5.24}$$

and *ergo,* the energy dissipation rate is

$$\varepsilon(l) = \frac{15\nu}{l} \int_r^{r+l} \left(\frac{dv}{dr} \right)^2 dr \tag{5.25}$$

If we define $D_i \equiv \frac{dv}{dr}\big|_i \left[\frac{\eta\sqrt{15\varepsilon}}{(\eta\varepsilon)^{1/3}} \right]$ and $N \equiv \frac{l}{K\eta}$ (where, η is Kolmogorov scale, $(\eta\varepsilon)^{1/3}$ is Kolmogorov velocity scale and K is the number of Kolmogorov scales over which one obtains smoothness), then equation (5.25) may be rewritten, upon discretization, as:

$$\varepsilon_l - \varepsilon = \frac{1}{N} \sum_{i=1}^{N} Y_i \tag{5.26}$$

Here, $Y_i \equiv D_i^2 - \varepsilon$. The link between the phenomenology of turbulence and the theory of large deviation comes from the above equation where we assume each Y_i to be an independently distributed random variable. It is the possibility that the experimental average as expressed in equation (5.26) can show significant departure from zero for large $N(N \propto l)$ leads to the l-dependence of the powers of the deviation $\epsilon_l - \epsilon$ and thus to the multifractality of turbulence.
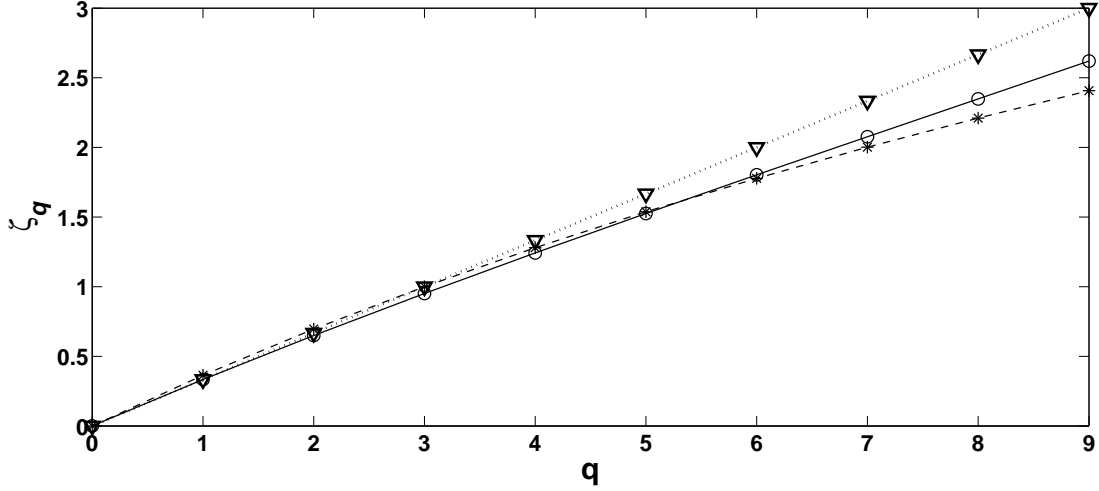
Figure 5.5: ζ_q *vs.* q **curve in fully developed fluid turbulence**. The dashed line joining the asterisks is the celebrated She-Leveque scaling law. The circles joined by the solid line denote the values of ζ_p (for corresponding q) as obtained by dint of the model proposed herein. To appreciate the convexity of the aforementioned curves, a dotted line joining triangles, in accordance with the classical linear Kolmogorov prediction, has also been plotted. For every q, first $\langle |\varepsilon_l - \varepsilon|^q \rangle$ *vs.* N is plotted in log-log scale using the data yielded during the numerical integration of equation (5.27) and then the observation that for $N = 30$ to 60, we get a fairly straight line leads us to attempt fitting the range linearly. The process gives a value for τ_q. The relation $\zeta_q = q/3 + \tau_q$, then, tells us what is the corresponding value for ζ_q. One can see, the fit is remarkable. There is room for improvement in extending the inertial range and in getting better fit for higher ζ_q's. As mentioned in this letter, the form of Z_T is crucial.

As we would like to emphasize that this is a very direct way of quantifying the link between turbulence phenomenology and the theory of large deviations with the help of the binomial distribution. The fact that the results are not as good as She and Leveque [13] is merely a statement of the fact that the assumed binomial distribution is not the most accurate one. Here, we have assumed the relation (5.26) to be the parallel of equation (5.4). Owing to the contraction principle, the rate functions for $\varepsilon_l - \varepsilon$ and $Z(\varepsilon_l)$ are same. Thus, using equations (5.9), (5.22) and (5.23), we can write:

$$\langle |\varepsilon_l - \varepsilon|^q \rangle = \left| \frac{\Xi}{2} \right|^q \left[\frac{\int_0^1 \left| \ln\left(\frac{x}{1-x}\right) \right|^q \left\{ \left(\frac{p}{x}\right)^x \left(\frac{1-p}{1-x}\right)^{1-x} \right\}^N dx}{\int_0^1 \left\{ \left(\frac{p}{x}\right)^x \left(\frac{1-p}{1-x}\right)^{1-x} \right\}^N dx} \right] \tag{5.27}$$

We assume that to the leading order $\langle |\varepsilon_l - \varepsilon|^q \rangle \sim l^{\tau_q}$. By trial and error, we fix the inertial range as $N = 30$ to 60 and calculate numerically $\mu(= -\tau_2) = 0.16$. Similarly, we calculate $\zeta_q(= q/3 + \tau_{q/3})$ for various q. Note that to obtain the numerical solution for the integrals in equation (5.27), we have dropped the diverging terms from the finite series that represent the integrands as they are suitably discretized for their evaluation by Simpson's one-third rule.

Our model's inherent bias for the value 0.26 for the parameter p in order to closely mimic the realistic turbulent fluid's scaling properties would seem so natural when it is compared with a particular successful multifractal cascade model[56] based on a generalized two-scale Cantor set. In that model, as the eddies breakdown into two new ones, the flux of kinetic energy into the smaller scales is hypothesized to be dividing into non-equal fractions $p = 0.3$ (quite close to our value of $p = 0.26$!) and $1 - p = 0.7$. It could fit remarkably well the entire spectrum of generalized dimensions[57] and (equivalently) the singularity spectrum (the so-called $f - \alpha$ curve[58]) for the energy dissipation field in many a turbulent flow.

Finally we would like to point out the simplicity of biased coin-toss models and its reasonably astonishing success in predicting μ reduces the need for more complicated models. We believe just by being able to find a more appropriate function Z_T, we can make big leaps in the rather complex theory of turbulence. One should note that the refined large deviation theorem, which implies the presence of the factor $\sqrt{N}$ in the probability density, has no extra effect on the results derived herein using large deviation theorem. As readers must have appreciated, we

could derive results concerning anomalous exponents (showcasing intermittency in turbulence) merely by focusing on the presence of rare events in the distribution of energy dissipation rate and by mapping them appropriately on the phenomenon of large deviations found in simple coin toss. Therefore, it is in accordance with our contention that the simple coin toss is the 'Gaussian model' for the problems where rare events play significant role. Within this very framework, we hope to model various other physical phenomena that are dominated by rare events; after all, now we have a working approach to arrive at quantitative results for such processes that cannot be usually solved otherwise.

5.3 Summary

In this chapter we show that why rare events should be considered as an important ingredient to understand various nonequilibrium phenomena, starting from stretching of RNA molecule to a fully turbulent fluid. Using a probability distribution that takes care of large deviations, here we have calculated full work probability distributions for different systems and the multifractal exponents of the order structure factors in fully developed turbulence. Results are satisfactorily close to the experiments.

Bibliography

[1] Y. Oono, Prog. Theor. Phys. Supp. 99, 165, 1989.

[2] J. Kurchan, J. Stat. Mech. P07005 (2007), doi.10.1088/1742-5468/2007/07/P07005.

[3] D. J Evans and D J Searles, Phys. Rev. Lett. **96**, 120603 (2006).

[4] E. M Shevick et al, Ann. Rev. Phys. Chem. **39**, 2007.

[5] T. Bodineau and B Derrida, Phys. Rev. Lett. **92**, 180601 (2004).

[6] G. Gallavoti and E G D Cohen, Phys. Rev. Lett. **74**, 2694 (1995).

[7] D. J Evans and D J Searles, Phys. Rev. E **50**, 1645 (,) 1994.

[8] C. Jarzynski, Phys. Rev. Lett. **78**, 2690 (1997)

[9] G. E. Crooks, J. Stat. Phys. 90, 1481, 1998

[10] U. Seifert, Phys. Rev. Lett. **95**, 040602 (2005)

[11] A. N. Kolmogorov, J. Fluid Mech. 12, 82 (1962), L. D. Landau and E M Lifshitz, Fluid mechanics, course of theoretical physics (Pergamon, Oxford, 1962) Vol. 6.

[12] C. Meneveau and K R Sreenivasan, Phys. Rev. Lett. **59**, 1424 (1987).

[13] Z. She and E Leveque, Phys. Rev. Lett. **72**, 336 (1994).

[14] V-Lvov and I Procaccia, Phys. Rev. E **52**, 3840 (1995); Phys. Rev. E **54**, 6268 (1996); Phys. Rev. E **55**, 7030 (1997).

Bibliography

[15] A. Das and J K Bhattacharjee, Europhys. Lett. **26**, 527 (1994).

[16] A. Sain, Manu and R Pandit, Phys. Rev. Lett. **81**, 4377 (1998).

[17] D. Mitra and R Pandit, Phys. Rev. Lett. **93**, 024501 (2004).

[18] K. R. Sreenivasan and R A Antonia, Ann. Rev. Fluid Mech., 29, 435, 1997.

[19] U. Frisch, Turbulence (Cambridge University Press, 1996).

[20] B. Derrida, A J Bray and C Godreche, J. Phys. A, 27, L357 (1994).

[21] S. N. Majumdar and C Sire, Phys. Rev. Lett. **77**, 1420 (1996)

[22] S. N. Majumdar, Curr. Sci. 77, 370 (1996)

[23] J. Krug et al, Phys. Rev. E **56**, 2702 (1997)

[24] M. Constantin et al, Phys. Rev. E **69**, 061608 (2004)

[25] H. Cramer, Actualités Scientifiques et Industrielles **736**, 5 (1938).

[26] R. S. Ellis, Physica D **133**, 106 (1999).

[27] A. Dembo and O. Zeitouni, Large Deviations Techniques and Applications, (Springer), (1997).

[28] S. R. S. Varadhan, *Large Deviations and Applications* (SIAM), (1984).

[29] A. Imparato and L. Peliti, Phys. Biol. **6**, 1 (2009).

[30] F. Douarche, S. Ciliberto, A. Petrosyan and I. Rabbiosi, Europhys. Lett **70**, 593 (2005).

[31] A. Dhar, Phys. Rev. E. **71**, 036126 (2005).

[32] R. Marathe and A. Dhar, Phys. Rev. E. **72**, 066112 (2005).

[33] J. Liphardt, S. Dumont, S. Smith, I. Tinoco, and C. Busta-mante, Science **296**, 1832 (2002).

[34] V. Blickle, T. Speck, L. Helden, U. Seifert and C. Bechinger, Phys. Rev. Lett. **96**, 070603 (2006).

[35] A. Saha and J. K. Bhattacharjee, J.Phys A **40**, 13269 (2007).

[36] T. Mai and A. Dhar Phys. Rev. E. **75**, 061101 (2007).

[37] J. Kurchan, J.Phys A **31**, 3719 (1998).

[38] J. L. Lebowitz and H. Spohn, J. Stat. Phys **95**, 333 (1999).

[39] J. Farago, J. Stat. Phys **107**, 781 (2002).

[40] R. Von. Zon, S. Ciliberto and E.G.D. Cohen, Phys. Rev. Lett. **92**, 130601 (2004).

[41] O. Narayan and A. Dhar, J.Phys A **37**, 63 (2004).

[42] A. M. Obukov, J. Fluid. Mech. **13**, 77 (1962).

[43] C. Meneveau and K. R. Sreenivasan, J. Fluid Mech. **224**, 429 (1991).

[44] G. Stolovitzky and K. R. Sreenivasan, Rev. Mod. Phys. **66**, 229 (1994).

[45] R. Benzi, G. Paladin, G. Parisi and A. Vulpiani, J. Phys. A: Math Gen. **17**, 3521 (1984).

[46] G. Parisi and U. Frisch, *Turbulence and Predictibility of Geohysical Fluid Dynamics* ed. M Ghil, R. Benzi and G. Parisi (Amsterdam: North Holland), (1985).

[47] G Boffetta, A Mazzino and A Vulpiani, J. Phys. A: Math Theor. **41**, 363001 (2008).

[48] B. B. Mandelbort, J. Fluid Mech. **62**, 331 (1974).

[49] U. Frisch, M. Afonso Martins, A. Mazzino and V. Yakhot, J. Fluid Mech. **542**, 97 (2005).

[50] R. R. Bahadur and R. Ranga Rao, Ann. Math. Stat. **31**, 1015 (1960).

[51] C. Meneveau and K. R. Sreenivasan, Phys. Lett. A **137**, 103 (1989).

Bibliography

[52] A. N. Kolmogorov, Dokl. Akad. Nauk SSSR, **32**, 1 (1941); (English translation: Proc. R. Soc. Lond. A **434**, 15 (1991)).

[53] L. F. Richardson, Cambridge University Press (Cambridge), (1922).

[54] G. I. Taylor, Proc. R. Soc. London, Ser. A **151**, 421 (1935).

[55] S. Chen, G. D. Doolen, R. H. Kraichnan and Z-S. She, Phys. Fluids A **5**(2), 458 (1993).

[56] C. Meneveau and K. R. Sreenivasan, Phys. Rev. Lett. **59**, 1424 (1987).

[57] H. G. E. Hentschel and I. Procaccia, Physica D **8**, 435 (1983).

[58] T. C. Halsey, M. H. Jensen, L. Kadanoff, I. Procaccia and B. I. Shraiman, Phys. Rev. A **33**, 1141 (1986).

6 Drive-induced lamellar ordering in binary suspensions

In this chapter we will study the feasibility of driven segregation of suspensions of soft colloidal particles using space (x) and time (t) dependent optical trapping potentials in one dimension. The fact that by radiation pressure the particles in a colloidal suspension can be forced into rows aligned along the light-intensity interference fringes produced by crossed laser beams [3, 4, 5], is employed to create externally tunable optical potential for the suspensions. Two kinds of potentials are used— a symmetric oscillatory ramp ($|x|$) potential and a sawtooth flashing ratchet potential; with a mirror plane at the origin . We show that flashing of the ratchet potential leads to a micro-phase segregated lamellar steady state at large t though the oscillation of the $|x|$ potential does not. Potential applications of our study will also be discussed.

6.1 Soft matter- a pedagogical introduction

In this chapter we will deal with the physical system that belongs to a broad class, called '*soft matter*' in recent literatures (a nice review on the subject may be [1]). The term 'soft matter' describes a very large class of materials whose common characteristic is that they are composed of mesoscopic particles, i.e., particles with typical sizes 1 nm - 1 μm, dispersed into a solvent whose molecules are much smaller in size (typically of atomic dimensions). In addition, soft matter systems may contain other, smaller units such as short polymeric chains, salt dissociated

into ions, etc. Other terms that are used as synonyms are complex fluids as well as colloidal suspensions.

Colloids are abundant in everyday experience. From mayonnaise to blood and from ink to smoke, soft matter is what we are made of and what we use in countless industrial applications in the chemical, pharmaceutical and food industries. Microemulsions as well as self-organized micelles of soap molecules in aqueous solutions also belong to the same category. According to the definition of the International Union of Pure and Applied Chemistry, the term 'colloid' describes supramolecular entities whose extension in at least one spatial direction lies between 1 nm and 1 μm. Hence, not only spherical but also ellipsoidal particles in solution, as well as platelets and rods in suspension can be classified as colloidal systems. The macromolecules form the disperse phase and the solvent the dispersion medium. Both can be in any of the three states of matter, thus giving rise to a large variety of colloidal dispersions. We rather focus our attention on a particular type of soft matter systems, namely on suspensions of spherical mesoscopic particles in liquid medium.

The mesoscopic size of the constituent suspended particles is the key in understanding the fact that such systems are indeed soft, i.e., they have a rigidity against mechanical deformations which is many orders of magnitude smaller than that of their atomic counterparts. To illustrate this point, let us consider a perfect crystal having lattice constant 'a'. This crystal is sheared by an external force with the result that every lattice plane is displaced parallel to itself by an amount x, with respect to the plane immediately below it. Associated with this deformation is an energy per unit area $u(x)$ which, for small values of x, is a quadratic function of the deformation, as $x = 0$ is an equilibrium position. In a crystal, this energy depends on the direction of the applied shear and it is given in general by a relation as $u(x) = \frac{G}{2} \left(\frac{x}{a} \right)^2$, where G stands for any one of the several elastic constants of the solid. The elastic constants can be calculated within the framework of the theory of the harmonic crystal and the expression giving these constants can be written in terms of the microscopic interactions and the crystal structure [2] . Assuming that the pairwise, spherically symmetric interaction between the particles is given by $\phi(r)$ and that only nearest neighbour interactions are relevant, one can show that in a simple cubic crystal the elastic constant c_{xxxx}, taken as representative for G, is given

through the expression $c_{xxxx} = G = \frac{\epsilon}{v}\phi''(r = a, \mathbf{p})$ [2], where ϵ is the energy scale of the atomic interaction, v is the volume of a unit cell and the set of parameters $\mathbf{p}$ determines the range of the atomic interaction potential or the relative extent of its repulsive and attractive parts. The energy scale ϵ for atomic systems, ranges from 0.1 eV for the noble gases to 10 eV for the alkali halides and the metals. For typical colloidal crystals, ϵ ranges between $1K_BT - 100K_BT$ (K_B is Boltzmann constant and T is the temperature). As $K_BT \sim 1/40$ eV, at room temperature, we can conclude that the energy scales for atomic and colloidal systems are about the same. The family of functions ϕ is rather insensitive to the set of parameters $\mathbf{p}$. Therefore, the major difference in the values of the elastic constants comes from v of the expression of G because the typical length scales involved in colloidal crystals exceed those of their atomic counterparts by three to four orders of magnitude, the ratio between the elastic constants of colloidal and atomic systems is extremely small — $G_{colloidal} : G_{atomic} = 10^{-12} - 10^{-9}$. This shows that there is an enormous difference in the critical stress required to cleave an atomic and a colloidal crystal. One can shear the latter by moving one's little finger but one needs to apply extreme shear stresses in order to shear the former.

6.2 Segregation and mixing

Segregation and mixing of dissimilar 'objects'- representing biomolecules, colloidal particles, polymers etc, are important problems in physics as well as other branches of science like biology, chemistry etc, both from fundamental and practical points of view. There are two fundamentally different circumstances under which mixing and demixing can occur: first it can happen in the bulk towards thermodynamically stable equilibrium phases. The end stages of demixing is then governed by the equilibrium bulk phase diagram which can allow for coexistence of two phases with different concentrations (macro-phase- separation) [6, 7] or for stable internally segregated structures on the particle scale (micro-phase-separation) [8]. Second, mixing can occur under full nonequilibrium conditions in the sense that an external drive will bring the system into a nonequilibrium steady state (NSS) [9, 10]. While the former case has been explored

by now and many fluid-fluid demixing bulk phase diagrams and stable micro-phase-separated states are known by experiment [11, 12], theory [13, 14] and simulation [15, 16, 17], most of the applications happen under full nonequilibrium conditions. This is true for techniques like density gradient centrifugation [18], liquid chromatography [19], and applies also to the traditional brazil nut effect [20] of shaken granular matter. Whether and how an external drive stimulates separation in binary colloidal mixtures is a fascinating question even for relatively simple situations: A constant drive (as realized in sedimentation and electrophoresis) can yield lanes of separated particles [21, 22, 23], sheared colloidal mixtures can aggregate into bands in the shear directions [24, 25, 26]. What is by far less understood, however, is the efficiency of a *time-dependent* (e.g. oscillatory) external drive on particle separation. Here we explore this for time dependent confining fields acting on a binary colloidal mixture. The field is periodically compressing and releasing the particles such that the system reaches an oscillatory steady state. The constituents of a binary mixture, having a density higher than a critical density ρ_c, spontaneously segregate over a microscopic length scale producing a stable micro-phase separated lamellar steady state. If the initial density is below the critical one, no phase separation occurs in equilibrium. We find that even if the initial density of the mixture is below ρ_c, time dependent external drive, depending on its spatial structure, can enhance the density of the mixture above ρ_c, so that finally a microscopically phase segregated steady state is produced far from equilibrium. Here dynamics, as well as the spatial structure play an important role behind phase segregation. To illustrate this we use two different external drives, one of which allows dynamical phase segregation and the other which does not. The results in contrast will manifest the role of dynamics and the structure as well, necessary for phase separation. First we use an oscillatory $|x|$ potential to drive the system. This external time dependent potential is such that it cannot enhance the density sufficiently and consequently there is no phase separation. Next we use a particularly arranged flashing ratchet potential, described later in detail, as the external drive. In this case we get a microscopically phase segregated steady state far from equilibrium.

6.3 Model

We consider a one dimensional system of interacting soft polymeric particles attached to a thermal bath at temperature T and placed in space and time dependent external potentials. The particles follow overdamped Brownian motion and interact with each other via soft, repulsive, Gaussian core potential [27, 28, 29]. This interparticle pair potential is a good description for soft colloidal particles like polymer coils, dendrimers or weakly charged poly-electrolyte chains [30]. Dynamical density functional theory (DDFT)[33, 34] is applied to solve for the time dependent density of the system which approaches a NSS. A brief introduction of DDFT is given in the appendix of this chapter for completeness. The interparticle Gaussian potential is given by $V_{ij}^{\alpha\beta} = A^{\alpha\beta} \exp(\frac{-(x_i^\alpha - x_j^\beta)^2}{2\sigma_{\alpha\beta}^2})$ where $\alpha, \beta = 1, 2$ are the species index and indices i, j go over the number of particles N. The strengths of the interaction $A^{\alpha\beta}$ have been set equal to each other and is scaled to $K_B T$, where K_B is the Boltzmann constant and T is the temperature of the system. The length scales $\sigma_{11} = \sigma_1$, $\sigma_{22} = \sigma_2$ and σ_{12} are proportional to radius of gyration of the polymer chains. We take, $\sigma_1 \neq \sigma_2$ and $\sigma_{12} < \frac{\sigma_1 + \sigma_2}{2}$. Thus, the polymers differ from each other only by their radius of gyration; the latter constraint helps the polymers to form a mixed state in equilibrium. Here we consider only the equiatomic binary mixture for simplicity.

Starting with a uniform density $\rho < \rho_c(\sigma_1, \sigma_2, T)$, we prepare a mixed state of the polymers at equilibrium, confined by the time independent external potential $V_0|x|$. Then we switch on the oscillation with frequency ω. The time dependent external drive can be written as $V_1(x,t) = V_0|x|\cos^2(\omega t)$ which produces a particle-current towards $x = 0$, finally resulting a nonequilibrium steady build-up around the minima of the external potential in NSS. In this case the density never goes above ρ_c and consequently no phase-segregation is observed for the dynamics. We get the final density profile by solving DDFT equations. The effect of the oscillatory dynamics on the polymeric mixed state shows up prominently in the variation of density at $x = 0$, (say, $\rho(0)$) with increasing driving frequency (i.e. ω). When the driving frequency is zero we get maximum density at $x = 0$ and it decreases as ω increases. For very large frequency $V_0 \rightarrow \frac{V_0}{2}$, because $\lim_{\omega \rightarrow \infty} \frac{1}{\tau_0} \int_0^{\tau_0} \cos^2(\omega t) dt = \frac{1}{2}$, where τ_0 is the duration of the external drive. So, dynamics reduces the "effective" amplitude of the oscillation and

consequently the density. This suggests, if we start with subcritical density, it will become even lower in NSS when we apply $V_1(x,t)$ and we have no phase separation at the end of the process. These results are in excellent agreement with independent Brownian dynamics simulations which constitutes stringent test for our numerics.

Now we consider a system of flashing ratchets - $V_2(x,t)$, given by

$$
\begin{aligned}
V_2(x,t) &= V_{on}(x) \qquad mt_0 \leq t \leq (m+1/2)t_0 \\
&= 0 \qquad\qquad else
\end{aligned}
\tag{6.1}
$$

where $V_{on}(x)$ is

$$
\begin{aligned}
V_{on}(x) & \tag{6.2}\\
&= +\frac{h}{3l}(x-4nl) \qquad +4nl < x < +(4n+3)l \\
&= -\frac{h}{3l}(x+4nl) \qquad -4nl > x > -(4n+3)l \\
&= -\frac{h}{l}(x-4(n+1)l) \qquad +(4n+3)l < x < +4(n+1)l \\
&= +\frac{h}{l}(x+4(n+1)l) \qquad -(4n+3)l > x > -4(n+1)l
\end{aligned}
$$

Here $m, n = 0, 1, 2, ...$ and t_0 is the time period of flashing, h is the height and $4l$ is the base of each tooth of the ratchet potential (see figure (6.2)). The teeth of the ratchet potential have a mirror symmetric plane at the middle (i.e. $x = 0$) so that, as the potential flashes, a particle current sets in initially towards the center of the system and finally the opposite currents nullify each other giving rise to a nonequilibrium build-up around the center at NSS of the system. The ratchet potential works by rectifying Brownian motion, usually producing a non-equilibrium flow with a direction set by the nature of the asymmetry. This potential is very similar to ratchet potentials for Brownian motors discussed for example in [36, 37]. However unlike in these studies, where the potential is constructed to produce a net flow of particles, here we can have a NSS in spite of periodic pumping of energy. Consider an initial equilibrium state with $V(x) = V_{on}$ and density $\rho(x) < \rho_c$ everywhere. As the potential starts flashing periodically, particles start to flow towards the central minima of the system from the

other minima(s). This causes the increment of $\rho(0)$ which eventually becomes larger than ρ_c. This results a microscopic phase separation around the central minima of the system, only due to the ratchet-controlled dynamics, even if we start with a subcritical density.

6.4 Particle Dynamics And Density Dynamics

We assume that the particles of both the species follow overdamped Langevin dynamics, i.e. the dynamical equation for the "i"-th particle from any of the species is

$$\frac{dx_i}{dt} = -\Gamma\frac{\partial V}{\partial x_i} + \Gamma f_i. \tag{6.3}$$

Neglecting hydrodynamic effects, we replace the mobility tensor $\mathbf{\Gamma}_{ij}$ by its mean field value $\Gamma\delta_{ij}$ even far away from equilibrium and assume that it does not depend on the particle species. Here V is the total configuration-dependent potential energy arising from the Gaussian interactions and the external potential imposed. Thermal noise from the bath f_i, has the usual properties,

$$< f_i(t) >= 0; \quad < f_i(t)f_j(t') >= 2\frac{K_B T}{\Gamma}\delta_{ij}\delta(t - t'). \tag{6.4}$$

DDFT [33, 34], is used to coarse grain from the particle picture to the density picture in order to compute the time-dependent density profiles of each species present in the mixture. For Gaussian interactions, it has been shown that the mean-field expression for the equilibrium density functional is an excellent approximation at intermediate and high densities [38, 39]. Let $\rho_1(\tilde{x}, \tau)$ and $\rho_2(\tilde{x}, \tau)$ are dimensionless densities of species 1 and 2 respectively, where $\tilde{x} = \frac{x}{\sigma_1}$ and $\tau = \frac{t}{\tau_B}$ are dimensionless variables. Here $\tau_B = \sigma_1^2/\Gamma K_B T$ is Brownian time scale. The coupled dynamical equation of ρ_1 and ρ_2 in presence of time dependent external potential $V_{ext}(\tilde{x}, \tau)$ and inter particle soft Gaussian core potentials (all potentials are in units of $K_B T$) is the following

$$
\begin{aligned}
\frac{\partial \rho_\alpha}{\partial \tau} &= \frac{\partial^2 \rho_\alpha}{\partial \tilde{x}^2} + \frac{\partial}{\partial \tilde{x}}\left[\rho_\alpha(\tilde{x}, \tau)\frac{\partial V_{ext}}{\partial \tilde{x}}\right] \\
&+ \frac{\partial}{\partial \tilde{x}}\left[\rho_\alpha(\tilde{x}, \tau)\frac{\partial}{\partial \tilde{x}}\right. \\
&\qquad \left. \sum_\beta \int d\tilde{x}' \rho_\beta(\tilde{x}', \tau)A^{\alpha\beta}\exp\left(\frac{-(\tilde{x} - \tilde{x}')^2}{r_{\alpha\beta}^2}\right)\right].
\end{aligned}
\tag{6.5}
$$

Here, $r_{\alpha\beta}$ represents ratios of the widths of interparticle interactions. Here $r_{11}(=\frac{\sigma_1}{\sigma_1})=1$, $r_{22}=\frac{\sigma_2}{\sigma_1}$, $r_{12}=\frac{\sigma_{12}}{\sigma_1}$ and $r_{12}=r_{21}$ (because, $\sigma_{12}=\sigma_{21}$). We take $\sigma_{\alpha\beta}=|\sigma_\alpha-\sigma_\beta|$ for $\alpha\neq\beta$.

We solve the coupled dynamical equations for the densities (equation (6.5)) numerically using a "forward-time centered space" algorithm [39] to solve the initial value problem with spatial periodic boundary conditions. As the method is accurate only to $\mathcal{O}(\Delta t)$, we need to take sufficiently small $\Delta t=10^{-6}\tau_B$.

We initially prepare the system in equilibrium such that it is in a mixed state where the total number of particles of both the species are identical, i.e. $N_1=\int dx\rho_1=N_2=\int dx\rho_2$. We have chosen $N_1=N_2=50$ here throughout the calculation. We then switch on the time dependence at $t=0$, i.e. it starts to oscillate (for V_1) or to flash (for V_2) and perturb the mixture. Finally the system reaches a NSS for both V_1 and V_2. In case of V_2 only the binary mixture is micro-phase separated, i.e. the constituents of the mixture form alternate lamellae with widths of the order of the range of the inter-particle interactions. In case of V_1, as stated earlier, no phase separation can be obtained. The results are depicted in the figures 6.1 and 6.2.

6.5 Results and discussions

In figure (6.1a) we show the potential $V_1(x,t)$ schematically at fixed time. It has only one minimum at $x=0$. In figure (6.1a) we also show the final steady state density profile, where no phase segregation is observed. In figure (6.1b) we plot the driving frequency Vs. central density calculated from DDFT and in figure (6.1c) the same graph from BD simulation is plotted. These graphs clearly show the fall of density of a single species with ω.

In figure (6.2) we show the 'on' state of flashing ratchet potential ($V_2(x,t)$) along with the final steady state density profiles, where a nonequilibrium enhancement of density near $x=0$ as well as the lamellar structure, both are clearly shown. Lamellar structure, i.e. the segregated phases are clear from the figure. Assuming local equilibrium, microphase separation is controlled by
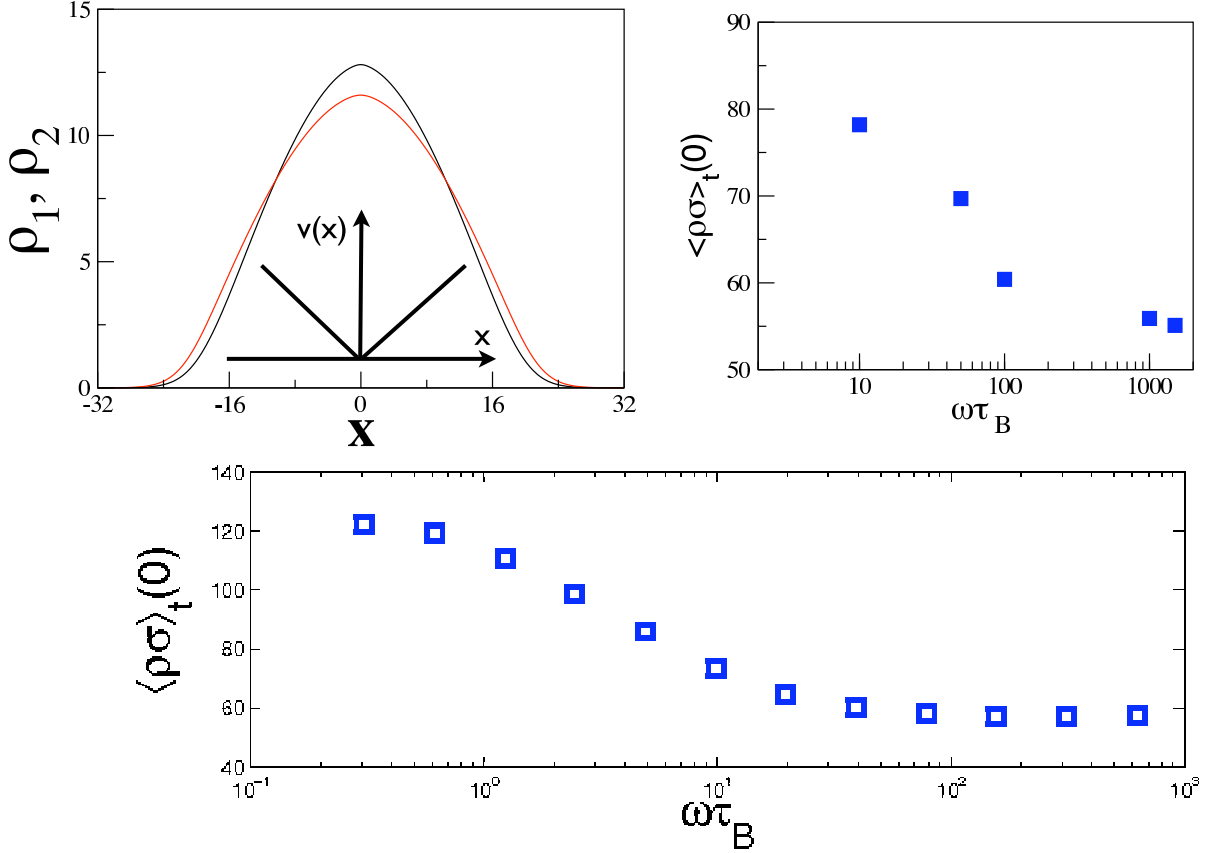
Figure 6.1: Final density profiles in (a) of the NSS obtained after driving the system by an oscillatory $|x|$ potential with slope $10K_BT/\sigma_1$, which is schematically shown also in (a). Red and black profiles are final density profiles of two constituent species. Decrease of central density of a single component with frequency is shown in (b) from DDFT and in (c) it is shown from BD simulation also. Here units used in space and time axis are τ_B and $\sigma = \sigma_1$ respectively. We take $r_{22} = 1/3$, $r_{12} = 2/3$, $A^{\alpha\beta} = k_B T$.
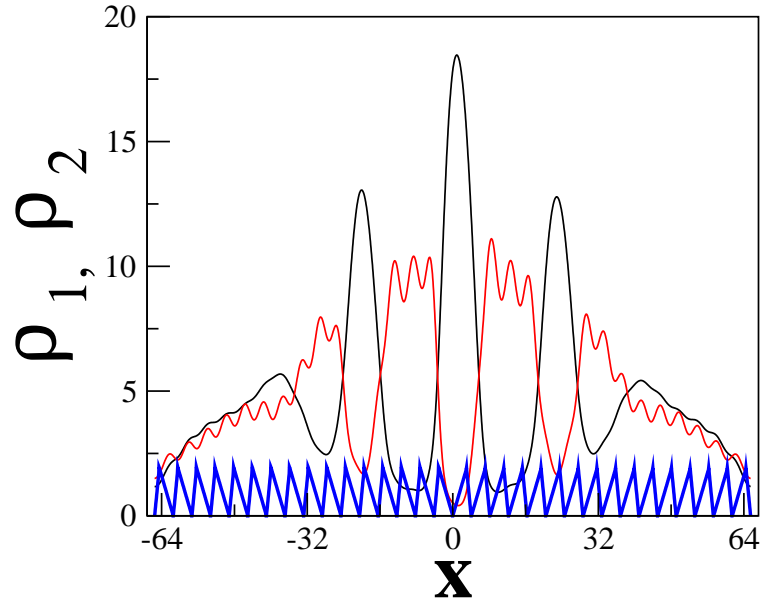
Figure 6.2: Final density profiles of the NSS obtained after driving the system by a flashing ratchet potential, are shown in Red and black. The "on" state of flashing ratchet potential is shown in blue. Here units used in space and time axis are τ_B and σ_1 respectively. The base of a tooth is $4\sigma_1$. The height of a tooth of the ratchet is $10k_BT$. Our system contains total number of 32 teeth. The parameters of the inter-particle potentials are same as in figure(1). Here the total time $\tau_o = 1000\tau_p$ where τ_p is the time period for flashing.

the local total density $\rho_0 = \rho_1 + \rho_2$ and occurs when $\rho_0 > \rho_c$ a composition dependent critical density. The time derivative $\dot{\rho}_0$, contains, $\dot{\rho}_0 = -(j'_{int} + j'_{ext})$ where j_{int} is the total particle current due to internal interactions and j_{ext} is that due to the external potential. In the NSS, $\dot{\rho}_0 = 0$ everywhere and these two currents balance each other. Since j_{int} depends on density, tuning j_{ext} using the external potential provides a way of controlling the density and hence the structure of the fluid. The flashing ratchet potential sets up j_{ext} in opposing directions producing a net accumulation of particles in the center in the NSS. The enhanced density then causes microphase separation. If $V_2(x, t)$ is always 'on' $j_{ext} = 0$ and the equilibrium density $\propto \exp(-\beta V_2(x, t))$ is not large enough to produce phase segregation.

Our system may have several practical applications. For example, it can be used as a method of fabrication to improve optical extraction efficiency from a semiconductor light emitting device [40]. To improve optical extraction, two processes are well known—(i) by inducing gradient of refractive index to prevent reflection and (ii) taking out the first order diffracted light from a diffraction grating. For both the processes, fabrication of subwavelength columnar structure on the surface of semiconductor light emitting devices, is an indispensable tool. To fabricate the structures, microphase-separated patterns of a block copolymer [8], as we have here, can be used as an etch mask.

6.6 Summary

In conclusion, we have considered the possibility of micro-phase separation of a mixture of soft colloidal particles using spatially varying time-oscillatory potentials. We have shown this by employing DDFT. The steady state density profile which shows phase separation, has alternating layers of particles of each constituent species. The thickness of the layers are of the order of corresponding sizes of the particles. This non-equilibrium steady state is purely dynamic in origin and may be controlled by tuning the amplitude and frequency of the external potential. The drive-induced lamellar ordering found in simple models here should be a general effect independent of details of the particle interactions and shapes of the external potentials. In principle, it is possible to observe the effect by real-space experiments of particle in optical

tweezers [35]. The test of micro-phase separation in case of flashing ratchet potential through Brownian dynamics simulation is an ongoing project.

6.7 Appendix

Dynamical Density Functional Theory:- Here we will briefly derive DDFT by following [34] closely. For details one should go through [34] and [33] both.

We have the following equation of motion for i-th soft colloidal particle, representing the center of mass of a polymeric coil, as

$$\dot{\mathbf{x}}_i = -\Gamma\nabla_i V + \Gamma\eta_i, \qquad (A1)$$

where V is the sum of external (time and space dependent) and inter-particle potential (only space dependent) felt by the particle and can be written as

$$V(\mathbf{x}^N, t) = \sum_{i=1}^{N} V_{ext}(\mathbf{x}_i, t) + \frac{1}{2}\sum_{j\neq i}\sum_{i=1}^{N} v_2(\mathbf{x}_i, \mathbf{x}_j) + \frac{1}{6}\sum_{k\neq j\neq i}\sum_{j\neq i}\sum_{i=1}^{N} v_3(\mathbf{x}_i, \mathbf{x}_j, \mathbf{x}_k) + ... \qquad (A2)$$

Here, $\mathbf{x}^N \equiv \{\mathbf{x}_1, \mathbf{x}_2...\mathbf{x}_N\}$ provided there are N number of particles, V_{ext} is the time dependent externally tunable potential on the particle (e.g. - flashing ratchet potential) and v_1, v_2... are respectively two body, three body... terms of the inter-particle interaction. η is usual Gaussian white noise acts on the particle due to the medium at temperature T.

The dynamics of the probability of getting a particle between $\mathbf{x}^N$ and $\mathbf{x}^N + d\mathbf{x}^N$ at time t is given by the following equation:-

$$\frac{\partial P(\mathbf{x}^N, t)}{\partial t} = \Gamma\sum_{i=1}^{N}\nabla_i.[k_B T\nabla_i + \nabla_i V(\mathbf{x}^N, t)]P(\mathbf{x}^N, t) \qquad (A3)$$

Now we define a n-particle density of the particles as

$$\rho^{(n)}(\mathbf{x}^n, t) = \frac{N!}{(N-n)!}\int d\mathbf{x}_{n+1}...\int d\mathbf{x}_N P(\mathbf{x}^N, t) \qquad (A4)$$

where the combinatorial pre-factor can easily be understood in the following way. The number of ways one can choose one particle from N independent particles are exactly N and after

picking that choosing another one can be done in $N - 1$ ways. As these two events (picking the first one and picking the next one from the rest) are independent, there are $N \times (N - 1)$ ways of doing those events together. Similarly if one wants to choose n number of particles, it can be done in $N \times (N - 1) \times (N - 2)... \times (N - n) = \frac{N!}{(N-n)!}$ number of ways. This factor is required to multiply with normalised probability distribution to get density out of it.

Integrating the dynamical equation for probability and using above definition of n-particle density with the expansion of the potential V, one can have the following equation

$$
\begin{aligned}
\Gamma^{-1}\frac{\partial\rho(\mathbf{x}_1,t)}{\partial t} &= k_B T \nabla_1^2 \rho(\mathbf{x}_1,t) \\
&+ \nabla_1.[\rho(\mathbf{x}_1,t)\nabla_1 V_{ext}(\mathbf{x}_1,t)] \\
&+ \nabla_1. \int d\mathbf{x}_2 \rho^{(2)}(\mathbf{x}_1,\mathbf{x}_2,t)\nabla_1 v_2(\mathbf{x}_1,\mathbf{x}_2) \\
&+ \nabla_1. \int d\mathbf{x}_2 \int d\mathbf{x}_3 \rho^{(3)}(\mathbf{x}_1,\mathbf{x}_2,\mathbf{x}_3,t)\nabla_1 v_3(\mathbf{x}_1,\mathbf{x}_2,\mathbf{x}_3) \\
&+ ....
\end{aligned} \tag{A5}
$$

where we have used $\rho^1 = \rho$. This equation is not tractable because it is not a closed relation—even if we consider such potential which has only two body term (simplest one), then also to calculate $\rho^{(n)}$ we need $\rho^{(n+1)}$, where $n = 1, 2, 3....$ From these relations, one obtains an infinite hierarchy of relations, analogous to the Born-Bogoliubov-Green-Kirkwood-Yvon (BBGKY) equations [33].

To make it tractable, we assume two relations, which are strictly true for equilibrium fluids, also work far from equilibrium. For a fluid in equilibrium, an exact sum rule [43] relates the gradient of the one-body direct correlation function—$c^1(\mathbf{r})$ to the inter particle forces acting on a particle, as:-

$$
- k_B T \rho(\mathbf{x}_1)\nabla c^{(1)}(\mathbf{x}_1) = \sum_{n=2}^{\infty} \int d\mathbf{x}_2 ... \int d\mathbf{x}_n \rho^{(n)}(\mathbf{x}^n)\nabla_1 v_n(\mathbf{x}^n). \tag{A6}
$$

and from equilibrium statistical mechanics one can also have one body direct correlation function as a functional derivative of the Helmholtz free energy (F_{ex}, a functional of density of the system) due to the inter particle interaction,

$$
c^{(1)}(\mathbf{x}) = -\beta \frac{\delta F_{ex}[\rho(\mathbf{x})]}{\delta\rho(\mathbf{x})}. \tag{A7}
$$

In above equation F_{ex} signifies the excess (over the ideal) Helmholtz free energy due to the inter particle interaction. The full form of the free energy is given by

$$F[\rho(\mathbf{x})] = k_B T \int d\mathbf{x}\rho(\mathbf{x})[\ln(\rho(\mathbf{x})\Lambda^3) - 1] + F_{ex}[\rho(\mathbf{x})] + \int d\mathbf{x}V_{ext}(\mathbf{x})\rho(\mathbf{x}). \qquad (A8)$$

where the first term of the r.h.s is the ideal part and the last term is due to the external potential. Here Λ is the thermal De Broglie wave length. All the length scales that we are concerned here, are much greater than this wave length to ensure that the fluctuations we are dealing here are only thermal in nature.

In DDFT it is assumed, as we have said before, that all the above equilibrium results hold good even if we go far from equilibrium, i.e. even if we replace $V_{ext}(\mathbf{x})$ by $V_{ext}(\mathbf{x}, t)$, $\rho(\mathbf{x})$ by $\rho(\mathbf{x}, t)$ and $c^{(1)}(\mathbf{x})$ by $c^{(1)}(\mathbf{x}, t)$ in above relations, they will hold good. This assumptions work well for the Brownian fluids in nonequilibrium conditions, where momentum degrees of freedom of the fluid relax instantaneously. Using the assumptions, finally we get a closed dynamical equation for density as,

$$\Gamma^{-1}\frac{\partial\rho(\mathbf{x}, t)}{\partial t} = \nabla.\left[\rho(\mathbf{x}, t)\nabla\frac{\delta F[\rho(\mathbf{x}, t)]}{\delta\rho(\mathbf{x}, t)}\right] \qquad (A9)$$

which is the central result of this formulation.

If the colloidal particles interacting via Gaussian potential, things become even simpler after the mean field approximation, because the excess free energy becomes

$$F_{ex} = \int\int dxdx'V_{int}(|x - x'|)\rho(x, t)\rho(x', t) \qquad (A10)$$

which works very accurately in static as well as dynamic cases [27, 28, 41, 42]. Using this it is straight forward to arrive at the DDFT equation (6.5) that we have used in our present work.

Bibliography

[1] C. N. Likos, Physics Reports, **348**, 267-439, (2001).

[2] N.W. Ashcroft, N.D. Mermin, Solid State Physics, Holt Saunders, Philadelphia, 1976

[3] A. Ashkin, Science, **210**, 1083, (1980)

[4] Smith et. al., Opt. Letter, **6**, 284, (1981)

[5] Aslam Chowdhury, Bruce J. Ackerson Phys. Rev. Lett. **55**, 08 (,) 1985

[6] H. Löwen, Physica A **235**, 129 (1997).

[7] H. Tanaka, J. Phys.: Condensed Matter **12**, R207 (2000).

[8] G. Krausch, Material Science & Engineering R - Reports **14**, 1 (1995).

[9] H. Löwen, J. Phys.: Condensed Matter **13**, R415 (2001).

[10] S. Ramaswamy, Advances in Physics **50**, 297 (2001).

[11] H. Frielinghaus, N. Hermsdorf, K. Almdal, K. Mortensen, L. Messe, L. Corvazier, J. P. A. Fairclough, A. J. Ryan, P. D. Olmsted, I. W. Hamley, Europhys. Letters **53**, 680 (2001).

[12] N. Hoffmann, F. Ebert, C. N. Likos, H. Löwen, G. Maret, Phys. Rev. Letters **97**, 078301 (2006).

[13] T. Uneyama, M. Doi, Macromolecules **38**, 196 (2005).

[14] P. Sollich, J. Phys.: Condensed Matter **14**, R79 (2002).

Bibliography

[15] N. B. Wilding, F. Schmid, P. Nielaba, Phys. Rev. E **58**, 2201 (1998).

[16] H. Tanaka, T. Araki, Chemical Engineering Science **61**, 2108 (2006).

[17] N. Hoffmann, C. N. Likos, H. Löwen, J. Phys.: Condensed Matter **18**, 10193 (2006).

[18] V. N. Manoharan, M. T. Elsesser, D. J. Pine, Science **301**, 483 (2003).

[19] L. R. Snyder, J. J. Kirkland, Introduction to Modern Liquid Chromatography, Wiley, New York (1979).

[20] D. C. Hong, P. V. Quinn, Phys. Rev. Lett. **86**, 3423 (2001)

[21] J. Dzubiella, G. P. Hoffmann, H. Löwen, Phys. Rev. E **65**, 021402 (2002).

[22] M. Rex, H. Löwen, Phys. Rev. E **75**, 051402 (2007).

[23] M. Rex, H. Löwen, European Physical Journal E **26**, 143 (2008).

[24] J. K. G. Dhont, Phys. Rev. E **60**, 4534 (1999).

[25] S. M. Fielding, Soft Matter **3**, 1262 (2007).

[26] S. A. Rogers, D. Vlassopoulos, P. T. Callaghan, Phys. Rev. Letters **100**, 128304 (2008).

[27] A. Lang, C. N. Likos, M. Watzlawek, H. Löwen, J. Phys.: Condensed Matter **12**, 5087 (2000).

[28] A. A. Louis, P. G. Bolhuis, J. P. Hansen, Phys. Rev. E **62**, 7961 (2000).

[29] C. N. Likos, M. Schmidt, H. Löwen, M. Ballauff, D. Pötschke, P. Lindner, Macromolecules **34**, 2914 (2001).

[30] A. Jusufi, J. Dzubiella, C. N. Likos, C. von Ferber, H. Löwen, J. Phys.: Cond. Mat. 1361772001

[31] C. N. Likos, S. Rosenfeldt, N. Dingenouts, M. Ballauff, P. Lindner, N. Werner, F. Vogtle, J. Chem. Phys. **117**, 1869, 2002

[32] M. Konieczny, C. N. Likos, H. Löwen, J. Chem. Phys.**121**, 4913, 2004

[33] U. Marini Bettolo Marconi, P. Tarazona, J. Chem. Phys. **110**, 8032, 1999

[34] A. J. Archer, R. Evans, J. Chem. Phys. **121**, 4246, 2004

[35] A possible realization is e.g. described in: C. Lutz, M. Reichert, H. Stark, C. Bechinger, Europhysics Letters **74**, 719 (2006).

[36] R. Eichhorn, P. Reimann, P. Hänggi, Phys. Rev. Letters **88**, 190601 (2002).

[37] P. Reimann, Phys. Rep.361572002

[38] J. Dzubiella, C. N. Likos, J. Phys.: Condensed Matter **15**, L147 (2003).

[39] M. Rex, C. N. Likos, H. Löwen, J. Dzubiella, Mol. Phys. **104**, 527 (2006).

[40] K. Asakawa, A. Fujimoto, Applied Optics, **44**, 34 (2005)

[41] C. N. Likos Phys. Rev. E **63**, 031206 (,) 2001

[42] A. J. Archer, R. Evans Phys. Rev. E **64**, 041501 (,) 2001

[43] R. Evans, Adv. Phys. **28**, 143, 1979